NOVEL ENCAPSULATION TECHNOLOGIES FOR SMALL SIZE-SCALE SELF-HEALING APPLICATIONS

BY

AARON CHRISTOPHER JACKSON

DISSERTATION

Submitted in partial fulfillment of the requirements
for the degree of Doctor of Philosophy in Materials Science and Engineering
in the Graduate College of the
University of Illinois at Urbana-Champaign, 2011

Urbana, Illinois

Doctoral Committee:

Professor Paul V. Braun, Chair
Professor Nancy R. Sottos
Professor Jeffrey S. Moore
Assistant Professor Shen J. Dillon

Abstract

Self-healing technology offers an autonomic route to repairing damage in advanced polymers to extend their lifetime. A variety of self-healing systems have been developed for mechanical self-healing, protective coatings, and electronic self-healing. These self-healing systems rely on functional groups within the polymer, microvascular networks, or compartmentalization in capsules and particles. The healing agents become active in the crack plane upon damage, forming new bonds that heal the material. Of these systems, compartmentalization offers a simple and inexpensive means to apply self-healing to current advanced polymer applications.

In this research, the primary motivation is to address challenges associated with small size-scale self-healing in compartmentalized systems. The term "small size-scale" in self-healing technology is applied to technologies where components are between 100 and 2000 nm. As the size of the capsules and particles decreases, current encapsulation methods do not ensure that self-healing components disperse well in a polymer matrix and that the components retain their contents during processing. The ring-opening metathesis polymerization reaction between dicyclopentadiene and Grubb's catalyst is especially important to self-healing applications and provides a model system that uses both encapsulated liquid and solid healing agents. DCPD is encapsulated in polyureaformaldehyde (PUF) capsules while catalyst is protected in wax particles.

Silica coatings, applied using a variety of silica condensation chemistries, help to improve the functionality of liquid-filled capsules. Fluoride-catalyzed silica condensation offers the best route to coating PUF capsules with a variety of sizes and contents. Coated capsules, 1.5 μm in diameter, can be dried to a powder without aggregates, something that cannot be achieved without the coating. Although a silica shell adds an additional diffusion barrier to the capsules,

the stability of PUF capsules relies more on the washing conditions and capsule contents than on the addition of a silica shell.

Polymer protection of Grubbs' catalyst allows the catalyst to be incorporated into an epoxy matrix at smaller size scales without deactivation. The final particles contain catalyst encapsulated in particles made of polystyrene (PS) and polymethylmethacrylate (PMMA) and coated with silica. At larger size-scales, the polystyrene is sufficient to protect the particles and helps to improve the thermal stability of the particles compared to as-received Grubbs' catalyst or catalyst encapsulated with wax.

One important application requiring small size-scale self-healing components is in fiber-rich regions of epoxy composites where the spacing between fibers is limits the size of the components that can be used for self-healing. The small size scale self-healing components, DCPD capsules and Grubbs' catalyst particles, are successfully incorporated into epoxy without aggregation or deactivation and demonstrate nominal healing. The size of the capsules limits the amount of healing agent delivered to the crack plane so pressure is applied across the crack plane, decreasing the crack volume and improving healing. PS in the catalyst particles also contributes to healing as it is dissolved by the DCPD and redeposits in the crack plane. The full system provides a healing efficiency of approximately 25%.

Another important application requiring small size-scale self-healing components is in optical self-healing. 10 μm thick PMMA coatings containing 1.5 μm in diameter dibutyl phthalate (DBP) capsules scatter minimal light as a result of index matching. The capsules are capable of partially healing sub-micron damage in 100 μm PMMA films that have been mechanically damaged. The healed material scatters minimal light and retains the protective capabilities of the original PMMA coating. Larger capsules, 80 μm in diameter, containing DBP provide more healing allowing full healing at 6 wt.% capsules in polymer. They scatter more

light than the 10 μm coatings containing 1.5 μm in diameter capsules but are still more optically clear than systems with poor index matching.

Acknowledgments

My scientific career owes everything to my parents who facilitated my science interests throughout grade school and high school. Whether coaching me in Science Olympiad or building a bell jar vacuum in our basement, they were my first research advisors and have been tremendous role models. I also owe a great deal of gratitude to my brother and sisters, Meredith, Becca, and Brendon, who have all challenged me at home to be my best. Becca deserves special thanks for looking over my thesis during its initial stages.

My research career would not have been successful without the guidance of my current research advisor, Paul Braun, who kept me focused throughout my graduate school career and was patient through all of the rookie mistakes I made as a graduate student. I appreciate the scientific discussions as well as the opportunities he has opened up for me.

I owe a great deal of gratitude to my committee members, Professor Nancy Sottos, Professor Jeffrey Moore and Professor Shen Dillon. Their suggestions, questions and criticisms have helped me hone in on the key details in my work. I owe special thanks to Professor Sottos and Professor Scott White who were instrumental in my earlier work with self-healing materials. They helped to nudge me in the right directions and pushed me to my comfort level and beyond.

Of the colleagues I have worked with here at the University of Illinois, the Braun group has provided a significant amount of support towards helping me reach my goals. Jon Bartelt and Kamil Marczewski provided great help in the labs and Special thanks go to Dr. Dara Gough, Dr. Abby Juhl, Sid Gupta, Dr. Mark Losego, Corissa Lee, Kevin Arpin, Austin Pickett, and Nihan Yonet who have made insightful comments on my work and supported me over the last few years. Whether it has been research related, teaching related or extracurricular, I have enjoyed my time here with you and hope to keep in touch.

Folks in the Autonomic Materials Group have been important in providing technical assistance. I would like to thank Dr. Ben Blaiszik and Dr. David McIlroy for helping me during

my first year become more familiar with the AMS labs. Dr. Mary Caruso and Dr. Susan Odom have been great collaborators for my side work with self-healing electronics. Jason Patrick, Marta Baginksi, Dr. Ben Blaiszik, and Dr. Magnus Anderson have all done a great job keeping the AMS labs clean and organized as lab managers of the AMS labs. Lab manager is usually a thankless job but it is time to make an exception; thanks!

I would also like to thank the other grad students who started with me in 2006, especially Andrew Carlson, Dr. Hunter McDaniel, Sid Gupta, Dr. Jericho Moll, and Phil Heil. We all stayed close and they helped to keep Graduate School in perspective during my time here.

Finally, I would like to thank facilities and funding including Beckman Institute's Imaging Technology Group and MRL facilities. Scott Robinson has been an especially important resource for learning about all of the microscopy techniques I used and has helped keep my images sharp.

TABLE OF CONTENTS

CHAPTER 1: INTRODUCTION 1
1.1 Autonomic Self-healing Polymers 1
1.1.1 Microvascular Self-healing Systems 2
1.1.2 Molecular Self-healing Systems 3
1.1.3 Compartmentalized Self-healing Systems 4
1.1.3.1 Mechanical Self-healing 4
1.1.3.2 Protective Coatings 5
1.1.3.3 Electronic Self-healing 6
1.2 Challenges for Compartmentalized Self-healing 6
1.2.1 Small Size-scale Self-healing 6
1.2.2 High Temperature Processing 9
1.2.3 Solution Processing 10
1.3 Statement of Purpose 11
1.4 References 12

CHAPTER 2: MODIFICATION OF CAPSULES VIA SILICA COATINGS 17
2.1 Motivation 17
2.2 Surface Chemistry 18
2.3 Silica Coating Methods 20
2.3.1 Stöber Condensation 20
2.3.2 Fluoride-catalyzed Silica Condensation 24
2.3.3 Chemical Vapor Deposition 28
2.4 Capsule Stability 29
2.4.1 Modeling the Diffusion Coefficient of Solvents in a Capsule Shell 30
2.4.2 Thermal Stability 32
2.4.3 Solvent Stability 39
2.5 Conclusions 42
2.6 Experimental 43
2.6.1 Materials 43
2.6.2 Capsule Manufacture 43
2.6.3 Stöber Condensation 44
2.6.4 Fluoride-catalyzed Condensation 45
2.6.5 FBR-CVD 46
2.6.6 Capsule Analysis 47
2.7 References 49

CHAPTER 3: POLYMER PARTICLES CONTAINING GRUBBS' CATALYST 52
3.1 Motivation 52
3.2 Sub-micron Polystyrene Particles Containing Grubbs' Catalyst 53
3.3 PS-protected Grubbs' Catalyst for Thermal Stability 56
3.4 Conclusions 59
3.5 Experimental 60
3.5.1 Materials 60
3.5.2 Polymer-protected Catalyst Particles 60
3.5.3 Catalyst Particle Analysis 61
3.6 References 62

CHAPTER 4: MECHANICAL SMALL SIZE-SCALE SELF-HEALING IN EPOXY .. 64
4.1 Motivation 64
4.2 System Overview 66
4.3 Dispersing Micron Size Components in Epoxy 68
4.4 Activity of Grubbs' Catalyst Particles in Epoxy 71
4.5 Small Size-scale Self-healing in an Epoxy Matrix 73
4.6 Conclusions 74
4.7 Experimental 75
4.7.1 Materials 75
4.7.2 Self-healing Composites 76
4.8 References 77

CHAPTER 5: OPTICAL SELF-HEALING IN POLYMETHYLMETHACRYLATE ... 78
5.1 Motivation 78
5.2 System Overview 80
5.3 Optical Properties of Capsule-containing Films 83
5.4 Optical and Barrier Properties of the Healed Polymer 86
5.5 Rate and Extent of Thermoplastic Self-healing 90
5.6 Conclusions 92
5.7 Experimental 93
5.7.1 Materials 93
5.7.2 Fabrication of Self-healing Coatings 93
5.7.3 Analysis of Self-healing Coatings 94
5.8 References 95

CHAPTER 6: CONCLUSIONS AND FUTURE DIRECTIONS 97
6.1 Conclusions 97
6.2 Future Directions 100
6.2.1 Capsule Stability 101
6.2.2 Active Particle Stability 103
6.2.3 New Applications with Thermoplastic Self-healing 104
6.3 References 105

AUTHOR'S BIOGRAPHY 106

CHAPTER 1

INTRODUCTION

1.1 Autonomic Self-healing Polymers

Self-healing technology offers an important mechanism for extending the lifetime of advanced polymers in many applications. Similar to the biology of a cut where proteins, platelets and other components from the blood are recruited to the damaged skin, healing agents are incorporated into a polymer, and are recruited to damage in polymers, polymerizing to form new material in the damaged region. White *et al.* demonstrated a self-healing system where healing agents are incorporated into polymer as capsules or particles (**Figure 1.1**).[1] As a crack propagates through the polymer matrix, the healing agents release into the crack plane, mix, and form new polymer. Newer self-healing technologies rely on an expanded set of solutions for incorporating healing agents into a polymer.[2] The original self-healing system where self-healing agents are phase separated in a polymer matrix is considered a compartmentalized self-healing system.[3-19] A microvascular system incorporates the healing agents into the polymer matrix through microchannels similar to blood vessels in biology.[20-24] Finally, molecular systems incorporate reactive agents into the backbone of the polymer.[25-33]

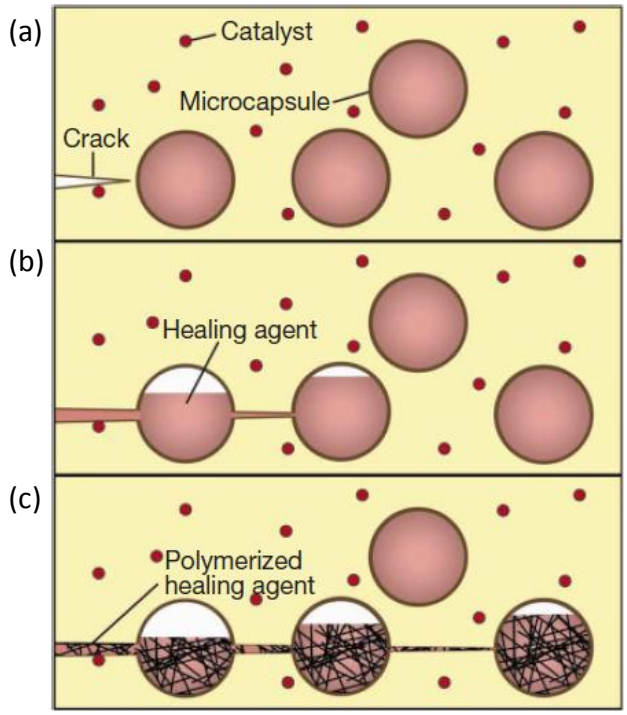

Figure 1.1. Schematic of the self-healing process. Catalyst and microcapsules are incorporated into a polymer matrix (a). As a crack propagates through the polymer, healing agent is released into the crack plane (b). When the healing agent meets catalyst in the polymer, it polymerizes creating new polymer (c). Figure adapted from [1].

1.1.1 Microvascular Self-healing Systems

Microcascular self-healing systems incorporate healing agents into a polymer matrix through microchannels similar to blood vessels in biology (**Figure 1.2**). The primary advantage to these systems is that multiple healing events can occur as long as the vascular networks can be refreshed. The original concept proposed by Toohey *et al.* was made of a microchannel network containing dicyclopentadiene (DCPD). The microchannels delivered DCPD to an epoxy surface coating containing Grubbs' catalyst.[20] One of the advantages to this system is the variety of healing that can be used. Molecular self-healing systems are limited by synthetic routes to modifying a polymer while compartmentalized systems are limited by solution encapsulation methods that require good phase separation. As a result, more recent work demonstrated healing

using a 2 microchannel system where one set of channels contained epoxy resin and the other contained epoxy hardener.[21, 22] These systems are limited to healing a coating only but other microvascular systems use microchannels that can heal in bulk epoxy. Trask *et al.*[23] use hollow microfibers to deliver healing agents throughout a composite material while Hamilton *et al.* [24] fabricated 3-D microvascular networks in epoxy using a robocasting method.

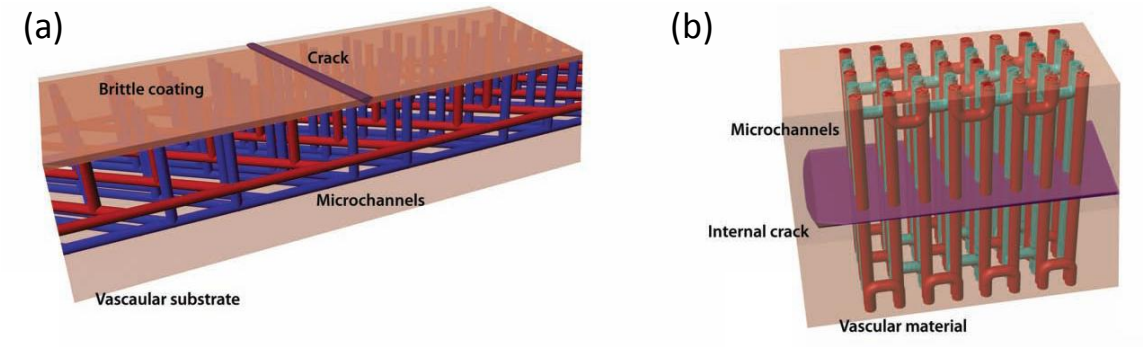

Figure 1.2. (a) microvascular network where healing agents are delivered to an epoxy coating, and (b) a microvascular network where healing agents are delivered throughout the polymer matrix. Adapted from reference [24].

1.1.2 Molecular Self-healing Systems

Molecular self-healing systems incorporate mechanically responsive moieties into the backbone of the polymer. In many cases, these moieties are reversible bonds that rely on hydrogen bonding or high temperature for construction and deconstruction.[25-27] This is a promising route because multiple healing events can be achieved due to the reversibility. More recently, mechanochemistry has demonstrated promise where mechanical force in the polymer matrix opens new functionalities within the polymer backbone. Hickenboth *et al.* demonstrated such a phenomenon using benzocyclobutanes [28, 29] while Potisek *et al.* later demonstrated chemical reactions that could take place using the benzocyclobutane group.[29] Since then other

mechanoresponsive moieties have been used for color changing,[30, 31] unveiling of cyanoacrylates,[32] and opening of gem-dichlorocyclopropanes.[33] One of the challenges with molecular self-healing systems is the low quantity of mechanically responsive moieties present in a damaged region.

1.1.3 Compartmentalized Self-healing Systems

Compartmentalized self-healing systems require encapsulation of healing agents and these encapsulated healing agents are incorporated into a polymer matrix. Due to its simplicity, low cost and the relatively high volume of healing agent delivered, much work has been done towards implementing the system in a variety of applications using a variety of chemistries. These systems and chemistries can be divided into the properties they are capable of healing.

1.1.3.1 Mechanical Self-healing

Mechanical properties, including fracture toughness and fatigue, require good bonding between the healed polymer and the crack surface. The self-healing chemistry chosen by White *et al.* is based on the ring opening methathesis polymerization of Dicyclopentadiene (DCPD) in the presence of Grubbs' catalyst (**Figure 1.3**). These components are incorporated into an epoxy matrix based on diglycidal ether of bisphenol A (DGEBA) and diethylene triamene (DETA). The resulting healed region maintains its mechanical integrity through mechanical and Van der Waals bonding. The recovery of a material's mechanical properties using the DCPD/Grubbs' catalyst system is particularly applicable to composites where subsurface damage occurs that is difficult to detect and fix manually.[3-6] The chemistry has also been used in the development of self-healing adhesives.[7]

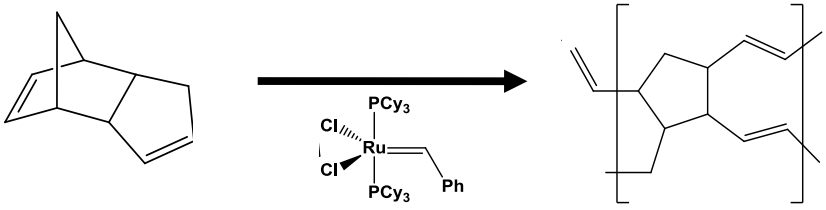

Figure 1.3 Schematic of the reaction between Grubbs' catalyst and DCPD.

A variety of self-healing chemistries have been developed more recently to improve the interaction between the healed material and an epoxy matrix. These include epoxy,[8, 9] isocyanate,[10] and solvent welding [11] chemistries. In addition, other chemistries have been developed that work with other matrices. Siloxane chemistries, for example have been used in vinyl ester matrices [12] and PDMS.[13]

1.1.3.2 Protective Coatings

Protective coatings require that the healing chemistry provide a barrier between the coating's substrate and the outside environment. The barrier does not need to fill the crack plane and does not need an excellent mechanical bond with the coating. Initial work in this area encapsulated film forming liquids, such as castor oil, into a polymer coating.[14] As the liquid released into the crack plane, it coated the substrate and provided the barrier between the substrate and the surrounding environment. By including corrosion inhibitors, the efficacy of the film was enhanced. More recently, polymerization reactions involving siloxane chemistry have been used to improve the mechanical properties of the films released (**Figure 1.4**).[15, 16]

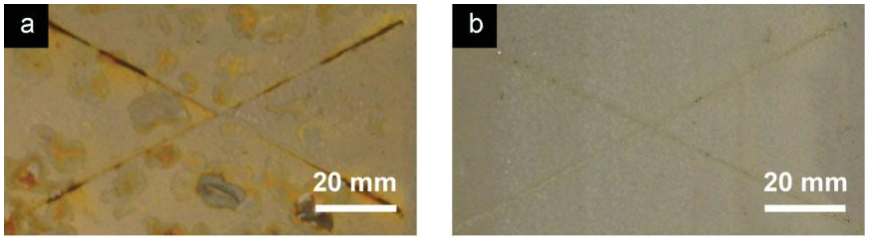

Figure 1.4. An epoxy vinyl ester matrix (a) without and (b) with an encapsulated self-healing siloxane chemistry.

1.1.3.3 Electronic Self-healing

A more recent type of self-healing involves release of conductive healing agents that can bridge gaps in a circuit and regain the electrical properties of the undamaged circuit. Initial work by Caruso *et. al.* demonstrated encapsulation of carbon nanotubes (CNT) in polyureaformaldehyde capsules and demonstrated release of the CNTs upon capsule rupture.[17] Odom *et. al.* demonstrated the use of charge transfer salts as a conductive healing agents.[18] More recent work has demonstrated device architecture where low melting point eutectics were released into an active circuit.[19] Instead of releasing conductive components, Odom *et. al.* also developed a device where solvents dissolved and redeposited electronic circuits made of conductive paint.[19]

1.2 Challenges for Compartmentalized Self-healing

1.2.1 Small Size-scale Self-healing

Small size-scale self-healing systems are important in applications where space is limited. In composites, interstitial spaces between fibers, where the volume is micron size or smaller,

requires encapsulated healing agents with sub-micron diameter.[34, 35] Blaiszik *et al.* demonstrated successful healing of interfacial damage between fibers and epoxy using micron size capsules.[34] For optical polymers, self-healing components on the order of 1 μm in diameter provide several advantages. First, many optical polymers are used as coatings where the thickness of the coating limits the size of the capsules. The use of thinner coatings also limits scattering from the capsules and is therefore important for obtaining optically clear polymers containing capsules. Finally, many optical polymers are thermoplastic and are subject to crazing damage [36, 37] which may not effectively rupture capsules on the order of 100 μm in diameter due to the nanometer wide damage created. This damage may not have enough force to rupture capsules or may occur in the space between capsules.

One of the challenges for developing small size-scale self-healing systems is to design liquid-filled capsules and active particles on the order of 1 μm in diameter. Kessler and *et al.* developed an emulsion surface polymerization of polyureaformaldehyde (PUF) to encapsulate DCPD in capsules larger than 20 μm in diameter.[38] Blaiszik *et al.* demonstrated the synthesis of 1.4 μm DCPD-filled PUF capsules using a sonication during the emulsification step of the DCPD encapsulation process.[35] While these capsules can be decorated onto glass fibers,[34] they do not disperse well in epoxy.

Silica condensation chemistries have been used to help improve colloid functionality and may potentially decrease aggregation of sonicated capsules. The silica coatings are relatively well studied[39-42] and provide a chemically modifiable surface.[43, 44] The Stöber method is particularly useful for coating colloids with a wide variety of functionalities and sizes (**Figure 1.5**).[39] A variety surface functionalities can be added to decrease capsule aggregation, including charged groups for charge repulsion or polymer brushes for steric hindrance.[45]

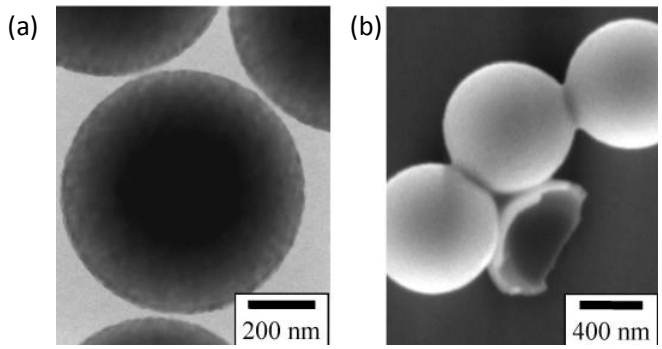

Figure 1.5. (a) TEM and (b) SEM of polystyrene particles coated with silica using a modified Stöber silica condensation method. Figure adapted from reference [39].

An analogous method for making active particles, particularly Grubbs' catalyst particles, on the order of 1 μm in diameter has not been devised yet. Part of the challenge is that Grubbs' catalyst is susceptible to deactivation by a number of reactive groups.[46-48] Rule *et al.* developed a scheme for encapsulating the catalyst in wax particles [49] but as the size of the wax particles approaches 1 μm, aggregation prohibits the use of the encapsulation method. Gibson developed a method for encapsulating Grubbs' catalyst in polystyrene but did not demonstrate well defined catalyst particles.[50] Regardless, polymer encapsulation is a promising route to catalyst encapsulation and has been used frequently in the drug delivery industry to protect and slowly release drugs in the human body. To encapsulate drugs in polymer, researchers use an emulsion solvent evaporation procedure.[51-54] In these procedures, a hydrophobic drug is dissolved in an organic solvent with a hydrophobic polymer. The organic phase is emulsified in water and the solvent is driven off leaving behind drug-loaded polymer particles (**Figure 1.6**).

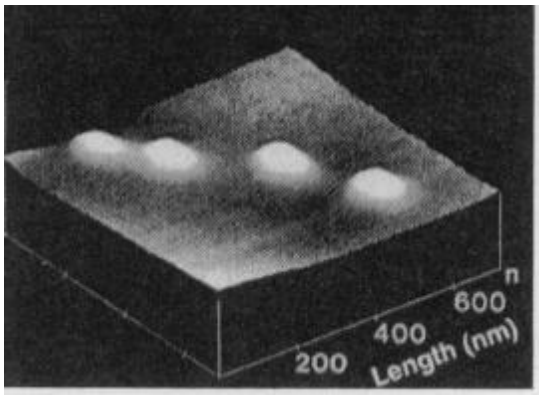

Figure 1.6. Atomic force microscopy (AFM) of polymer nanospheres made with a poly(lactic-co-glycolic acid) functionalized with polyethylene glycol using an emulsion solvent evaporation method. Figure adapted from [52].

Another challenge for small size-scale self-healing is to maximize healing response as the capsule size decreases. Rule and co-workers show that, for a given concentration of capsules, as the capsule size decreases, the amount of healing agent available in the crack plane decreases linearly.[55] They also show that maximum healing occurs when the crack plane is full and this requires a minimum size capsule and capsule concentration for a given damage size. The typical crack widths tested using this work are between 3-10 μm for which capsules larger than 10 μm are capable of providing maximum healing. To demonstrate healing with micron size capsules, sub-micron wide damage events need to be tested. Blaiszik *et. al.* attained sub-micron wide damage events by generating interface damage between fibers and epoxy.[34] Others reduce damage volume by applying pressure across the damaged region.[5, 56]

1.2.2 High Temperature Processing

High temperature processing is important in the composites industry where high temperature, combined with high pressure, can help decrease voids or allow the use of more

viscous resins. For the DCPD and Grubbs' catalyst system, DCPD is encapsulated in polyureaformaldehyde (PUF) capsules, while Grubbs' catalyst can be used as received. Kessler demonstrated high temperature stability in air for DCPD-filled PUF capsules both with temperature ramps and 150 °C isotherms.[4] Temperature ramps demonstrated that the capsules maintained their expected contents after capsule synthesis while 150 °C isotherms demonstrated how quickly the capsules lost their contents. DCPD-filled PUF capsules lose a significant quantity of their contents over 2 hours at 150 °C.[4] To improve upon the thermal stability of capsules, Caruso *et. al.* used a polyurethane (PU) encapsulation method in addition to the PUF encapsulation.[57]

Not as much work has been done to improve the thermal stability of catalyst particles. Rule *et. al.* noted that Grubbs' catalyst tends to deactivate in epoxy even at room temperature and used wax to help protect the catalyst better.[49] Wax, however, melts above 80 °C so its use is limited.

1.2.3 Solution Processing

Thermal stability in air provides a rough measure of capsule stability but does not reflect conditions that capsules see during processing or use. Many thermoplastic materials and paints require solvents and a solvent evaporation step for the processing of the materials. Other polymers have low viscosity resins and may be considered a solvent in the initial stages of processing. Kumar *et. al.* described what happens to capsules in solvents used for paints.[14] They suggest that core contents diffuse into the paint and, as material is lost, the capsule collapses. Yuan *et. al.* attempted to quantify healing agent loss from epoxy-filled capsules by measuring the quantity of material released into solution.[58] They did not, however, compare this to the initial sample weight to determine the percent of sample released. High temperature

solvent stability has not been considered but is also important since heat is often required to drive off solvents.

Drug delivery offers more examples of solvent stability measurements that can be applied to capsules and particles. Researchers in drug delivery engineer drug-loaded devices that can release their contents slowly over a long period of time.[53, 54] In those cases, the capsules or particles are dispersed in a solvent for a given time, centrifuged, and the supernatant analyzed to determine the amount of drug delivered during exposure to an *in vitro* environment. Similar methods can be used to determine healing agent loss, as opposed to drug release.

1.3 Statement of Purpose

This thesis demonstrates small size-scale self-healing systems for composites and optical polymers where the self-healing components are on the order of 1 μm or smaller. Current encapsulation methods do not ensure that self-healing components can be well dispersed in a polymer matrix and that the components retain their contents during processing. To build better self-healing components at this size-scale, this thesis considers modifications of existing encapsulation methods for both liquid healing agents, such as dicyclopentadiene, and solid healing agents, such as Grubbs' catalyst. For liquid-filled capsules, this thesis addresses the encapsulation requirements by employing a silica coating procedure that adds an additional layer to previously synthesized capsules. This layer can act as a base for functionality allowing better interaction with the capsules' environment or it can act as an additional diffusion barrier. For active particles, this thesis addresses the encapsulation requirements by first demonstrating the encapsulation of Grubbs' catalyst in polymer, then modifying the encapsulation with a silica coating similar to that used for liquid-filled capsules.

This thesis also considers the qualification and quantification of the properties improved by a silica modification. Functionality is demonstrated by successful dispersion of self-healing components in polymer matrices. Stability is demonstrated using a variety of testing methods that mimic the liquid-filled capsule and active particle environment. Current research in capsules and particle stability for self-healing do not adequately address the environment of the application in which the self-healing components will be used. As a result, many of the testing methods demonstrated are new to self-healing and a comprehensive discussion of these and other stability testing methods are discussed in Chapter 6.

Finally, within the framework of small size-scale self-healing applications in composites and optical polymers, this thesis explores the limitations of employing such a system while demonstrating its advantages. Small size-scale self-healing in epoxy is important for composites but also demonstrates the importance of the damage size when healing with capsules on the order of 1 μm in diameter. Optical self-healing using a compartmentalized system requires a new chemistry and new self-healing concepts that expands the library of self-healing applications.

1.4 References

[1] White, S. R.; Sottos, N. R.; Geubelle, P. H.; Moore, J. S.; Kessler, M. R.; Sriram, S. R.; Brown, E. N.; Viswanathan, S. Autonomic healing of polymer composites *Nature* **2001**, *409*, 794-797.

[2] Blaiszik, B. J.; Kramer, S. L. B.; Olugebefola, S. C.; Moore, J. S.; Sottos, N. R.; White, S. R. Self-Healing Polymers and Composites. *Ann. Rev. Mater. Res.* **2010**, *40*, 179.

[3] Kessler, M. R.; Sottos, N. R.; White, S. R. Self-healing structural composite materials. *Comp. Part A - Appl. S.* **2003**, *34*, 743-753.

[4] Kessler, M. R. Characterization and Performance of a Self-healing Composite Material. Ph D. Thesis. University of Illinois Urbana Champaign, 2002.

[5] Patel, A. J.; Sottos, N. R.; Wetzel, E. D.; White, S. R. Autonomic healing of low-velocity impact damage in fiber-reinforced composites. *Comp. Part A - Appl. S.* **2010**, *41*, 360-368.

[6] Moll, J. L.; White, S. R.; Sottos, N. R. A Self-sealing Fiber-reinforced Composite *J. Composite Mater.* **2010**, *44*, 2573-2585.

[7] Jin, H.; Miller, G. M.; Sottos, N. R.; White, S. R. Fracture and fatigue response of a self-healing epoxy adhesive. *Polymer* **2011**, *52*, 1628-1634.

[8] McIlroy, D. A.; Blaiszik, B. J.; Caruso, M. M.; White, S. R.; Moore, J. S.; Sottos, N. R. Microencapsulation of a Reactive Liquid-Phase Amine for Self-Healing Epoxy Composites. *Macromolecules* **2010**, *43*, 1855-1859.

[9] Yuan, Y. C.; Rong, M. Z.; Zhang, M. Q.; Chen, J.; Yang, G. C.; Li, X. M. Self-Healing Polymeric Materials Using Epoxy/Mercaptan as the Healant. *Macromolecules* **2008**, *41*, 5197-5202.

[10] Yang, J.; Keller, M. W.; Moore, J. S.; White, S. R.; Sottos, N. R. Microencapsulation of Isocyanates for Self-Healing Polymers. *Macromolecules* **2008**, *41*, 9650-9655.

[11] Caruso, M. M.; Delafuente, D. A.; Ho, V.; Sottos, N. R.; Moore, J. S.; White, S. R. Solvent-Promoted Self-Healing Epoxy Materials. *Macromolecules* **2007**, *40*, 8830-8832.

[12] Cho, S. H.; Andersson, H. M.; White, S. R.; Sottos, N. R.; Braun, P. V. Polydimethylsiloxane-Based Self-Healing Materials. *Adv. Mater.* **2006**, *18*, 997-1000.

[13] Keller, M. W.; White, S. R.; Sottos, N. R. Torsion fatigue response of self-healing poly(dimethylsiloxane) elastomers. *Polymer* **2008**, *49*, 3136-3145.

[14] Kumar, A.; Stephenson, L.; Murray, J. Self-healing coatings for steel. *Prog. Org. Coat.* **2006**, *55*, 244-253.

[15] Cho, S. H.; White, S. R.; Braun, P. V. Self-Healing Polymer Coatings. *Adv. Mater.* **2009**, *21*, 645-649.

[16] Park, J.; Braun, P. Coaxial Electrospinning of Self-Healing Coatings *Adv Mater* **2010**, *22*, 496-499.

[17] Caruso, M. M.; Schelkopf, S. R.; Jackson, A. C.; Landry, A. M.; Braun, P. V.; Moore, J. S. Microcapsules containing suspensions of carbon nanotubes. *J. Mater. Chem.* **2009**, *19*, 6093.

[18] Odom, S. A.; Caruso, M. M.; Finke, A. D.; Prokup, A. M.; Ritchey, J. A.; Leonard, J. H.; White, S. R.; Sottos, N. R.; Moore, J. S. Restoration of Conductivity with TTF-TCNQ Charge-Transfer Salts. *Adv. Func. Mater.* **2010**, 1721-1727.

[19] Blaiszik, B. J.; Odom, S. A.; Caruso, M. M.; Jackson, A.; Baginska, M.; Ritchey, J. A.; Finke, A. D.; White, S. R.; Moore, J. S.; Sottos, N. R.; Braun, P. V.; Amine, K. US Patent 13/168,166, 2011.

[20] Toohey, K. S.; Sottos, N. R.; Lewis, J. A.; Moore, J. S.; White, S. R. Self-healing materials with microvascular networks. *Nat. Mater.* **2007**, *6*, 581-585.

[21] Toohey, K. S.; Hansen, C. J.; Lewis, J. A.; White, S. R.; Sottos, N. R. Delivery of Two-Part Self-Healing Chemistry via Microvascular Networks. *Adv. Func. Mater.* **2009**, *19*, 1399-1405.

[22] Hansen, C. J.; Wu, W.; Toohey, K. S.; Sottos, N. R.; White, S. R.; Lewis, J. A. Self-Healing Materials with Interpenetrating Microvascular Networks. *Adv. Mater.* **2009**, *21*, 4143-4147.

[23] Trask, R. S.; Williams, G. J.; Bond, I. P. Bioinspired self-healing of advanced composite structures using hollow glass fibres *J. R. Soc. Interface* **2007**, *4*, 363-371.

[24] Hamilton, A. R.; Sottos, N. R.; White, S. R. Self-Healing of Internal Damage in Synthetic Vascular Materials. *Advanced Materials* **2010**, *22*, 5159-5163.

[25] Chen, X.; Dam, M. A.; Ono, K.; Mal, A.; Shen, H.; Nutt, S. R.; Sheran, K.; Wudl, F. A thermally re-mendable cross-linked polymeric material. *Science* **2002**, *295*, 1698-1702.

[26] Beck, J. B.; Rowan, S. J. Multistimuli, multiresponsive metallo-supramolecular polymers *J. Am. Chem. Soc.* **2003**, *125*, 13922-13923.

[27] Cordier, P.; Tournilhac, F.; Soulie-Ziakovic, C.; Leibler, L. Self-healing and thermoreversible rubber from supramolecular assembly. *Nature* **2008**, *451*, 977-980.

[28] Hickenboth, C. R.; Moore, J. S.; White, S. R.; Sottos, N. R.; Baudry, J.; Wilson, S. R. Biasing reaction pathways with mechanical force. *Nature* **2007**, *446*, 423-427.

[29] Potisek, S. L.; Davis, D. A.; Sottos, N. R.; White, S. R.; Moore, J. S. Mechanophore-Linked Addition Polymers. *J. Am. Chem. Soc.* **2007**, *129*, 13808-13809.

[30] Davis, D. A.; Hamilton, A.; Yang, J.; Cremar, L. D.; Van Gough, D.; Potisek, S. L.; Ong, M. T.; Braun, P. V.; Martinez, T. J.; White, S. R.; Moore, J. S.; Sottos, N. R. Force-induced activation of covalent bonds in mechanoresponsive polymeric materials *Nature* **2009**, *459*, 68-72.

[31] Lee, C. K.; Davis, D. A.; White, S. R.; Moore, J. S.; Sottos, N. R.; Braun, P. V. Force-Induced Redistribution of a Chemical Equilibrium. *J. Am. Chem. Soc.* **2010**, *132*, 16107-16111.

[32] Kryger, M. J.; Ong, M. T.; Odom, S. A.; Sottos, N. R.; White, S. R.; Martinez, T. J.; Moore, J. S. Masked Cyanoacrylates Unveiled by Mechanical Force. *J. Am. Chem. Soc.* **2010**, 4558-4559.

[33] Lenhardt, J. M.; Black, A. L.; Craig, S. L. gem-Dichlorocyclopropanes as Abundant and Efficient Mechanophores in Polybutadiene Copolymers under Mechanical Stress. *J. Am. Chem. Soc.* **2009**, *131*, 10818-10819.

[34] Blaiszik, B. J.; Baginska, M.; White, S. R.; Sottos, N. R. Autonomic Recovery of Fiber/Matrix Interfacial Bond Strength in a Model Composite. *Adv. Func. Mater.* **2010**, *20*, 3547-3554.

[35] Blaiszik, B. J.; Sottos, N. R.; White, S. R. Nanocapsules for self-healing materials. *Compos. Sci. Technol.* **2008**, *68*, 978.

[36] Ishiyama, C.; Sakuma, T.; Shimojo, M.; Higo, Y. Effects of humidity on environmental stress cracking behavior in poly(methyl methacrylate). *J Polym Sci Pol Phys* **2002**, *40*, 1-9.

[37] Miller, D. C.; Gedvilas, L. M.; To, B.; Kennedy, C. E.; Kurtz, S. R. Durability of poly(methyl methacrylate) lenses used in concentrating photovoltaic modules. *Proc SPIE* **2010**, 777303.

[38] Brown, E. N.; Kessler, M. R.; Sottos, N. R.; White, S. R. In situpoly(urea-formaldehyde) microencapsulation of dicyclopentadiene. *J. Microencapsul.* **2003**, *20*, 719-730.

[39] Graf, C.; Vossen, D. L. J.; Imhof, A.; van Blaaderen, A. A General Method to Coat Colloidal Particles with Silica. *Langmuir* **2003**, *19*, 6693-6700.

[40] Fowler, C. E.; Khushalani, D.; Mann, S. Interfacial synthesis of hollow microspheres of mesostructured silica. *Chem. Comm.* **2001**, 2028-2029.

[41] Bégu, S.; Durand, R.; Lerner, D. A.; Charnay, C.; Tourné-Péteilh, C.; Devoisselle, J. M. Preparation and characterization of siliceous material using liposomes as template. *Chem. Comm.* **2003**, 640.

[42] Steinmetz, N. F.; Shah, S. N.; Barclay, J. E.; Rallapalli, G.; Lomonossoff, G. P.; Evans, D. J. Virus-Templated Silica Nanoparticles. *Small* **2009**, *5*, 813-816.

[43] Howarter, J. A.; Youngblood, J. P. Optimization of silica silanization by 3-aminopropyltriethoxysilane *Langmuir* **2006**, *22*, 11142-11147.

[44] Liu, Y.; Hsu, C.; Wang, M.; Chen, H. A novel approach of chemical functionalization on nano-scaled silica particles. *Nanotechnology* **2003**, *14*, 813-819.

[45] Cosgrove, T. In *Colloid science: theory, methods and applications* Blackwell Pub. Professional: Ames, Iowa, 2005, pp 288.

[46] Wilson, G. O.; Porter, K. A.; Weissman, H.; White, S. R.; Sottos, N. R.; Moore, J. S. Stability of Second Generation Grubbs' Alkylidenes to Primary Amines: Formation of Novel Ruthenium-Amine Complexes. *Adv. Synth. Catal.* **2009**, *351*, 1817-1825.

[47] Wilson, G. O.; Caruso, M. M.; Reimer, N. T.; White, S. R.; Sottos, N. R.; Moore, J. S. Evaluation of Ruthenium Catalysts for Ring-Opening Metathesis Polymerization-Based Self-Healing Applications. *Chem. Mater.* **2008**, *20*, 3288-3297.

[48] Dinger, M. B.; Mol, J. C. Degradation of the First-Generation Grubbs Metathesis Catalyst with Primary Alcohols, Water, and Oxygen. Formation and Catalytic Activity of Ruthenium(II) Monocarbonyl Species. *Organometallics* **2003**, *22*, 1089-1095.

[49] Rule, J. D.; Brown, E. N.; Sottos, N. R.; White, S. R.; Moore, J. S. Wax-Protected Catalyst Microspheres for Efficient Self-Healing Materials. *Adv. Mater.* **2005**, *17*, 205-208.

[50] Gibson, S. E.; Swamy, V. M. Micronencapsulation of a Metathesis Catalyst. *Adv. Synth. Catal.* **2002**, *344*, 619.

[51] Pekarek, K. J.; Jacob, J. S.; Mathiowitz, E. Double-walled polymer microspheres for controlled drug release *Nature* **1994**, *367*, 258-260.

[52] Gref, R.; Minamitake, Y.; Peracchia, M.; Trubetskoy, V.; Torchilin, V.; Langer, R. Biodegradable long-circulating polymeric nanospheres. *Science* **1994**, *263*, 1600-1603.

[53] Edlund, U.; Albertsson, A. Degradable Aliphatic Polyesters; Degradable Polymer Microspheres for Controlled Drug Delivery. *Adv. Polym. Sci.* **2002**, *157*, 67-112.

[54] Mu, L.; Feng, S. S. A novel controlled release formulation for the anticancer drug paclitaxel (Taxol®): PLGA nanoparticles containing vitamin E TPGS. *J. Controlled Release* **2003**, *86*, 33-48.

[55] Rule, J. D.; Sottos, N. R.; White, S. R. Effect of microcapsule size on the performance of self-healing polymers. *Polymer* **2007**, *48*, 3520-3529.

[56] Kirkby, E. L.; Rule, J. D.; Michaud, V. J.; Sottos, N. R.; White, S. R.; Månson, J. E. Embedded Shape-Memory Alloy Wires for Improved Performance of Self-Healing Polymers. *Adv. Func. Mater.* **2008**, *18*, 2253-2260.

[57] Caruso, M. M.; Blaiszik, B. J.; Jin, H.; Schelkopf, S. R.; Stradley, D. S.; Sottos, N. R.; White, S. R.; Moore, J. S. Robust, Double-Walled Microcapsules for Self-Healing Polymeric Materials. *ACS Appl. Mater. Interfaces* **2010**, *2*, 1195-1199.

[58] Yuan, L.; Liang, G.; Xie, J.; Li, L.; Guo, J. The permeability and stability of microencapsulated epoxy resins. *J. Mater. Sci.* **2007**, *42*, 4390-4397.

CHAPTER 2:

MODIFICATION OF CAPSULES VIA SILICA COATINGS

Parts of this chapter were previously published by the author:

Jackson, A. C.; Bartelt, J. A.; Marczewski, K.; Sottos, N. R.; Braun, P. V. Silica-Protected Micron and Sub-Micron Capsules and Particles for Self-Healing at the Microscale. *Macro. Rap. Comm.* **2010**, *31*, 82-87.

2.1 Motivation

While PUF capsules have been successful in a variety of epoxy applications, additional shell layers are sought that can improve upon the capsules' stability and functionality without requiring entirely new encapsulation methods. New applications and processing conditions are the primary driving force for this method of modifying the capsules. In particular, 1.5 μm size-scale PUF capsules [1] are known to aggregate easily and are not expected to have good stability. The lack of surface functionality limits the concentration of micron size PUF capsules that can be dispersed in epoxy. In addition, the high capsule surface area and thin shell wall is not ideal for retaining healing agent. Temperature ramps and high temperature isotherms demonstrate that ca. 100 μm PUF capsules lose a significant quantity of their contents at high temperatures [2, 3] and this is expected to be worse at smaller size-scales. Two size scales of capsules are considered for this work: micron size PUF capsules made via a sonication step and large PUF capsules [1] made without a sonication step.[2] The former are approximately 1-2 μm in diameter. The latter are larger than 20 μm in diameter where the exact size of the batch depends on the shear forces applied by stir blade during capsule preparation.

Silica coatings for capsules provide a generalized route for improving both functionality and stability. Silica chemistries are well studied, often utilize mild synthetic conditions,[4-7] are

amenable to functionalization,[8, 9] and silica is a potentially good diffusion barrier. There are a variety of ways to add a silica coating to liquid-filled capsules. These include Stöber condensation,[4, 10] fluoride catalyzed condensation,[7] and chemical vapor deposition (CVD).[12] The Stöber condensation and fluoride catalyzed methods are both solution-based reactions that require careful engineering of the capsule surface, the solvent used, the catalyst for condensation, and ionic environment. Similar to sizings used in the composites industry, functional silanes can be chemically attached to the silica coating to add polymer specific functionality to the capsules and this functionality can be used to improve the interface between the capsules and polymer matrix.[8, 9] CVD offers less strict reaction conditions, especially where the capsule surface is concerned. It also requires a fluidized bed reactor setup[12, 13] to conformally coat the capsules: without fluidization, contact points between capsules are devoid of the silica coating. This research develops the procedures to coat capsules using each silica coating method while exploring the potential improvements in functionality and stability that can be gained with a silica coating.

2.2 Surface Chemistry

Previous research has demonstrated the importance of surface charge on silica condensation. The first steps toward silica condensation are to understand PUF capsule surface functionality and to understand how to change the surface functionality. These capsules are prepared using an emulsion surface polymerization method.[1, 2] As a result, the two functionalities that are potentially present on the capsule surface are the amines in the PUF and the carboxylic acids present in the emulsifier, ethylene maleic anhydride (EMA). Work done by Blaiszik *et al.* demonstrates that a negative charge exists on the surface of these capsules above

pH 5 suggesting that EMA is the primary functional group exposed on the surface of the capsules.[1]

To change the surface chemistry, layer-by-layer coating methods can be used.[14] The most intriguing method, developed by Graf *et al.*,[5] used polyvinylpyrolidone (PVP) as a universal coating to enhance surface nucleation of silica in a Stöber condensation reaction. PUF capsules coated with PVP did not have any characteristic that could confirm the adsorption of PVP to the capsule surface. Silica and other oxides adsorbed to the capsule surface may also provide a nucleation center for silica regrowth. Electroless deposition of gold employs this strategy by growing the metal off of gold nanoparticles adsorbed on a surface.[15, 16] Chang *et al.* also used silica to seed monodisperse silica colloids.[17] Due to the slightly negative charge of PUF capsules, alumina nanoparticles, positively charged below pH 8, can be adsorbed to the capsules by electrostatic interactions and potentially act as nucleation spots. Although samples are not sufficiently consistent to obtain zeta potential measurements of the alumina modifications, SEM shows visual evidence of alumina adsorption on capsules containing dicyclopentadiene (DCPD) (**Figure 2.1**). EDAX of the capsule surface confirms that there is a large aluminum presence on the capsule surface compared to its background.

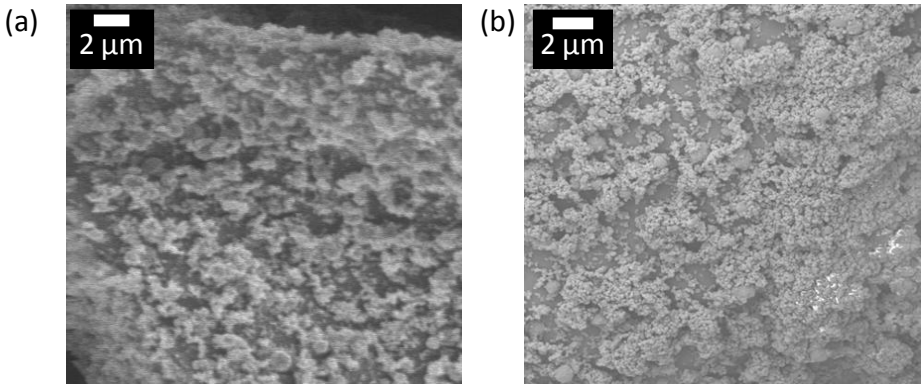

Figure 2.1. Surface of DCPD containing PUF capsules that are unmodified (a) and modified with alumina particles (b).

2.3 Silica Coating Methods

2.3.1 Stöber Condensation

The Stöber condensation chemistry is a well understood route to coating a wide variety of colloids with silica.[4] Stöber conditions require that capsules be dispersed in water, an alcohol, ammonium hydroxide, and a silica precursor, usually tetraethylorthosilicate (TEOS). The first challenge to using this method is that the alcohol solvent is a good solvent for many capsule core materials, especially dicyclopentadiene (DCPD) which is relevant for this work. Since a typical Stöber reaction requires a minimum of 4 hours to complete, capsules should not lose significant amounts of core material during that time. DCPD capsules, approximately 80 μm in diameter, lose all of their contents after 4 hours in ethanol (**Figure 2.2b**). To minimize loss, ethanol is replaced with a saturated solution of DCPD in methanol. DCPD capsules in the saturated solution remain full after 4 hours (Figure 2.2c). Despite this improvement, 80 μm capsules continued to rupture when mechanically mixed in the DCPD-methanol solution suggesting that their shell wall is weakened. PUF capsules 1.5 μm in diameter did not rupture during mechanical stirring and were used in all Stober silica condensation reactions. For the successful coating of other liquids in PUF capsules without loss of core contents, the core solvent must have a saturation concentration in methanol or ethanol.

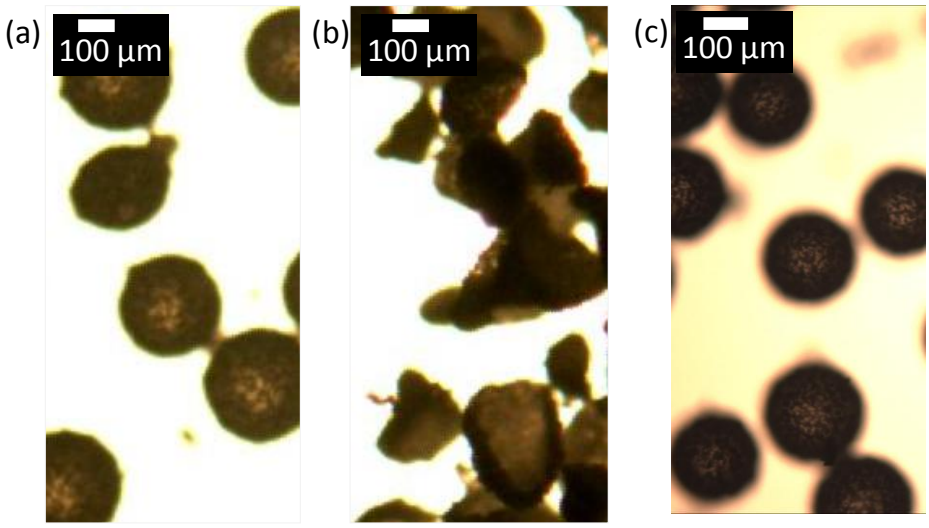

Figure 2.2. (a) Optical microscopy of PUF capsule containing DCPD. (b) Capsules soaked in ethanol for 4 hours and (c) capsules soaked in methanol/DCPD solution for 4hours.

Another challenge towards implementing the Stöber condensation chemistry is to reduce secondary nucleation produced during the reaction. Secondary nucleation occurs when silica precursor molecules react faster with themselves than they do with the capsule surface. These secondary nucleations manifest themselves as silica particles less than 200 nm in diameter (**Figure 2.3**). The particles make it difficult to purify the capsules, often resulting in gelation of the final reaction solution. In addition, the final product contains a high fraction of silica, reducing the volume of solvent that can be incorporated into a polymer matrix.

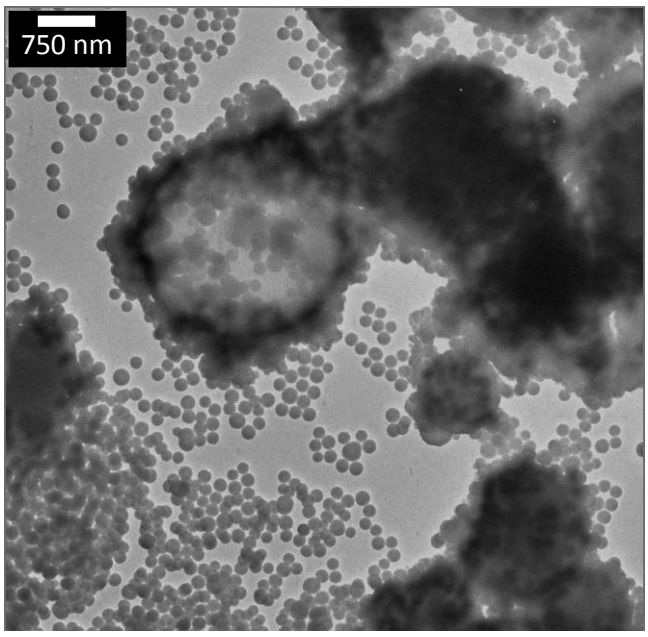

Figure 2.3. SEM of capsules produced using an unmodified Stöber procedure.

In a Stöber regrowth method, secondary nucleation can be reduced by either functionalizing the capsules with better nucleation sites or by changing reaction conditions to slow nucleation reactions in solution.[17-19] Coating the capsules with PVP or alumina to change the surface functionality of the capsules did not decrease secondary nucleations to an appreciable extent. In addition, excess reactants from the capsule synthesis procedure do not increase silica secondary nucleation in solution although EMA surfactant does form a porous core in the secondary nucleations found in samples where the capsules are not properly centrifuged. Instead, the Stöber conditions were the primary source of secondary nucleations. Here, the key factor that reduces secondary nucleation is the concentration of silica precursor in solution.[17, 19] At lower concentrations, the precursor molecules are more likely to find a capsule's surface than find other precursor molecules. Reducing precursor interactions reduces secondary nucleation. By adding the precursor to the capsule solution over an extended period of time with a syringe pump, a thick silica shell forms around the capsules without secondary nucleations.

1.5 μm capsules, coated using the Stöber method, are spherical with a rough surface (**Figure 2.4a**). Capsules are dried by filtering them and washing the sample with ethanol. The dried capsules have no aggregates and are easily broken up on a glass slide or dispersed in water. Based on TGA analysis (Figure 2.4b), they contain approximately 50% DCPD. Microtomed cross-sections of the capsules show that the silica shell produced is approximately 75 nm thick (Figure 2.4c).

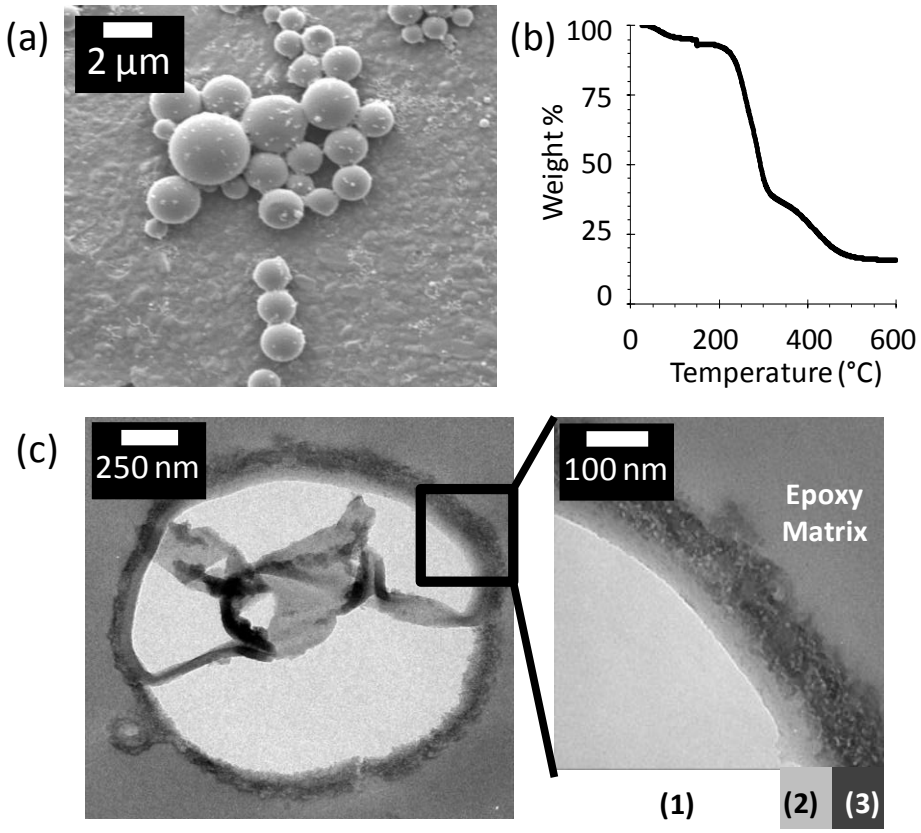

Figure 2.4. (a) SEM and (b) TGA of micron size capsules coated using the Stöber method. (c) TEM of the cross-section of the capsules as prepared using a microtoming process. The core (1) is removed during this process while the PUF (2) and silica (3) shells are observed.

There are several factors that limit the use of the Stöber process for coating other liquid-filled capsules. First, this system is optimized for DCPD and works because DCPD can form a

saturated solution in methanol. Second, only micron size capsules can be coated using this procedure. Finally, the window for good capsule dispersion in a methanol-DCPD environment is relatively small and capsules aggregate with any changes to the PUF chemistry. These problems are avoided by using the fluoride-catalyzed method and, as a result, the Stöber method is not a preferred coating method for capsules.

2.3.2 Fluoride-catalyzed Silica Condensation

Fluoride-catalyzed silica condensation is an aqueous-based chemistry that uses fluoride ions as the catalyst [7, 20] and requires a relatively well controlled ionic environment. The primary advantage of this chemistry is that healing agent loss is inherently limited since capsules are not exposed to organic solvents. Work by Bégu *et al.* show that lipid micelles can be coated with a dense layer of silica using this method.[7] In that work, tetrabutylammonium fluoride (TBAF) serves as the silica condensation catalyst while monobasic sodium phosphate maintains an appropriate ionic environment. Other work demonstrates that surface charge and ionic environment can both affect the final condensation rate at a surface.[21] For PUF capsules, monobasic sodium phosphate and either ammonium chloride or cetyl trimethylamminum bromide give the solution its appropriate ionic environment.

Capsule size is an important factor in determining the processing conditions required to make and collect a free-flowing powder of coated capsules containing healing agent. During the coating step, large capsules frequently rupture when exposed to the shear forces created by a stir blade or stir bar. By mixing the large capsules on a vortexer, the capsule contents remain intact. Filtration results in a free-flowing powder of large capsules. 1.5 μm capsules remain stable when mixed via stir blade. However, filtration results in a gel of capsules and silica. Centrifuging and then freeze drying the capsules attains a free-flowing powder.

Sonicated DCPD capsules coated with silica are spherical with an average diameter of 1.5 μm (**Figure 2.5a**). TGA and elemental analysis suggest that DCPD is retained in the coated capsules at between 55 wt.% and 70 wt.% depending on the synthesis conditions of the sample (Figure 2.5b). TGA analysis also demonstrates that the micron size capsules retain almost all of their DCPD after being stored at room temperature for 7 days, providing sufficient time to incorporate them into a self-healing polymer. Figure 5c shows a TEM image of a representative cross-section of coated capsules in epoxy prepared by microtome. The DCPD and part of the polyureaformaldehyde (PUF) shell wall are removed during the microtoming process. The PUF shell wall is 20-25nm thick and the silica shell wall is 20-40nm thick. Based on geometry calculations, an ideal capsule should contain 90 wt.% DCPD. Similar results are obtained for capsules containing ethyl phenyl acetate (EPA) and dibutyl phthalate (DBP).

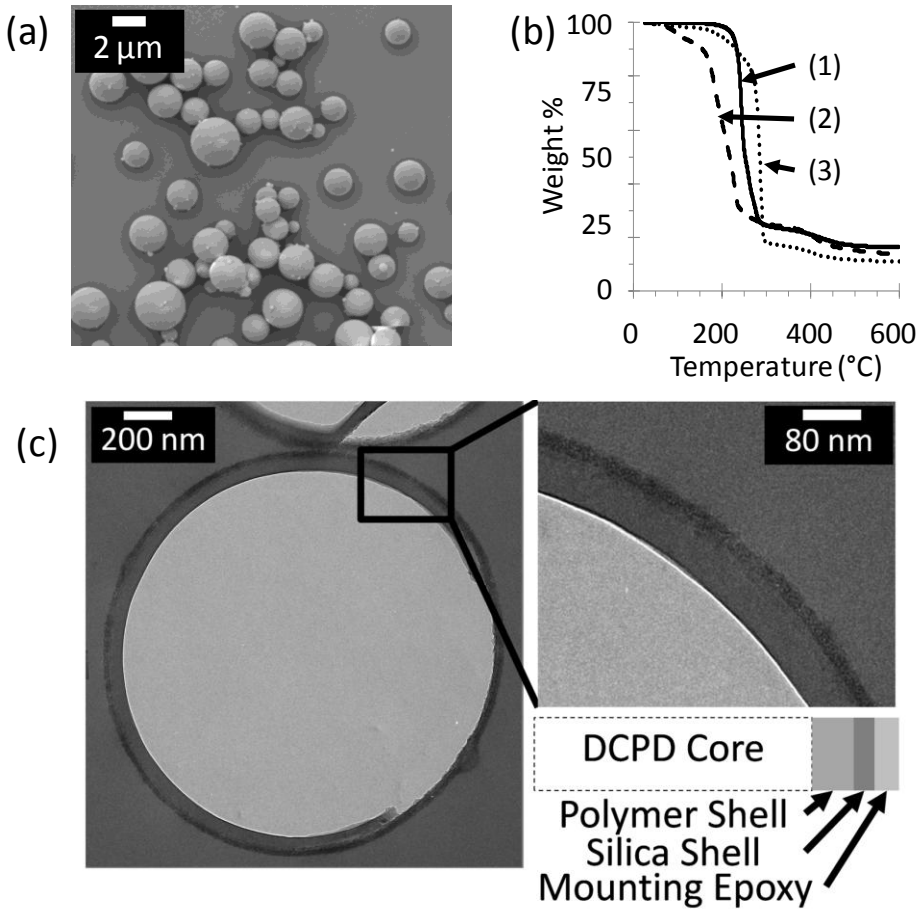

Figure 2.5. (a) SEM of DCPD-filled, micron size capsules coated using the Flouride-catalyzed condensation method. (b) TGA traces of micron size coated capsules containing DCPD (1), EPA (2), and DBP (3). (c) TEM shows a representative cross-section of the DCPD-containing capsules as prepared using a microtoming process.

As mentioned, silica chemistries are relatively simple and chemical functionalization can be added without changing the reaction conditions. This is important because the silica coating can serve as an initiator for polymer brush layers or other similar functionalities which are known to decrease the attraction between colloids in solution.[22] Aminopropyltrimethoxy silicate (APTES) reacts with the shell wall when added following the standard silica coating method. Zeta potential measurements demonstrate that functionalized capsules are more positively charged than the coated capsules without functionalization (**Figure 2.6**). At low pH, a capsule

functionalized with a dense coverage of amines should have a positive zeta potential. Because the zeta potential is negative for these samples across all pH, it is likely that the capsules do not have a high density of functionalization molecules on their surface.

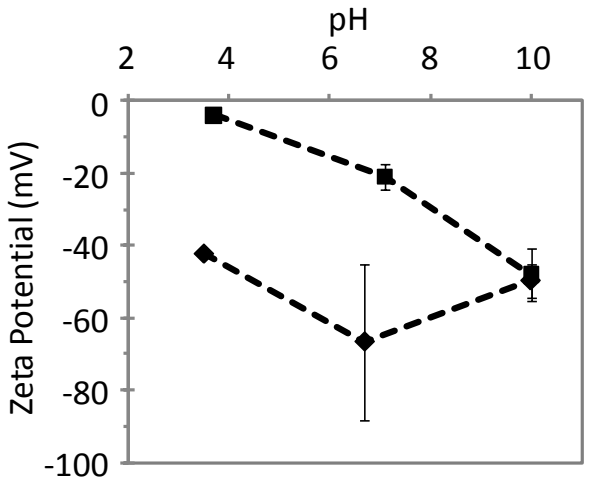

Figure 2.6. Zeta potential of silica coated capsules and amine functionalized silica coated capsules over a range of pH values.

Large coated capsules range in size depending on the initial batch of capsules used in the coating procedure. Similar to sonicated capsules, microtomed cross-sections of the large coated capsules show a conformal silica shell, approximately 20-40nm thick surrounding the PUF capsule (**Figure 2.7**). The large capsules lose less than 5% of their contents during the coating procedure. The procedure has been demonstrated for ca. 75 μm capsules containing DCPD and dibutyl phthalate (DBP).

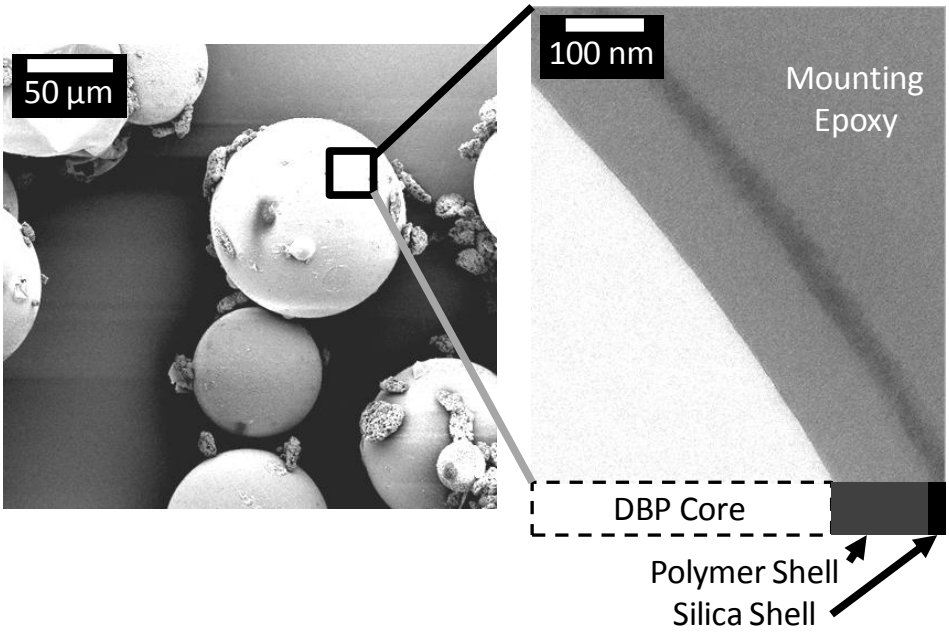

Figure 2.7. SEM (left) of silica coated DBP capsules. TEM (right) shows a representative cross-section of 75 µm DBP-containing capsules as prepared using a microtoming process.

2.3.3 Chemical Vapor Deposition

Chemical vapor deposition is an alternative method to capsule coating that does not require solution processing conditions. This is beneficial for capsules with relatively weak shell walls that cannot survive typical mixing conditions. For capsules, a fluidized bed reactor (FBR) is necessary to achieve full surface coverage. This technology has been used to coat a variety of other colloids.[12, 13] A successful FBR system disperses airflow through a sample of capsules, resulting in fluidization of the capsules and fully exposing capsules to reactants in the gas stream. The gas stream is bubbled through silicon tetrachloride or water in a series of cycles that allow silica growth at room temperature.[11] The primary limitation for this method is the size of the capsules. Van der Waals forces between sonicated colloids are too strong for the forces of fluidization to break them apart. As a result, this method is limited to larger capsules. 75 µm

DCPD capsules coated via FBR-CVD are shown in **Figure 2.8**. They are conformally coated and lose less than 5% of their contents during work-up.

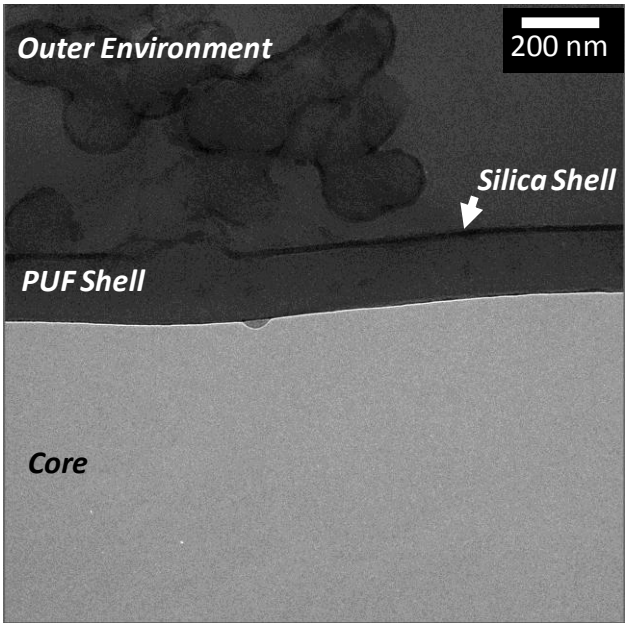

Figure 2.8. TEM of a representative cross-section of 75 μm DCPD-containing capsules as prepared using a microtoming process.

2.4 Capsule Stability

One of the potential advantages of silica coated capsules is improved capsule stability in adverse environments. Capsule stability, in particular stability to loss of core contents by diffusion across the shell wall, is important for processing steps and applications where capsule are exposed to extreme environments such as high temperatures or solvents. Past research has focused primarily on the thermal stability of capsules. Temperature ramps from room temperature to 600 °C give good qualitative evidence that the core material is encapsulated. The temperature at which weight loss begins is an important indicator for how stable the capsules are: capsules that begin to lose contents at higher temperatures are considered more stable.[3, 23]

Quantitative measurement of the thermal stability is attained in tests where the capsules weight is monitored in a high temperature, 150 °C, environment.[3, 23] Capsules that lose less mass over a two hour period are considered more stable.

Thermal stability, however, is insufficient alone to quantify the effects of a silica coating on capsule coating. In this section, several other factors are studied to help understand the stability of PUF capsules and make a better informed conclusion on effects of silica coatings on capsule stability. Capsule size, core contents and capsule washing are all important parameters that affect capsule stability. These factors are considered under a variety of new stability tests that more appropriately quantify stability for the environments to which the capsules are typically exposed than the previously used thermal stability tests. Under a variety of temperatures, the diffusion coefficient of core solvents in PUF is found and extrapolated to room temperature to make predictions on room temperature storage. Capsules are also exposed to high temperatures in an epoxy matrix and solvents to better understand how they behave during use and under extreme processing conditions.

2.4.1 Modeling the Diffusion Coefficient of Solvents in a Capsule Shell

The diffusion coefficient of solvents in PUF is calculated using simplified models to better compare stability across various samples and extrapolate high temperature stability to room temperature stability. Solvent stability presents the simplest case for modeling solvent loss in capsules. In this case, it is assumed that capsules are dispersed in an infinitely large body of solvent and instantaneous perfect mixing occurs inside and outside of the capsule. In addition, flux is assumed to be constant across the shell wall (**Figure 2.9a**). Using these assumptions, Fick's first law is simplified according to Equation 2.1 where the flux, J, is a function of the

diffusion coefficient (D), core concentration (C_{core}), solvent concentration (C_{Solv}), capsule volume (V) and shell wall thickness (w).

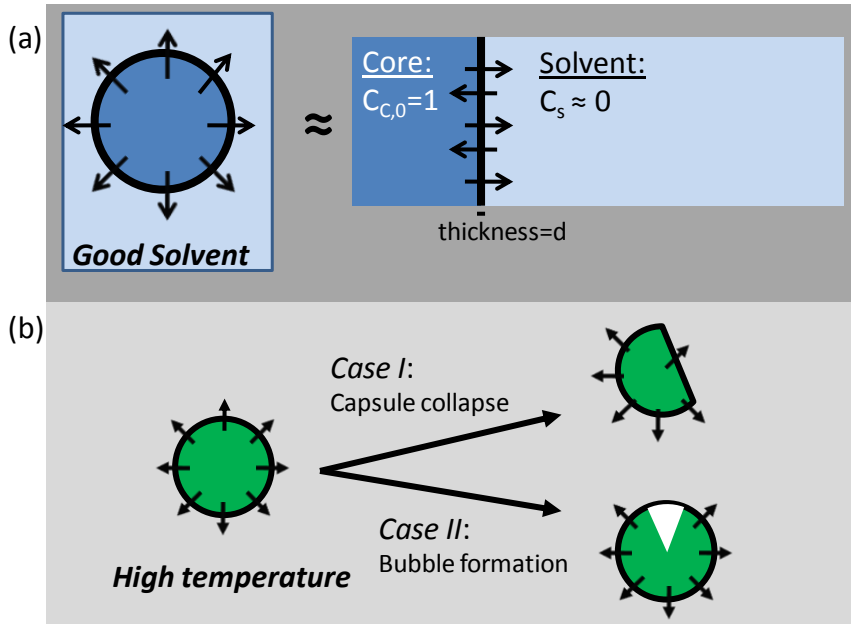

Figure 2.9. Schematic for assumptions made to calculate the diffusion coefficient for capsules in (a) solvent and (b) high temperature. For solvent stability, the core concentration (C) at time t=0 sec is 1 while the concentration of core material in the solvent (C_S) is approximated as 0 for all times since the capsules concentration is dilute.

$$J = -D\frac{d\Phi}{dx} = -D\frac{\Delta c}{V \cdot \Delta x} = -D\frac{(C_{Core} - C_{Solv})}{V \cdot w} \qquad \text{Equation 2.1}$$

Given the definition of Flux in Equation 2.2, Equation 2.1 and Equation 2.2 can be simplified to find the fraction of contents left in the capsule (c/c_0) as a function of diffusion coefficient, time (t) and capsule radius (r) (Equation 2.3).

$$J = \frac{\Delta C_{Core}}{\Delta t \cdot A} \qquad \text{Equation 2.2}$$

$$\frac{c}{c_0} = e^{-3Dt/wr} \qquad \text{Equation 2.3}$$

During thermal stability experiments, solvent from the surrounding environment does not replace the core contents. Instead, two limiting cases are possible. If the shell wall is weak, the capsule collapses as its contents are lost and the area through which solvent can diffuse remains constant. Assuming changes in pressure are negligible, the capsule contents within the capsule, $c/c_{0,}$ are linearly related to D, t, and r (Equation 2.4). If the shell wall is strong and outside air replaces lost contents, the surface area of shell in contact with the core material changes. Although physically impossible, if the air forms a bubble shaped like a cone, the capsule contents are related to D, t, and r as described in Equation 2.3. The capsule collapse case forms a lower bound while the bubble formation case forms an upper bound for expected thermal stability behavior. Over small times, Equation 2.4 serves as a good approximation to find the diffusion coefficient during high temperature isotherms.

$$\frac{c}{c_0} = 1 - 3Dt/wr \qquad \text{Equation 2.4}$$

2.4.2 Thermal Stability

Temperature ramps from room temperature to 600 °C are a good first approximation of capsule quality. The solvent core typically plays the most important role in affecting mass loss during a temperature ramp. The stability of capsules containing DCPD, DBP, and EPA is especially relevant in this work. For capsules made using a 1200 rpm stir rate, DBP capsules

(100 μm in diameter) begin to lose their contents at 200 °C while DCPD (120 μm in diameter) and EPA (70 μm in diameter) capsules lose their contents at lower temperatures, closer to 100 °C (**Figure 2.10**). Temperature ramps for 120 μm DCPD capsules coated using the fluoride-catalyzed silica condensation method show no differences compared to uncoated capsules. This is not surprising, however, since the silica shell wall (20-50 nm thick) is only a small fraction of the full shell wall (approximately 200 nm thick). In addition, although defects in the silica shell could not be observed via microscopy, defects cannot be ruled out.

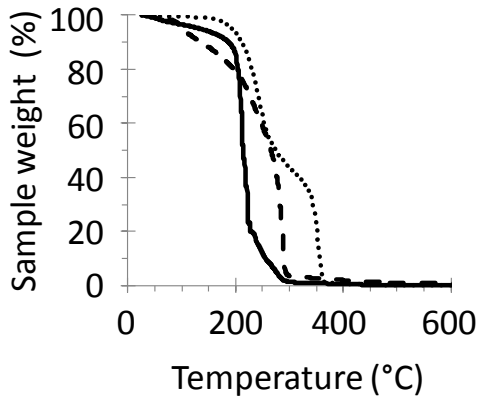

Figure 2.10. Temperature ramps for 70 μm EPA (dashed line), 100 μm DBP (dotted line), and 120 μm DCPD (solid line) capsules made using a 1200 rpm stir rate.

Due to the thinner PUF shell, the silica coating is expected to be more effective for sonicated capsules. However, silica coated, sonicated capsules once again have similar TGA traces to uncoated, sonicated capsules (**Figure 2.11a**). The only significant difference between the uncoated and coated capsules is the quantity of material left at 600 °C which corresponds to the silica content in the capsules. Similar to the large capsules, the encapsulated solvent plays the more important role in affecting mass loss during a temperature ramp. Sonicated EPA and DBP

capsules begin to lose their contents at similar temperatures to their large counterparts but silica-coated, sonicated DCPD capsules do not lose their contents until 200 °C (Figure 2.11b).

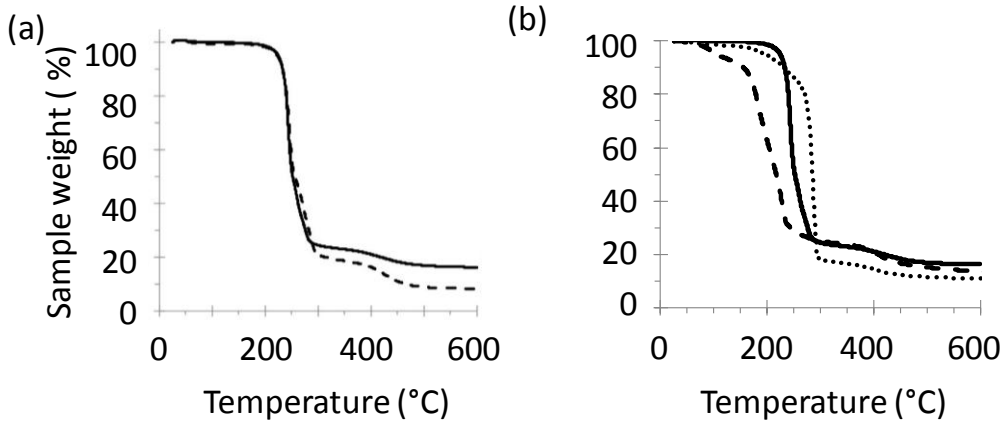

Figure 2.11. (a) Temperature ramps for coated (solid line) and uncoated (dashed line) sonicated DCPD capsules. (b) Temperature ramps for sonicated EPA (dashed line), DBP (dotted line) and DCPD (solid line) capsules. The average capsule diameter for these samples is 70 μm for EPA capsules, 100 μm for DCPD capsules and 120 μm for DBP capsules.

Isotherms at high temperatures are useful for determining capsule storage stability under accelerated conditions. For ca. 100 μm capsules, it is evident that the capsule work-up conditions affect stability more than the silica-coating method. Specifically, capsules washed with ethanol are significantly more stable than capsules washed with water only (**Figure 2.12a**). Mass loss from capsules washed with water is similar to the mass loss from capsules prepared by Kessler.[3] Consistency of capsule work-up conditions is important for quantifying capsule stability and, under the same work-up conditions, no improvements are observed between uncoated and coated capsules. 120 μm DCPD capsules coated using the fluoride-catalyzed silica condensation chemistry perform similarly to capsules washed in ethanol but DCPD capsules coated using the FBR-CVD method do not perform nearly as well (Figure 2.12b).

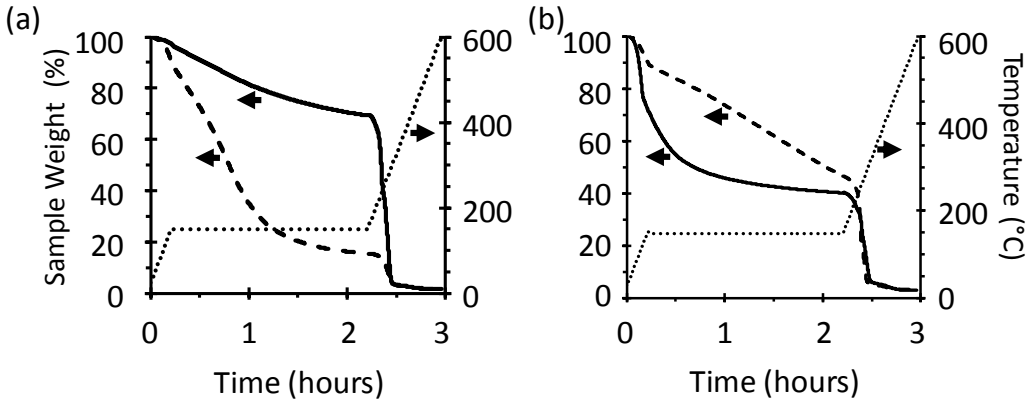

Figure 2.12. (a) 150 °C isotherms for 100 μm DCPD uncoated capsules rinsed with water (dashed line) or ethanol (solid line). (b) 150 °C isotherms for 100 μm DCPD capsules coated using either the fluoride-catalyzed silica condensation chemistry (dashed line) or using the FBR-CVD method (solid line). Dotted lines correspond to the temperature profiles of the TGA runs.

Unexpectedly, sonicated capsules are more stable than large capsules based on 150 °C isotherm experiments (**Figure 2.13**). As discussed earlier however, these capsules contain 50-70 wt% DCPD when geometry calculations suggest that they should contain closer to 90 wt% DCPD. In addition, the ratio of the sonicated capsule shell thickness to its radius, approximately 0.067, is significantly higher than the ratio for large capsules, 0.005. This is particularly interesting because if content loss is driven by pressure changes within the capsules, capsule stability should change with the ratio of capsule thickness to radius. Imaging of capsules subjected to high temperatures suggests that the core material does undergo a pressure change and that this pressure change is enough to increase the capsule radius for large capsules. It is unclear, however, how this should affect stability. A simple argument may also be made that sonicated capsules aggregate at higher temperatures making the diffusion of DCPD out of the mass of capsules slower than the diffusion of DCPD out of a mass of larger capsules. Although temperature isotherms were measured up to 210 °C for coated and uncoated sonicated capsules, PUF begins to degrade at 150 °C making this data purely academic.

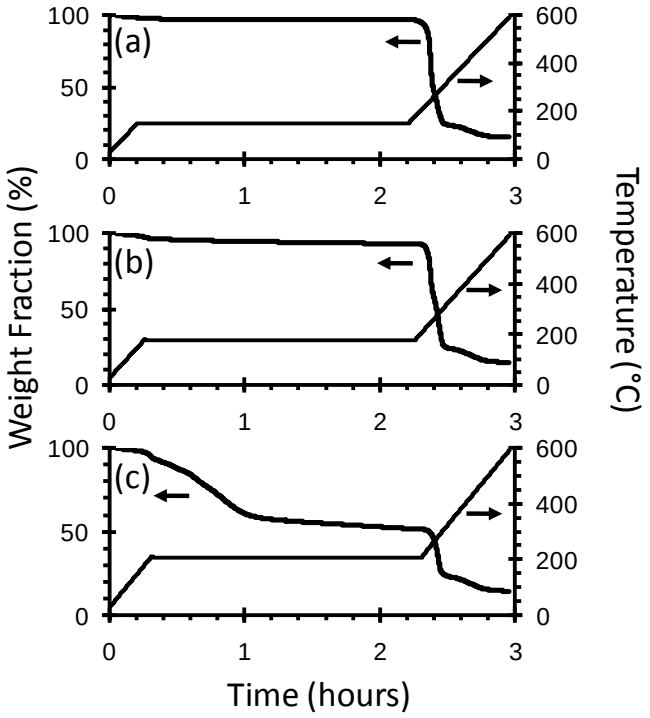

Figure 2.13. High temperature isotherms at (a) 150 °C, (b) 180 °C, and (c) 210 °C of DCPD-filled PUF capsules coated with silica using the fluoride-catalyzed silica condensation chemistry.

Capsules rarely see high temperature exposure during storage and, as a result, the diffusion constant of core material in PUF is extrapolated to room temperature to better understand stability. At 60 °C, DCPD loss from uncoated and coated PUF capsules is still similar and the more important factor for stability at 60 °C is still the capsule preparation (**Figure 2.14)**. Instead, to understand stability at lower temperatures, research focused on the core material. (**Figure 2.15**). Between EPA and DBP, solvents with similar molecular structure, DBP is more stable at all temperatures. Assuming an Arrehnius dependence on temperature, the diffusion coefficient of DBP in PUF at room temperature is calculated to be $10^{-14.8}$ cm^2/sec while the diffusion coefficient for EPA is calculated to be $10^{-12.7}$ cm^2/sec. These diffusion coefficients correspond to loss of 50% of the capsule's healing agent over 140 days and over 1 day

respectively. This does not agree with the capsule storage stability found in a lab setting. Specifically, EPA capsules retain a significant quantity of their contents at room temperature over 1 day. This is potentially a result of saturation of EPA in room temperature air that limits evaporation of EPA from the capsule surface. Without evaporation, the solvent concentration gradient across the capsule decreases and no further solvent leaks.

It is important to note that at low temperatures, DBP capsule stability, in addition to the stability of other capsules, may be limited by solvent evaporation as opposed to solvent diffusion across the capsule shell wall. During 50 °C isotherm experiments, weight loss from a sample of DBP liquid is similar in magnitude to the weight loss from DBP capsules. Weight loss at higher temperatures is greater for DBP liquid than DBP capsules confirming that weight loss is limited by diffusion at those temperatures. Indeed, DBP capsules, and other capsules, tend to aggregate after a week of storage as solvent on the capsule surface initiates capillary forces between capsules.

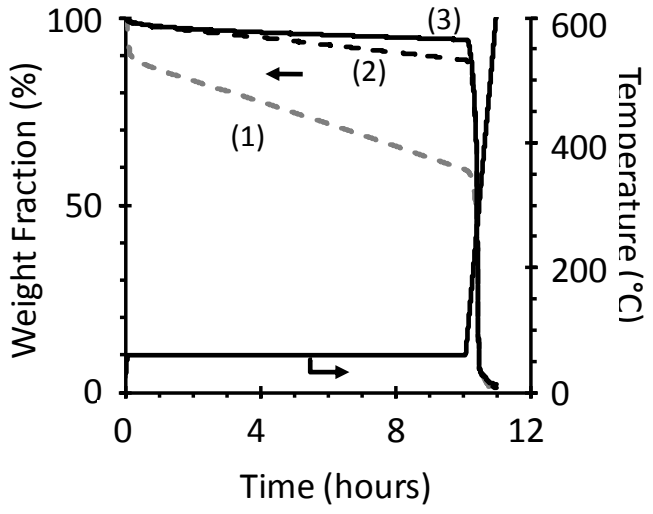

Figure 2.14. 60 °C Isotherms for 70 μm DCPD capsules washed with water (1), washed with ethanol (2) and coated with silica (3).

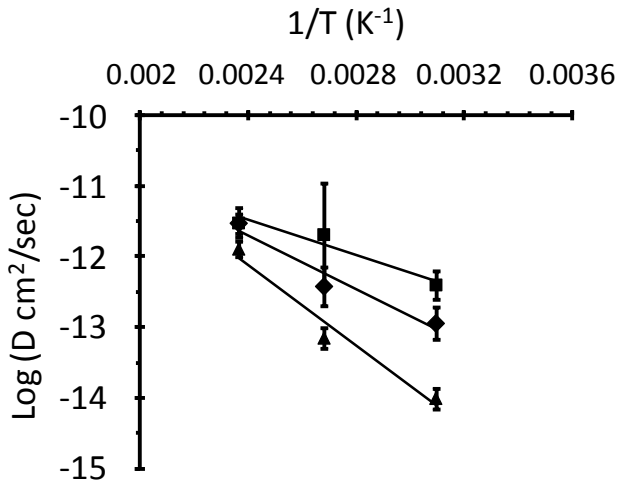

Figure 2.15. Inverse temperature vs. the log of the diffusion coefficient for 70 μm EPA capsules (squares), 100 μm DCPD capsules (diamonds), and 120 μm DBP capsules (triangles). All capsules are washed with ethanol. The shell thickness is approximated as 200 nm. Trendlines shown.

An unexpected result from the isothermal experiments is that the stability of DCPD capsules is consistently better than the stability of EPA capsules. This is interesting because DCPD has a lower boiling point, higher vapor pressure at 20 °C, and smaller molecular weight than EPA. While oligomerization of the DCPD molecules via a Diels-Alder reaction can increase the volatility of DCPD, this is unlikely below 100 °C over short times.[24] Instead this highlights the importance of the interaction between solvent molecules and the capsule shell wall.

Exposure of capsules to high temperatures is more likely to occur when the capsules are in a polymer matrix. Micro CT images of 80 μm uncoated DCPD capsules in epoxy show the effects of high temperature exposure for various times (**Figure 2.16**) at 80 °C. Bubbles form in the capsules very quickly, within 2 days, but remain the same size over a week. The plateau corresponds to approximately 6% volume loss. Given the thermal expansion for a typical liquid,

gasoline for example, is approximately 10^{-3} K^{-1}, the volume loss is consistent with the volume expansion of a liquid from 25 °C to 80 °C. It is hypothesized that the temperature increase in the sample increases pressure within the capsules driving diffusion of the solvent into the epoxy matrix. Upon reduction of the temperature from 80 °C to room temperature, the solvent contracts back to its original volume leaving bubbles corresponding to solvent lost in the polymer matrix. No further analysis was done to compare uncoated capsules to silica coated capsules since short-term DCPD loss is more dependent on volume expansion of the solvent rather than diffusion across the shell wall.

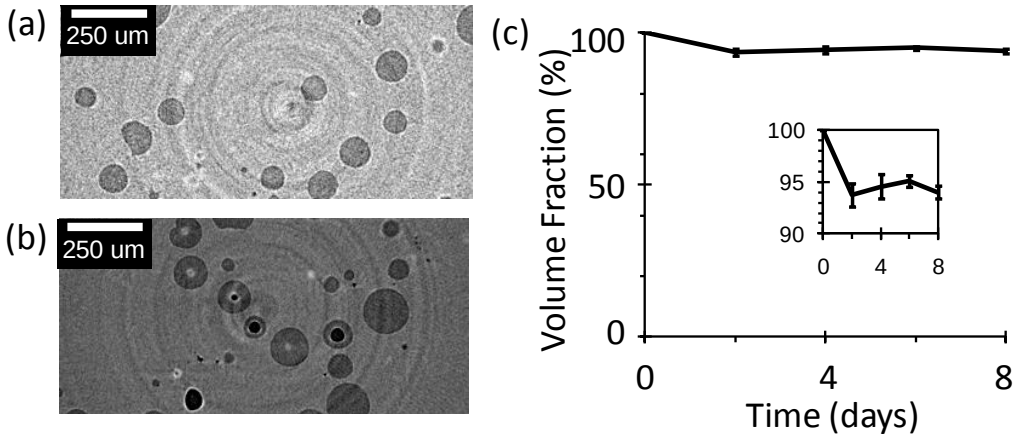

Figure 2.16. Slices of a reconstructed CT scan of 10 wt% DCPD capsules in epoxy after (a) 0 days and (b) 8 days at 80 °C. Average weight loss over time as calculated from the geometry of capsules scanned by micro CT. Capsules have an average diameter of 140 μm.

2.4.3 Solvent Stability

Solvent stability is especially important for self-healing materials made by solvent casting a thermoplastic polymer matrix. In proof of concept experiments, 30 μm chlorobenzene capsules consistently lost their contents after approximately 4 hours in ethanol corresponding to a

diffusion constant of approximately 10^{-12} cm^2/sec (**Figure 2.17**). This is relatively low compared to other solvents in polymer but similar to the diffusion coefficient calculated for DCPD capsules in thermal experiments (**Table 2.1**). Solvent stability of DCPD capsules could not be quantified as a result of a number of factors including inaccurate measurement of the initial DCPD content in the capsules and loss of the standard due to evaporation.

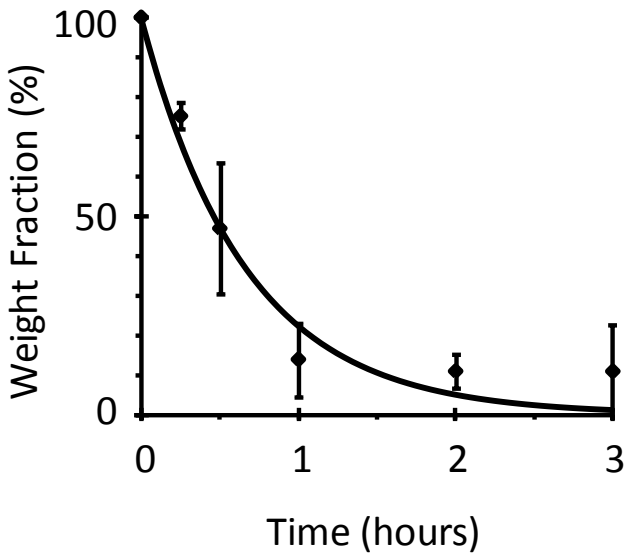

Figure 2.17. Weight loss from chlorobenzene capsules in ethanol as a function of time. Capsules have an average diameter of 30 μm and a shell wall thickness of 130 nm as measured by SEM.

Solvent	Polymer	Diffusion Coefficient (cm^2/sec)	Reference
DCPD	PUF	10^{-13} at 50 C	Thermal Stability
Chlorobenzene	PUF	10^{-12} at RT, in ethanol	Solvent Stability
Water	PVC	10^{-8} at RT	[25]
Propane	Cellulose nitrate	10^{-11} at RT	[25]

Table 2.1. Diffusion coefficients of various solvents in polymers.

Similar to thermal stability experiments, the core material is more important than the silica coating. As discussed in chapter 5, DBP and EPA capsules are important for thermoplastic self-healing of PMMA and, as a result, should be stable to the solvent casting techniques used to manufacture the self-healing components. One important problem with this system is that visual observations suggest that large EPA capsules, 70 μm in diameter, lose all of their contents during the processing of the films. Indeed, qualitatively, EPA capsules lose a significant portion of their contents when exposed to anisole and heated at 90 °C for 1 hour (**Figure 2.18a**) as measured by GC. DBP capsules, 100 μm in diameter, however, retain all of their contents under the same conditions (Figure 2.18b). The trend is similar for 1.5 μm diameter capsules (Figure 2.18c,d). This is an important factor for choosing DBP as a healing agent as opposed to EPA for thermoplastic self-healing of PMMA films.

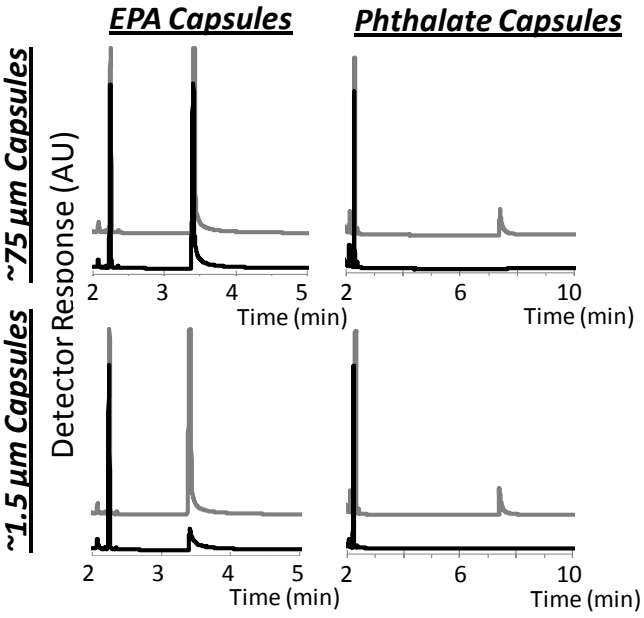

Figure 2.18. GC traces of filtered solution from DBP capsules or EPA capsules dispersed in anisole (1 wt.%) with a DCPD standard at 90°C for 1 hour (black lines). Controls of unencapsulated solvent dispersed in anisole (1 wt.%) with a DCPD standard are shown for qualitative comparison (gray lines).

2.5 Conclusions

Silica chemistries are useful for applying an additional functional layer to PUF capsules. Stöber chemistry, fluoride-catalyzed chemistry, and chemical vapor deposition techniques coat capsules with 20 – 50 nm of silica. The Stöber chemistry successfully coats micron size capsules but damages larger capsules. The CVD method successfully coats large capsules but sonicated, ca 1.5 μm, capsules cannot be dried effectively to be introduced into the FBR setup with aggregation. Aggregates lead to an incomplete coating of the capsules. The fluoride-catalyzed chemistry condenses silica onto both micron size capsules and larger capsules successfully and is a promising generalized method to coat a variety of PUF capsules with a functionalizable surface. The most important result for this coating process is that coated micron size capsules dry to a powder of individual capsules without aggregates, something that uncoated micron size capsules cannot do.

The silica shell is also expected to add an extra diffusion barrier around capsules. However, silica coated capsules do not consistently retain more contents than their uncoated counterparts. Improvements in stability can more easily be obtained by changing the capsule drying procedures and the type of core material used. DCPD capsules rinsed in ethanol show remarkably improved thermal stability than those rinsed with water. More importantly, both thermal and solvent stability improve when increasing the molecular size of the solvent used. Relevant to epoxy applications, capsules only lose 6 vol% over 24 hours at 80 °C and no further loss occurs after 1 week. This weight loss corresponds to a pressure increase in the capsule at high temperature due to volume expansion. Relevant to solvent casting applications, capsules containing DBP retain a significant portion of their contents in anisole after 1 hour at 90 °C

whereas capsules containing EPA lose a significant portion of their contents under similar conditions.

2.6 Experimental

2.6.1 Materials

Ammonium chloride was purchased from sigma. Monobasic sodium phosphate and sodium chloride were purchased from fisher. Brij 97, Resorcinol, urea, dibutylphthalate (DBP), ethyl phenyl acetate (EPA), formaldehyde solution, tetrabutyl ammonium fluoride (TBAF), ammonium chloride, glycidoxypropyltrimethoxy silane (GLYMO), and tetraethylorthosilicate (TEOS) were purchased from sigma-aldrich. Formaldehyde was purchased as a 37.5 wt.% solution and TBAF was purchased as a 75 wt.% solution in water. For all experiments, 1 mL TBAF was diluted with 100 mL Millipore water. Ethylene maleic anhydride (EMA) surfactant was donated by vertellus (chemical name ZeMac). For all experiments, a 2.5 wt.% solution of EMA in water was made and used. Methyltriethoxy silane (MTMS), cetyltrimethylammonium bromide (CTAB), dicyclopentadiene (DCPD), and anisole were purchased from Acros. Aminopropyltriethoxy silane (APTES) and silicon tetrachloride was purchased from Gelest.

2.6.2 Capsule Manufacture

Capsules were fabricated using the emulsion surface polymerization methods described previously.[1, 2] Two sizes were considered in this work: small capsules (1.5 μm in diameter) and large capsules (approximately 75 μm in diameter). Briefly, ammonium chloride, resorcinol, urea and EMA surfactant were dissolved into water and mixed under mechanical stirring. A hydrophobic solvent, DBP, EPA, or DCPD was added to the water phase and emulsified.

Emulsification for large capsules was accomplished using a stir blade setup between 600 rpm and 1500rpm while emulsification for micron size capsules was accomplished using a stir blade setup at 900 rpm. For micron size capsules, sonication was employed to decrease the emulsion droplets' size. Formaldehyde was then added, starting the reaction. The reaction temperature was increased to 55 °C at 60 °C/min and held at 55 °C for 4 hours. Large capsules (75 μm) were filtered to remove excess reactants while small (1 μm) capsules were centrifuged to remove reactants.

2.6.3 Stöber Condensation

The Stöber condensation method was only used with 1.5 μm DCPD capsules. A schematic of the setup used is shown in **Figure 2.19** and is based on work by Giesche.[18] Three solutions were prepared as described in **Table 2.2**. Solution C was mixed with 20 mL of sonicated capsules after centrifugation of the sample (4500 rpm, 20 minutes). This solution was stirred using a mixer blade in a reaction vessel at 600rpm. Solution A and Solution B were added to 60 mL syringes and pumped into solution C at 0.022 mL/min. If a functionalization was desired, the epoxide functionalization GLYMO for example, at 0.9 mL or the silane was added after 24 hours. The reaction continued for another 12 hours after the addition of the functionalization silane. The final sample was filtered and washed with ethanol only.

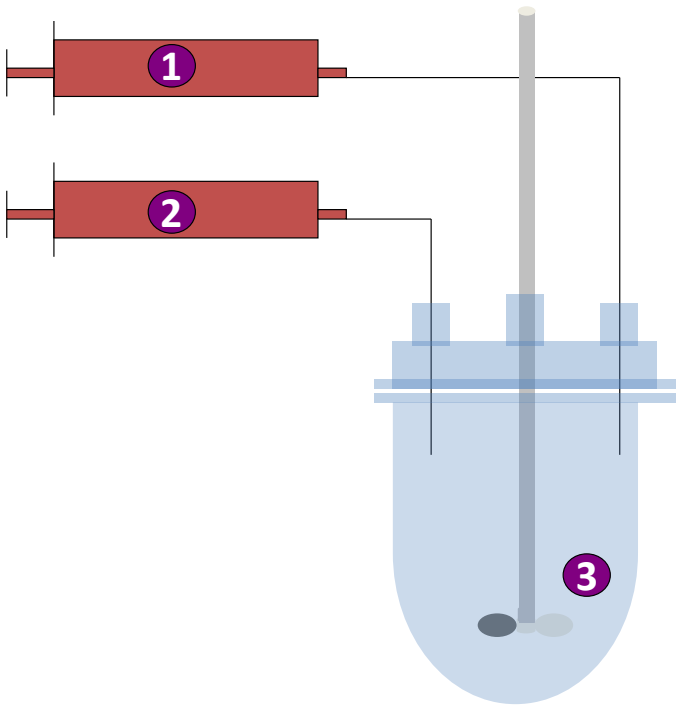

Figure 2.19. Schematic of the Stöber condensation reaction setup. Two solutions, one containing solvent and catalyst (1) and the other containing solvent and silica precursor (2) are injected into a flask containing solvent, catalyst and capsules (3). The solution in the flask is stirred at 600 rpm.

Solution	Saturated solution of DCPD in methanol (mL)	Water (mL)	Ammonium hydroxide (mL)	TMOS
Solution A	20	0.5	1.9	0
Solution B	20	0	0	0.3
Solution C	30	0.4	1.4	0

Table 2.2. Quantities of reactants added to the solutions required for Stöber silica condensation on capsules.

2.6.4 Fluoride-catalyzed Condensation

Sonicated capsules were coated with silica by first removing excess reactants through centrifugation (2 times at 4500 rpm for 20 minutes). Monobasic sodium hydroxide (0.2 g),

Ammonia chloride (0.05 g) and dilute TBAF solution (12 mL) was mixed in water (20 mL). Capsules (~8 % w/w in 40 mL of water) were mixed into this solution and stirred using an impeller blade at 500 rpm. Finally, TEOS (1 mL) was added and the reaction was stirred for 24 hours. Functionalization (optional, APTES or MPTMS, 0.1 mL) was added and the reaction allowed to continue for another 24 hours. The coated capsules were first centrifuged, and then freeze dried for 3 days.

To coat large capsules, a solution was prepared with CTAB (0.05 g), Monobasic sodium phosphoric acid (0.1 g), TBAF solution (6 mL), millipore water (20 mL), and capsules (0.7 g). This solution was vortexed on low for 5 minutes before adding TEOS (0.5g). The reaction continued under low vortexing for 24 hours. The capsules were finally filtered and washed with ethanol.

2.6.5 FBR-CVD

FBR-CVD was used to coat only large capsules, 50-300 μm. A typical CVD setup is shown in **Figure 2.20**. The setup allows Nitrogen, water rich nitrogen, and precursor (silicon tetrachloride) rich nitrogen to flow through a 2.54 cm diameter frit containing capsules. The initial nitrogen flow rate was increased until fluidization occurred, usually 25 cc/sec. To begin the CVD step, nitrogen flow was turned on for 30 seconds followed by flow of water rich nitrogen for 2 minutes. Subsequently, a full cycle was completed with each reactant gas stream run through the FBR as described in **Table 2.3**. For this work, 3 cycles were completed.

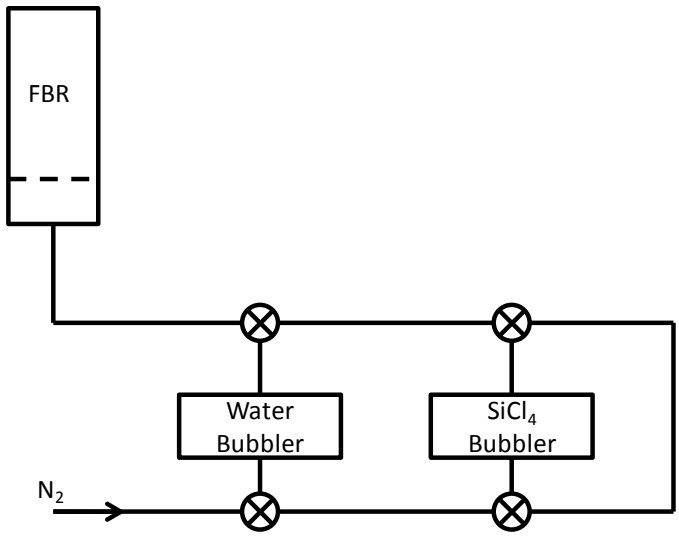

Figure 2.20. Schematic of FBR-CVD setup.

Step	Nitrogen (sec)	Water-rich Nitrogen (sec)	Precursor-rich Nitrogen (sec)
Step 1	30	0	0
Step 2	0	30	0
Step 3	30	0	0
Step 4	0	0	30
Step 5	30	0	0

Table 2.3. Steps in 1 cycle for the FBR-CVD setup.

2.6.6 Capsule Analysis

DCPD capsules were analyzed as follows. Shell morphology was determined by SEM (Philips XL30 ESEM-FEG) and TEM (Philips CM200). The shell wall was analyzed more closely by sectioning the samples via a microtome process followed by TEM analysis. Fill content of the capsules was determined using thermal gravimetric analysis (TGA) and elemental analysis. TGA was performed using a Mettler-Toledo TGA 851e under nitrogen atmosphere and

a heating rate of 10 °C min^{-1}. DCPD content was calculated by comparing the weight loss from PUF made without solvent to weight loss from capsules. The shoulders at 200 °C and 400 °C are indicative of the quantity of DCPD contained in the capsules (**Figure 2.21**). Elemental Analysis was performed on a CE440 by Exeter Analytical. The percent carbon (W_C), hydrogen (W_H), and nitrogen (W_N) were obtained from this method and plugged into **Equation 2.5** and **Equation 2.6** to find the percent PUF (W_{PUF}) and DCPD (W_{DCPD}). This equation has been derived previously [1, 3] and is based on the amount of carbon, hydrogen, and nitrogen in polyureaformaldehyde (PUF) and DCPD.

$$W_{PUF} = 4.009 \times W_N \qquad \text{Equation 2.5}$$

$$W_{DCPD} = 1.101 \times W_C - 0.5895 \times W_{PUF} \qquad \text{Equation 2.6}$$

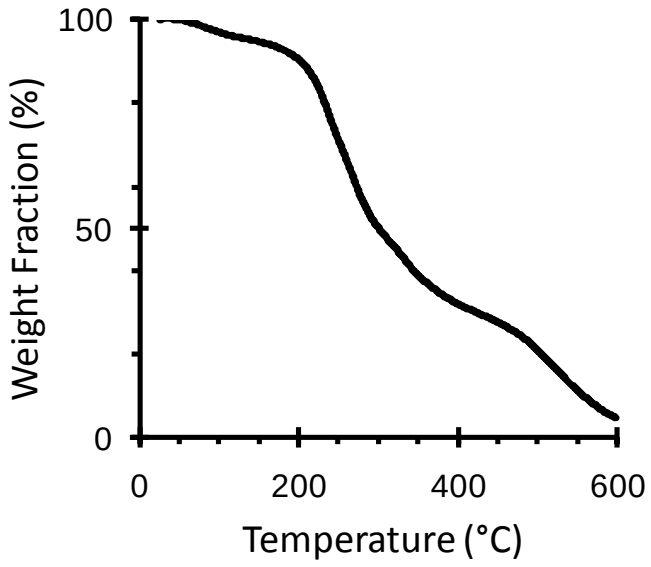

Figure 2.21. Degradation of PUF as measured by TGA.

Micro CT scans were taken on an XRadia MicroXCT-200. The weight loss from capsules was determined by measuring the diameter of bubbles in the capsules and the diameter of the respective capsules. The ratio of the cubes of the diameters was taken to be the volume loss from the capsules.

Solvent stability of capsules was tested by dispersing capsules in solvent with a standard. Chlorobenzene capsules were dispersed in ethanol with a DCPD standard. DCPD capsules were dispersed in ethanol with a chlorobenzene standard. DBP and EPA capsules were dispersed in anisole with a DCPD standard. All capsule concentrations and standard concentrations were 1 wt% capsules in solvent. After mixing the capsules on a vortexer at a low setting for a period of time, the capsules were filtered using a 0.45 μm pore size polytetrafluoroethylene syringe filter. The contents were then run through gas chromatography (GC) and the area of solvent peaks used to calculate the quantity of solvent remaining in the solvent. The area of the capsule solvent peak was normalized to the area of the standard with known concentration and no capsules. GC was run on a Hewlett Packard 5890 Series II with split injector and flame ionization detector. The GC run proceeded from 100 °C to 250 °C at 10 °C/min.

2.7 References

[1] Blaiszik, B. J.; Sottos, N. R.; White, S. R. Nanocapsules for self-healing materials. *Compos. Sci. Technol.* **2008**, *68*, 978.

[2] Brown, E. N.; Kessler, M. R.; Sottos, N. R.; White, S. R. In situpoly(urea-formaldehyde) microencapsulation of dicyclopentadiene. *J. Microencapsul.* **2003**, *20*, 719-730.

[3] Kessler, M. R. Characterization and Performance of a Self-healing Composite Material. Ph D. Thesis. University of Illinois Urbana Champaign, 2002.

[4] Graf, C.; Vossen, D. L. J.; Imhof, A.; van Blaaderen, A. A General Method To Coat Colloidal Particles with Silica. *Langmuir* **2003**, *19*, 6693-6700.

[5] Steinmetz, N. F.; Shah, S. N.; Barclay, J. E.; Rallapalli, G.; Lomonossoff, G. P.; Evans, D. J. Virus-Templated Silica Nanoparticles. *Small* **2009**, *5*, 813-816.

[6] Fowler, C. E.; Khushalani, D.; Mann, S. Interfacial synthesis of hollow microspheres of mesostructured silica. *Chem. Comm.* **2001**, 2028-2029.

[7] Bégu, S.; Durand, R.; Lerner, D. A.; Charnay, C.; Tourné-Péteilh, C.; Devoisselle, J. M. Preparation and characterization of siliceous material using liposomes as template. *Chem. Comm.* **2003**, 640.

[8] Howarter, J. A.; Youngblood, J. P. Optimization of silica silanization by 3-aminopropyltriethoxysilane *Langmuir* **2006**, *22*, 11142-11147.

[9] Liu, Y.; Hsu, C.; Wang, M.; Chen, H. A novel approach of chemical functionalization on nano-scaled silica particles. *Nanotechnology* **2003**, *14*, 813-819.

[10] Stober, W. Controlled growth of monodisperse silica spheres in the micron size range*1. *J. Colloid Interf. Sci.* **1968**, *26*, 62-69.

[11] Klaus, J. W.; George, S. M. SiO_2 Chemical Vapor Deposition at Room Temperature Using $SiCl_4$ and H_2O with an NH_3 Catalyst. *J. Electrochem. Soc.* **2000**, *147*, 2658.

[12] Hakim, L. F.; Blackson, J.; George, S. M.; Weimer, A. W. Nanocoating Individual Silica Nanoparticles by Atomic Layer Deposition in a Fluidized Bed Reactor. *Chem. Vapor Depos.* **2005**, *11*, 420-425.

[13] Hakim, L. F.; George, S. M.; Weimer, A. W. Conformal nanocoating of zirconia nanoparticles by atomic layer deposition in a fluidized bed reactor *Nanotechnology* **2005**, *16*, S375-81.

[14] Decher, G.; Schmitt, J. Trends in Colloid and Interface Science VI; Fine-Tuning of the film thickness of ultrathin multilayer films composed of consecutively alternating layers of anionic and cationic polyelectrolytes. *Prog. Coll. Pol. Sci.* **1992**, *89*, 160-164.

[15] Hrapovic, S.; Liu, Y.; Enright, G.; Bensebaa, F.; Luong, J. H. T. New Strategy for Preparing Thin Gold Films on Modified Glass Surfaces by Electroless Deposition. *Langmuir* **2003**, *19*, 3958-3965.

[16] Tong, H.; Zhu, L.; Li, M.; Wang, C. Electroless silver deposition on Si(100) substrate based on the seed layer of silver itself. *Electrochim. Acta* **2003**, *48*, 2473-2477.

[17] Chang, S. M.; Lee, M.; Kim, W. S. Preparation of large monodispersed spherical silica particles using seed particle growth *J. Colloid Interface Sci.* **2005**, *286*, 536-542.

[18] Bogush, G.; Tracy, M.; Zukoski, C.,IV Preparation of monodisperse silica particles: Control of size and mass fraction? *J. Non Cryst. Solids* **1988**, *104*, 95-106.

[19] Giesche, H. Synthesis of monodispersed silica powders II. Controlled growth reaction and continuous production process. *Journal of the European Ceramic Society* **1994**, *14*, 205-214.

[20] Brinker, C. J.; Scherer, G. W. In *Sol-Gel Science: The Physics and Chemistry of Sol-Gel Processing* Academic Press: 1990, pp 912.

[21] Wallace, A. F.; DeYoreo, J. J.; Dove, P. M. Kinetics of silica nucleation on carboxyl- and amine-terminated surfaces: insights for biomineralization. *J. Am. Chem. Soc.* **2009**, *131*, 5244-5250.

[22] Cosgrove, T. In *Colloid science: theory, methods and applications* Blackwell Pub. Professional: Ames, Iowa, 2005, pp 288.

[23] Caruso, M. M.; Blaiszik, B. J.; Jin, H.; Schelkopf, S. R.; Stradley, D. S.; Sottos, N. R.; White, S. R.; Moore, J. S. Robust, Double-Walled Microcapsules for Self-Healing Polymeric Materials. *ACS Appl. Mater. Interfaces* **2010**, *2*, 1195-1199.

[24] Palmová, I. Experimental and modeling studies of oligomerization and copolymerization of dicyclopentadiene. *Chemical Engineering Science* **2001**, *56*, 927-935.

[25] Bloch, D. In *Polymer Handbook, 4th Edition* Wiley-Interscience: 1999, pp 2336.

CHAPTER 3

POLYMER PARTICLES CONTAINING GRUBBS' CATALYST

Parts of this chapter were previously published by the author:

Jackson, A. C.; Bartelt, J. A.; Marczewski, K.; Sottos, N. R.; Braun, P. V. Silica-Protected Micron and Sub-Micron Capsules and Particles for Self-Healing at the Microscale. *Macro. Rap. Comm.* **2010**, *31*, 82-87.

3.1 Motivation

A new encapsulation scheme to protect Grubbs' catalyst is sought to improve the functionality and stability of current catalyst particles used in self-healing materials, especially for small size-scale and high temperature self-healing applications. To date, Grubbs' catalyst has been the primary component, combined with dicyclopentadiene (DCPD) capsules, for mechanical self-healing in epoxy. The primary challenge with using Grubbs' catalyst is that it deactivates upon reaction with amines and alcohols in epoxy resins forming a hydride or ruthenium metal.[1-3] The relevant epoxy system this work focuses on contains the epoxy resin EPON 828 (diglycidal ether of bisphenol A) and the epoxy hardener DETA where DETA is the primary cause for deactivation. Previously, a wax protection scheme has been used to improve the healing efficiency of self-healing composite where both capsules and catalyst particles are larger than 20 μm in diameter.[4] For small size-scale applications, however, wax particles less than 5 μm aggregate and are no longer a viable option for catalyst protection.

Encapsulating Grubbs' catalyst in polymer particles offers a means for building stable sub-micron catalyst particles. Previous work showed that Grubbs' catalyst encapsulated in polystyrene allows recovery of the catalyst in industrial applications.[5] While these particles are not clearly defined and therefore not useful in self-healing materials, the research does highlight a

promising route for catalyst encapsulation. Researchers in drug delivery successfully encapsulate drugs in polymer particles less than 5 μm using an emulsion solvent evaporation method.[6-8] Due to their elevated melting point compared to wax, polymers also offer potential improvements in thermal stability for catalyst encapsulation. Using a similar procedure, this chapter demonstrates the successful synthesis of polymer-protected catalyst particles on the order of 1 μm in diameter. The chapter also demonstrates potential improvements in thermal stability for particles larger than 15 μm in diameter. In particular, polystyrene (PS) is chosen as the encapsulant since it dissolves readily in DCPD.

3.2 Sub-micron Polystyrene Particles Containing Grubbs' Catalyst

Several factors in the emulsification process are investigated to optimize the procedure for making sub-micron polymer protected catalyst particles. In the emulsion solvent evaporation scheme, PS and Grubbs' catalyst are dissolved in methylene chloride and the solution is emulsified in water with the help of a surfactant. The surfactant can affect the morphology of the particles. A high molecular weight polymer surfactant, EMA for example, forms collapsed polymer shells while a shorter molecular weight polymer surfactant, Pluronic 127 or CTAB for example, forms spherical particles. CTAB is chosen as an appropriate surfactant for sub-micron catalyst particles since it has no groups that deactivate the catalyst. The emulsification method is also important for producing sub-micron particles. Similar to the procedure used to make 1.5 μm DCPD capsules, sonication is also employed here to reduce the emulsion size sufficiently. Once emulsified, the solvent is removed by evaporation with the assistance of nitrogen flow.

The resulting sample contains PS-protected catalyst particles with an average diameter of 1.5 μm (**Figure 3.1a**) although the standard deviation was large, 0.7 μm and a few particles exist that are larger than 5 μm. Rheology demonstrates that the catalyst particles remain active after synthesis. In rheology experiments, catalyst (as opposed to the catalyst particle) concentration

was kept constant at 0.0167 g mL^{-1} in DCPD. This value is consistent with the concentration of catalyst in a crack plane reported in previous literature.[4, 9] The gel time for the catalyst-containing polymer particles, 30 minutes, is similar to the gel time of unprotected catalyst in DCPD (Figure 3.1b). This gel time is faster than the kinetics described by Kessler *et al.* [10] because the concentration of catalyst used here is an order of magnitude higher than the concentration used in the work by Kessler.

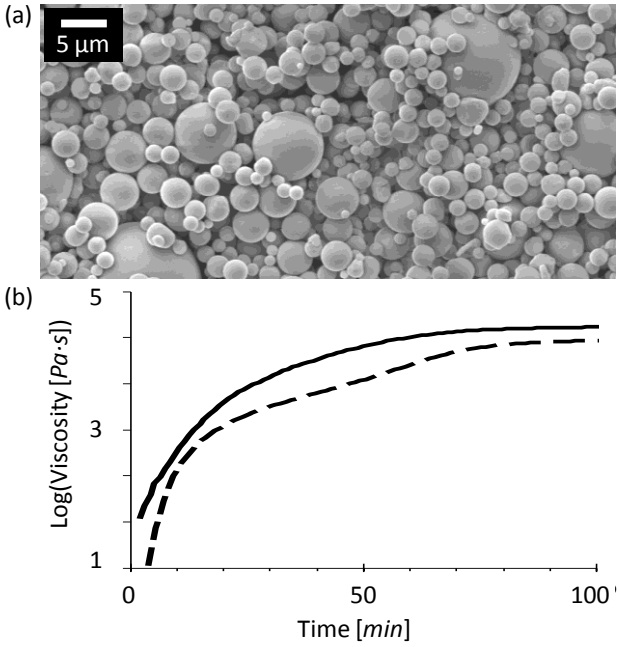

Figure 3.1. (a) SEM of polystyrene-protected catalyst particles. (b) The gel time of the polymer-protected catalyst particles (solid line) compared to that of the as-received Grubbs' catalyst (dotted line) as measured by rotating plate rheometry.

When incorporated into epoxy, the PS-protected catalyst particles react to form a ruthenium hydride that is yellow in color compared to the purple color of active catalyst. This hydride is unable to polymerize DCPD. A variety of individual changes to the synthesis procedure results in no improvements to particle stability. Molecular weight is important to the extent that higher molecular weight polymers swell more slowly in good solvents [11] and, as a

result should minimize swelling by components in the epoxy matrix. However, increasing the molecular weight of the PS from 35 kDa to 120 kDa did not improve stability. A silica coating, made via the fluoride-catalyzed silica-coating method described in Section 2.3.2, is expected to add an extra diffusion barrier to protect the particles from deactivating species but is insufficient alone. The type of polymer is import to the extent that epoxy and DETA swell some polymer better than others. Polymethylmethacrylate (PMMA) proved the most promising but was also insufficient alone. In addition, PMMA doesn't dissolve in DCPD making the catalyst inaccessible in a purely PMMA-protected catalyst particle.

A composite particle containing high molecular weight PS, PMMA, and silica proved to be most effective at protecting the catalyst in epoxy. The particles, after freeze drying, form a free-flowing powder with few aggregates. The composite particles are approximately 0.4 μm in diameter and have a uniform 20 nm thick shell of silica surrounding them (**Figure 3.2**). Based on SEM analysis, the particle size distribution is 0.4 ± 0.3 μm. The PMMA is expected to phase separate in the particles and either form a second barrier or improve the interface between the polystyrene and silica. SEM imaging shows a dumbbell shape to many of the particles suggesting that the PMMA does partially coat the PS. To demonstrate the activity of catalyst within the particles, the synthesized particles are prepared for ^{1}H NMR by etching the silica shell with HF solution and then dissolving the remaining particles in $CDCl_3$. Because there are many peaks from the polystyrene and polymethylmethacrylate, the presence of the carbene hydrogen peak at 20ppm is the best qualitative evidence for active catalyst in the particles.[1, 3] This peak is present in the spectrum of as-received Grubbs' catalyst, Grubbs' catalyst encapsulated in polystyrene, and the etched catalyst particles (Figure 3.2c). When as-received catalyst is dispersed in solvent containing an amine, the catalyst deactivates. The H^1 NMR spectrum of this deactivated catalyst sample shows no peak at 20ppm. The etched catalyst particles are also

dispersed in DCPD to directly test their activity. After 30 minutes, the mixture gels verifying catalyst activity.

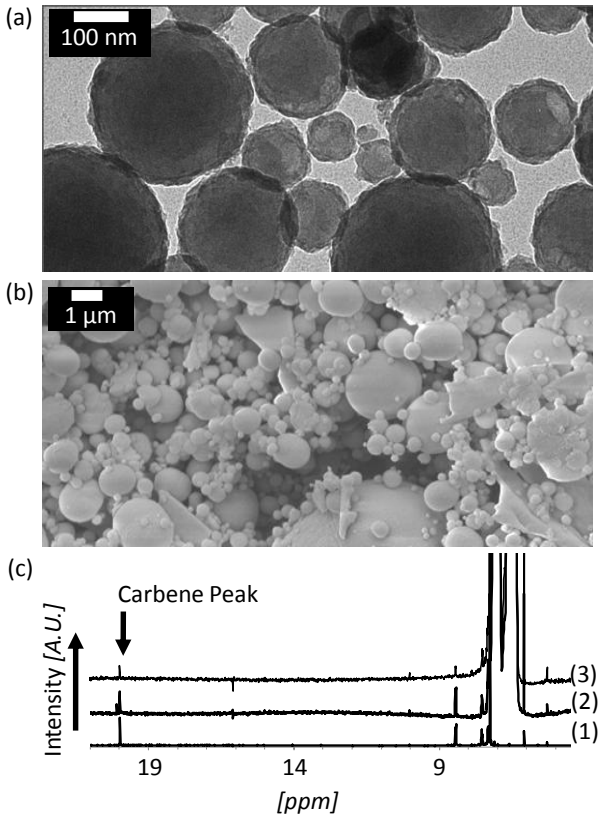

Figure 3.2. The morphology of the core-shell catalyst particles as observed via (a) TEM and (b) SEM. (c) H^1 NMR spectrum of as received Grubbs' catalyst (1), catalyst in polystyrene (2), and etched particles of catalyst in polystyrene, poly(methyl methacrylate) and silica (3).

3.3 PS-protected Grubbs' Catalyst for Thermal Stability

Because polystyrene's glass transition temperature (~100 °C) is higher than the melting point of wax (70-80 °C), 10-100 µm in diameter polymer protected catalyst particles are expected to retain more active catalyst at high temperatures. To build 10-100 µm PS particles without catalyst, an emulsion of PS and solvent, in this case toluene in water is produced and the solvent

evaporated to build PS particles. Unlike sub-micron capsules, the sonication step is removed and a mixer blade is used to create an emulsion with larger droplet size. However, when synthesizing larger PS particles containing the catalyst the resulting sample is an aggregated mass of polymer and catalyst. To make well dispersed particles, a quench bath, made of methanol and water, is required and removes sufficient solvent from the emulsion and eliminate aggregation in the sample by increasing the solubility of the hydrophobic solvent in water. No further protection is necessary at this size scale.

The final catalyst-containing particles are purple and spherical in shape. Changing the stir rate of the initial emulsion changes the particle size as long as the quench bath stir rate is kept low, typically 400 rpm. **Figure 3.3** shows the particle size as a function of stir rate for the initial emulsion solution and the quench solution. PS protected catalyst particles maintain their purple color after synthesis and remain active when dispersed in DETA, the primary deactivating species in an epoxy resin. NMR of the final sample shows a carbene peak near 20 ppm, indicative of active Grubbs' catalyst. When dispersed in DCPD, the PS-protected catalyst gel time, 40 minutes as measured by rheology, is comparable to the gel time of wax-protected catalyst (**Figure 3.4**). This is shorter than the gel time of as-received catalyst in DCPD and is expected due to the slow dissolution time of the crystallized catalyst in DCPD.

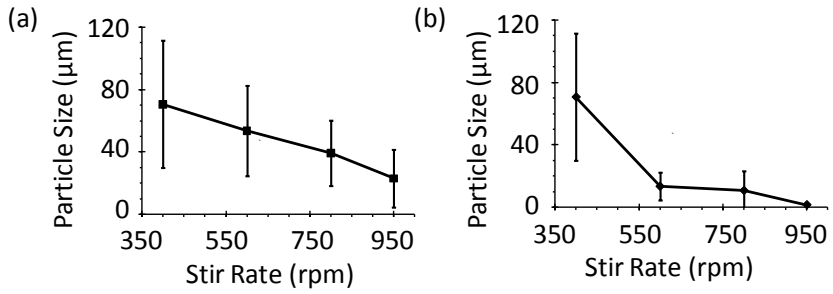

Figure 3.3. (a) Particle size as a function of initial emulsion stir rate with a constant quench solution stir rate of 400 rpm. (b) Particle size as a function of the quench solution stir rate with a constant initial emulsion stir rate of 400 rpm.

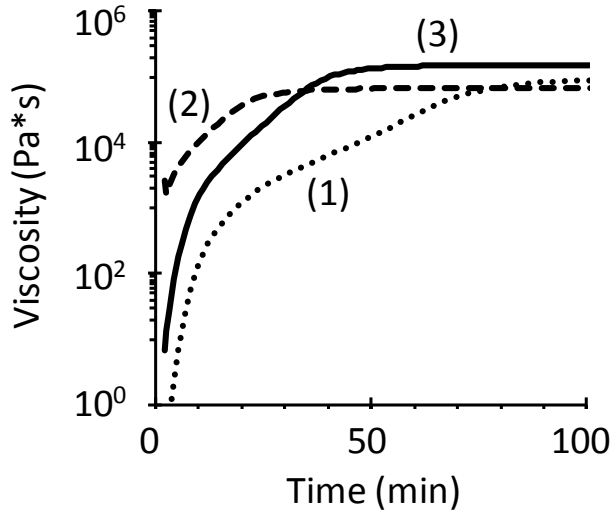

Figure 3.4. Viscosity of solutions of DCPD containing (1) unprotected catalyst, (2) catalyst in 15 µm wax particles, and (3) catalyst in 15 µm PS particles.

To test the PS particles for their resistance to deactivating species, the particles are dispersed in a solution of DETA and water. After exposing the PS-protected catalyst particles to DETA, the gel time increases slightly but remains less than 1 hour. This is also true for wax protected catalyst particles. The primary difference between PS-protected particles and wax-protected catalyst particles is the temperature at which the particles begin to coalesce and cannot

be collected from the DETA solution. Wax-protected particles fall cannot be collected for rheology tests above 35 °C while PS-protected catalyst particles remain intact until 65 °C. When cured in epoxy at 50 °C, the wax-protected particles dissolve into the epoxy matrix while PS particles remain relatively intact (**Figure 3.5**).

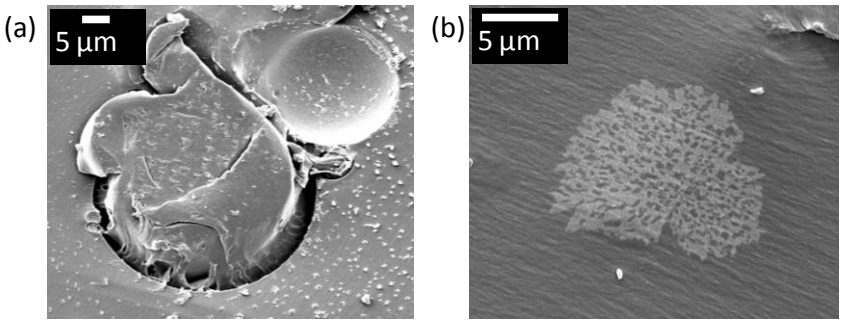

Figure 3.5. (a) PS-protected catalyst particles and (b) wax-protected catalyst particles dispersed in epoxy resin after curing at 50 °C for 24 hours.

3.4 Conclusions

Grubbs' catalyst is successfully encapsulated in polystyrene using an emulsion solvent evaporation procedure with minimal catalyst deactivation. Sub-micron PS-protected catalyst particles are important for small size-scale self-healing as a complimentary healing agent to the coated 1.5 µm diameter capsules discussed in Chapter 2. Sub-micron PS particles are made using sonication to emulsify a solution of catalyst, PS and solvent in water. The final particles form a dried powder with few aggregates. However, sub-micron PS particles do not provide sufficient protection at the sub-micron size-scale to be incorporated into epoxy. The sample turns yellow during the epoxy curing cycle as a result of the reaction between the catalyst and amines in the epoxy hardener, DETA. Instead a composite particle containing PS, PMMA, catalyst, and a silica shell is developed and maintains its active, purple color when incorporated in epoxy. 10-100 µm

diameter PS-protected catalyst particles are important for high temperature self-healing applications using the DCPD-Grubbs system. These particles maintain their activity in a solution of DETA up at up to 65 °C. The PS particles remain solid in epoxy at 50 °C while wax particles of similar size dissolve into the epoxy resin.

3.5 Experimental

3.5.1 Materials

Dicyclopentadiene (DCPD) was purchased from Alfa Aesar (90+%, stab. with 150-200ppm p-tert-butyl catechol). The DCPD was distilled to remove cyclopentadiene and any oligomeric units that might be present. Grubbs‘ catalyst, wax (mp=58-62 °C), and Polystyrene (PS, MW=280000 and MW=35000) were purchased from Aldrich. Grubbs‘ catalyst was kept in a nitrogen glovebox until use. Ethylene maleic anhydride copolymer was donated by Zeeland chemicals (EMA, MW=400000). This was used as a 2.5 % w/w solution in water. Pluronic was purchased from BASF. polymethylmethacrylate (PMMA, MW=120000), cetyltrimethylammonium bromide (CTAB), tetraethylorthosilicate (TEOS), and tetrabutylammonium fluoride (TBAF, 75wt% in water) were purchased from Sigma. TBAF was diluted to 0.75wt% for use. EPON 828 was purchased from Miller Stephenson and diethylaminetriamine (DETA) was received from Dow Chemical.

3.5.2 Polymer-protected Catalyst Particles

Composite polymer particles containing Grubbs’ catalyst were prepared using an emulsion solvent evaporation technique similar to those described in literature.[6, 7] First, CTAB (0.4 g) and dilute TBAF (18 mL) were dissolved in water (120 mL) at room temperature and stirred with a stir bar at medium speed. Next, PS (MW=35000, 0.8 g), PMMA (0.4 g), and

Grubbs' catalyst (0.08 g) were dissolved in methylene chloride (16 mL). For composite particles, PS (0.8 g) and catalyst (0.08 g) were dissolved in methylene chloride (16 mL). This organic phase was poured into the aqueous phase, emulsified for 1 minute via stir bar, and then sonicated for 30 seconds. The emulsion was stirred overnight with nitrogen flowing over the sample to assure evaporation of the methylene chloride. To add a silica coating, TEOS was added to the solution and allowed to react for 1 day. The final particles were centrifuged and then freeze dried for 4 days affording a dry powder.

Grubbs' catalyst particles larger than 5 μm were formed in a 2 part synthesis. In the first part, an oil in water emulsion was created with PS (MW=280000, 0.45 g), toluene (4.5 mL) and catalyst (0.045 g) in the oil phase. Water (40 mL) and pluronic 127 (0.05 g) formed the water phase. The solution was emulsified via mixer blade. After 2 minutes of emulsification, the solution was transferred to a quench bath containing methanol (110 mL), water (50 mL), and pluronic 127 (0.1g). The quench bath was stirred, via mixer blade, over night with nitrogen flow over the sample to help remove the solvent. The final particles were dried by filtration and washing the particles with water. The procedure is scaleable and has been successfully attempted at 3x the quantities listed.

3.5.3 Catalyst Particle Analysis

Grubbs' catalyst particles were analyzed as follows. Particle morphology was determined by SEM (Philips XL30 ESEM-FEG) and TEM (Philips CM200). For rheology experiments, catalyst (as opposed to the catalyst particle) concentration is kept constant at 0.0167 g mL^{-1} DCPD. This assumes a sample with 3 μm crack width and 5 % w/w 10 μm catalyst particles. This mixture was dripped onto a rotating plate geometry (25 mm diameter) set to have a 200 nm gap. Viscosity was measured every minute at a constant frequency (5 Hz). Gel time was determined by the peak in tan δ (loss modulus divided by the storage modulus). Because silica coated particles did not dissolve in organic solvents, the particles were etched in a solution of 20

% w/w HF in water for NMR and qualitative gel tests. NMR spectra were taken of various catalyst particles dissolved in deuterated methylene chloride with a trimethoxybenzene standard. In order to determine a qualitative gel time for the coated catalyst particles, the particles were etched and mixed into DCPD at 0.0167 g mL^{-1} DCPD. Due to the number of peaks for the other materials in the catalyst particles, no peaks could be used for catalyst quantification. Instead, the carbene peak at 20ppm was used as evidence of the presence of active Grubbs' catalyst.

To test the temperature of 15-45 μm catalyst particles, wax or PS particles (0.15 g) were dispersed in a water (5 mL) and DETA (0.5 g). The particles were stirred on low for 3 hours. The solution was then filtered and washed with water. The particles were considered inactive if they could not be collected or if the gel time, measured by rheology, of the particles was greater than 1.5 hours.

3.6 References

[1] Dinger, M. B.; Mol, J. C. Degradation of the First-Generation Grubbs Metathesis Catalyst with Primary Alcohols, Water, and Oxygen. Formation and Catalytic Activity of Ruthenium(II) Monocarbonyl Species. *Organometallics* **2003**, *22*, 1089-1095.

[2] Wilson, G. O.; Caruso, M. M.; Reimer, N. T.; White, S. R.; Sottos, N. R.; Moore, J. S. Evaluation of Ruthenium Catalysts for Ring-Opening Metathesis Polymerization-Based Self-Healing Applications. *Chem. Mater.* **2008**, *20*, 3288-3297.

[3] Wilson, G. O.; Porter, K. A.; Weissman, H.; White, S. R.; Sottos, N. R.; Moore, J. S. Stability of Second Generation Grubbs' Alkylidenes to Primary Amines: Formation of Novel Ruthenium-Amine Complexes. *Adv. Synth. Catal.* **2009**, *351*, 1817-1825.

[4] Rule, J. D.; Brown, E. N.; Sottos, N. R.; White, S. R.; Moore, J. S. Wax-Protected Catalyst Microspheres for Efficient Self-Healing Materials. *Adv. Mater.* **2005**, *17*, 205-208.

[5] Gibson, S. E.; Swamy, V. M. Micronencapsulation of a Metathesis Catalyst. *Adv. Synth. Catal.* **2002**, *344*, 619.

[6] Pekarek, K. J.; Jacob, J. S.; Mathiowitz, E. Double-walled polymer microspheres for controlled drug release *Nature* **1994**, *367*, 258-260.

[7] Gref, R.; Minamitake, Y.; Peracchia, M.; Trubetskoy, V.; Torchilin, V.; Langer, R. Biodegradable long-circulating polymeric nanospheres. *Science* **1994**, *263*, 1600-1603.

[8] Edlund, U.; Albertsson, A. Degradable Aliphatic Polyesters; Degradable Polymer Microspheres for Controlled Drug Delivery. **2002; 2002**, *157*, 67-112.

[9] Rule, J. D.; Sottos, N. R.; White, S. R. Effect of microcapsule size on the performance of self-healing polymers. *Polymer* **2007**, *48*, 3520-3529.

[10] Kessler, M. R. Characterization and Performance of a Self-healing Composite Material. Ph D. Thesis. University of Illinois Urbana Champaign, 2002.

[11] Ramkissoon-Ganorkar, C.; Gutowska, A.; Liu, F.; Baudyš, M.; Kim, S. W. Polymer Molecular Weight Alters Properties of pH-/Temperature Sensitive Polymeric Beads. *Pharm. Res.* **1999**, *16*, 819-827.

CHAPTER 4

MECHANICAL SMALL SIZE-SCALE SELF-HEALING IN EPOXY

Parts of this chapter were previously published by the author:

Jackson, A. C.; Bartelt, J. A.; Marczewski, K.; Sottos, N. R.; Braun, P. V. Silica-Protected Micron and Sub-Micron Capsules and Particles for Self-Healing at the Microscale. *Macro. Rap. Comm.* **2010**, *31*, 82-87.

4.1 Motivation

The use of small size-scale self-healing components in epoxy using a compartmentalized system is especially important in fiber reinforced composites where spacing between fibers limits the size of self-healing components that can be incorporated into the composite (**Figure 4.1a**). Previous work demonstrated the use of 1.5 μm capsules to heal fiber pull-out damage.[1] Glass fibers are decorated with these capsules and with Grubbs' catalyst (Figure 4.1b) and embedded in epoxy. As demonstrated in fiber pull-out tests, this system recovers a significant portion of its fiber pull-out strength after damage and healing. This chapter considers the next step, small size-scale self-healing in the epoxy matrix using the DCPD/Grubbs' catalyst chemistry.

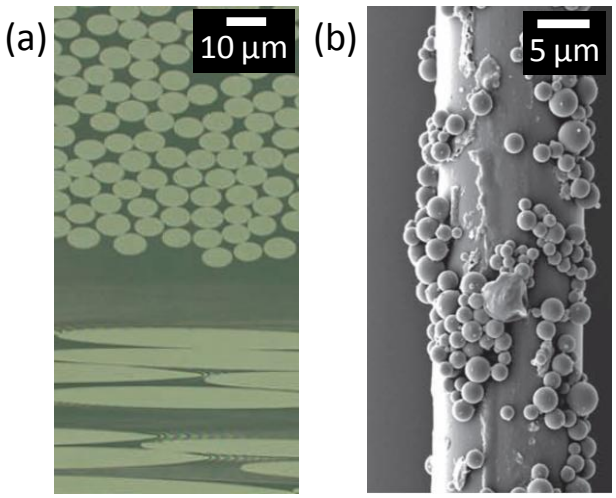

Figure 4.1. (a) Reflection optical microscopy of a carbon fiber composite (adapted from [2]). (b) SEM of glass fiber decorated with healing agents (adapted from [1]).

Small size-scale self-healing in bulk epoxy is not only important for limiting matrix damage between fibers but it is also important for understanding the limitations of mechanical self-healing for other applications requiring small size-scale self-healing. Rule *et al.* studied these limitations for capsules as small as 15 µm in diameter.[3] They found that maximum mechanical healing can only occur if the volume of the crack plane is equal to or less than the amount of healing agent supplied from capsules. By geometry, the relationship between the capsule size, d_c, and the mass of healing agent delivered, m, is linear as described by Equation 4.1. The healing agent delivered is also dependent on the density of the healing agent, ρ, and the fraction of capsules in epoxy, Φ.

$$m = \rho d_c \Phi \qquad \text{Equation 4.1}$$

Several challenges must be addressed to develop small size-scale self-healing in an epoxy matrix. Challenges with capsule dispersion in epoxy and catalyst encapsulation on the order of 1 µm in diameter are partially addressed in Chapter 2 and Chapter 3. This chapter further considers

how the DCPD-filled capsules and catalyst particles disperse in an epoxy matrix and retain activity. The final challenge to developing small size-scale self-healing is the size of damage that can be healed. DCPD-filled capsules as small as 30 μm in diameter effectively heal cracks as small as 3 μm.[3] However, capsules 1 μm in diameter are an order of magnitude smaller, so full healing is not expected unless damage is less than 300 nm wide. Other self-healing systems with similar limitations for healing agent delivery show improved healing as compression is applied across the crack.[4, 5] A similar strategy is applied here to decrease the damage volume.

4.2 System Overview

The epoxy matrix used in this work is based on the reaction of EPON 828 resin with diethylenetriamine (DETA) hardener. A tapered double cantilever beam (TDCB) specimen is used to test the mechanical properties of the self-healing epoxy.[3, 6] Due to the geometry of the TDCB (**Figure 4.2a**), crack propagation in the center portion of the TDCB is controlled and the crack toughness is independent of the crack length. As a result, the healing efficiency (η), the ratio of healed fracture toughness ($K_{IC,\ healed}$) to virgin fracture toughness ($K_{IC,\ virgin}$), is also equal to the ratio of the healed peak load (P_{healed}) to the virgin peak load(P_{Virgin}) as shown in Equation 4.2.[6]

$$\eta = \frac{K_{IC,healed}}{K_{IC,virgin}} = \frac{P_{healed}}{P_{Virgin}} \qquad \text{Equation 4.2}$$

For specimens with a center crack region of 50 mm, cracks propagate through the full sample and samples are manually placed together. The resulting crack width is approximately 10 μm based on work by Rule *et al.*[3] These samples are referred to as long-grove TDCBs. By decreasing the center region to 25mm long (Figure 4.2a), crack growth is arrested before full

damage to the sample occurs. As a result, alignment is easier and the crack width is approximately 3 μm. These samples are referred to as short-grove TDCBs.

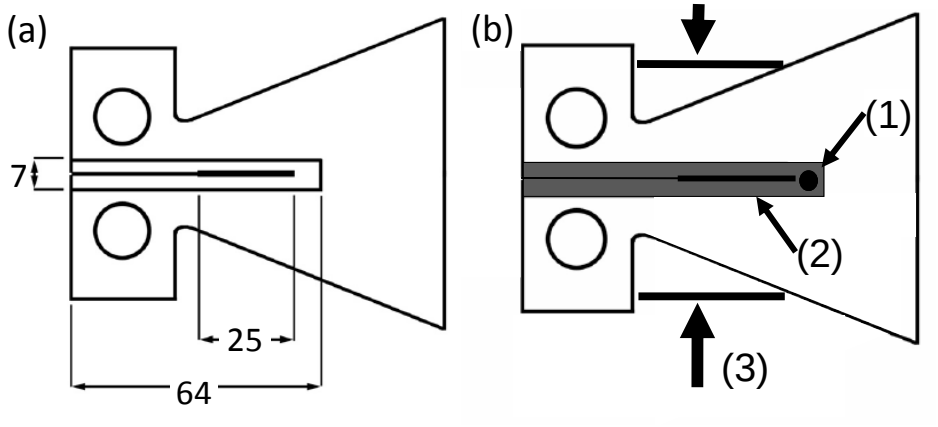

Figure 4.2. Short groove TDCB specimen. (a) Dimensions in mm. (b) Changes as compared to a standard short groove TDCB include: (1) a hole is drilled to arrest crack growth predictably; (2) healing agents are localized to the area surrounding the groove to minimize the quantity of healing agent used per sample; (3) force is applied during healing to artificially decrease the crack width.

For capsules larger than 15 μm, these specifications are sufficient for demonstrating healing. However, several changes must be made to accommodate capsules and particles on the order of 1 μm in diameter (Figure 4.2b). First, the quantity of capsules that can be produced does not fill a full TDCB sample. As a result, micron size capsules and catalyst particles were localized minimizing the quantity of components that are needed for each test. Second, cracking is inefficiently arrested in short grove TDCBs. To reduce loss of valuable sample, a hole is drilled at the end of the crack region to effectively arrest crack growth. Finally, as discussed previously, 3 μm wide cracks are theoretically too large to obtain effective healing. To reduce the crack width, force was applied across the crack plane using clamps. These clips apply a force of approximately 20-30 lb across the crack plane. SEM imaging of clamped TDCBs held together with super glue suggest the applied pressure reduces the crack width along portions of the crack to 1 μm or smaller (**Figure 4.3**).

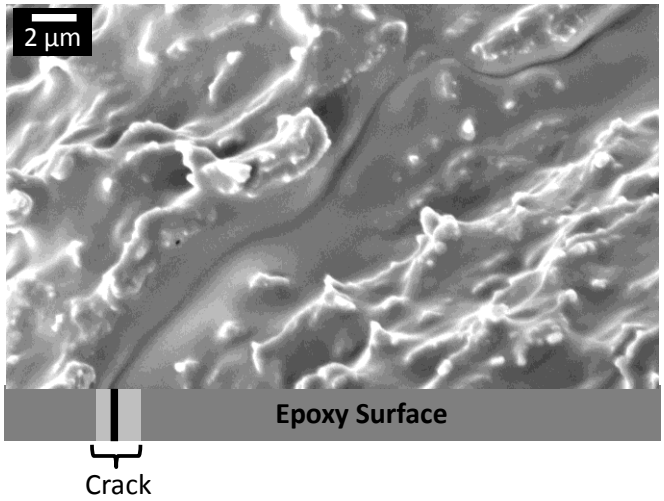

Figure 4.3. SEM of the edge of a crack in a TDCB specimen that has been cracked and mended with superglue while a force is applied across the crack plane using 20-30 lb of force.

4.3 Dispersing Micron Size Components in Epoxy

The importance of a silica shell on DCPD-filled capsules and catalyst particles is apparent when comparing the dispersion of coated capsules to the dispersion of uncoated capsules in an epoxy matrix. Uncoated capsules do not disperse well in epoxy at concentrations higher than 3 wt%. A powder of coated capsules, coated using the fluoride-catalyzed method, disperses in epoxy at significantly higher concentrations than the uncoated capsules without any aggregates. **Figure 4.4** shows a comparison of uncoated capsules and coated capsules dispersed in epoxy at 10 wt%. In all images, it is noted that all of the capsules rupture which is important for delivery of the healing agent.

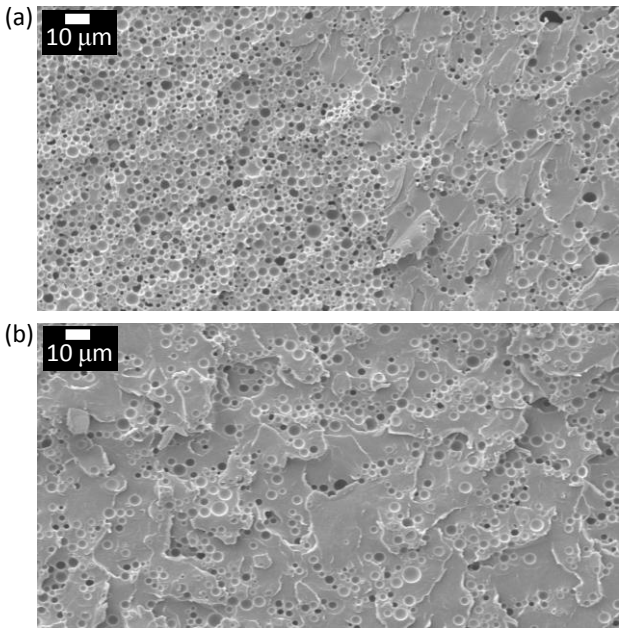

Figure 4.4. SEM of a fracture surface of an EPON 828/DETA epoxy containing (a) uncoated and (b) coated capsules at 10 wt%. Capsules are mixed into the uncured resin/hardener mixture as a dry powder.

The incorporation of micron size capsules and catalyst particles into epoxy alters the polymer's fracture toughness. Brown *et al.* showed previously [7] that capsules toughen epoxy through crack pinning, localized yielding and microcracking. Blaiszik *et al.* [8] showed that small (1 μm or less in diameter) capsules further enhance toughening of the epoxy through both crack pinning and crack deflection mechanisms. Crack deflection is evident in SEM analysis of the crack surface (Figure 4.4). A slight increase in fracture toughness is observed at 7 wt% capsules but no increase is observed at 15wt% capsules (**Table 4.1**). A dependence on capsule concentration is expected based on work by Brown *et al.*[7]

Sample	Micron size catalyst particles	1.5 μm DCPD capsules	Fracture Toughness (MPa $m^{1/2}$)
Blank	0 wt.%	0 wt.%	0.86 +/- 0.02
CGr	7 wt. %	0 wt.%	1.12 +/- 0.00
CCap (7)	0 wt.%	7 wt.%	0.95 +/- 0.11
CCap (15)	0 wt.%	15 wt.%	0.84 +/- 0.06
CCap (15) + CGr	7 wt.%	15 wt.%	0.76 +/- 0.09

Table 4.1. Fracture toughness of samples containing micron size catalyst and 1.5 μm DCPD capsules.

Similar results are observed for catalyst particles and samples containing both capsules and catalyst particles. As discussed, only silica-coated catalyst particles protected by polystyrene (PS) and polymethylmethacrylate (PMMA) stay active in epoxy so only these are studied for epoxy applications. These silica coated Grubbs' catalyst particles disperse well in epoxy at high concentrations (**Figure 4.5**). Although there is no visual evidence of particle cleavage, broken epoxy stubs do regain some mechanical properties when DCPD is injected into the damaged region suggesting that the catalyst is accessible. Fracture toughening mechanisms, specifically crack deflection, is observed in the crack plane. The fracture toughness of samples with 7wt% catalyst particles in epoxy is approximately 50% higher than samples without catalyst (Table 1).

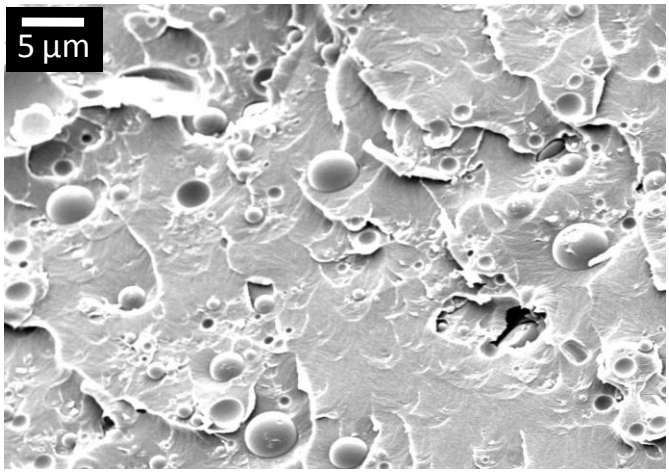

Figure 4.5. SEM of a fracture surface of an EPON 828/DETA epoxy containing 7 wt.% micron size catalyst particles. Particles are mixed into the uncured resin/hardener mixture as a dry powder.

4.4 Activity of Grubbs' Catalyst Particles in Epoxy

While chapter 3 demonstrates the successful synthesis of catalyst particles, this section demonstrates successful polymerization of DCPD injected into the crack plane of short grove epoxy TDCBs. TDCBs made with 2.5 wt% 45 μm in diameter PS particles containing 10 wt% Grubbs' catalyst have an average healing efficiency of 25 +/- 5% based on mechanical data from 3 samples (**Figure 4.6**). No healing is observed for samples containing 45 μm in diameter PS particles without catalyst. This healing efficiency is not quantitatively comparable to the healing efficiencies demonstrated in previous research due to differences in catalyst concentration and definition of healing efficiency.[9] Qualitatively, a key difference between the PS-protected particles and wax-protected particles is the ductility of the healed material. PS-protected catalyst particles make a more brittle healed material than the wax-protected catalyst particles. This is likely a result of the wax plasticizing the polyDCPD. The brittle nature of the healed material created by PS-protected particles is similar to the healed material made by unprotected catalyst.

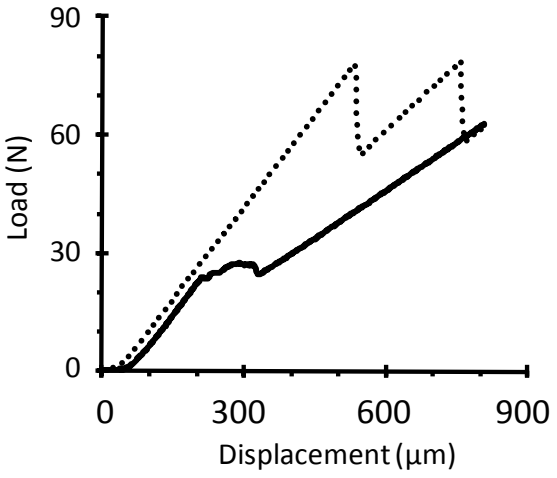

Figure 4.6. Virgin (dotted line) and healed (solid line) load displacement curves for epoxy short-grove TDCBs containing 45 μm Grubbs' catalyst particles. 5 μL DCPD is injected into the crack plane.

Micron size Grubbs' catalyst particles also provide sufficient catalyst to the crack plane to polymerize DCPD injected into the crack plane. As discussed in chapter 3, only silica-coated catalyst particles protected by PS and polymethylmethacrylate (PMMA) in the core remain active in epoxy. The healed peak load is approximately 20 N and the healed polymer is brittle in nature, similar to the nature of the healed polymer created by the 45 μm PS-protected catalyst particles. In controls, it is shown that at least a part of this healing is the result of a solvent welding mechanism where the PS from the catalyst particles dissolves and redeposits in the crack plane. Samples containing particles without catalyst have a healed peak load of approximately 7 N. The healed surface shows a polymer film in both cases (**Figure 4.7**). Unlike the 45 μm PS particles, samples with micron size particles have a higher surface roughness in the crack plane. It is likely that the higher surface area allows some mechanical interlocking between the matrix and healed polymer.

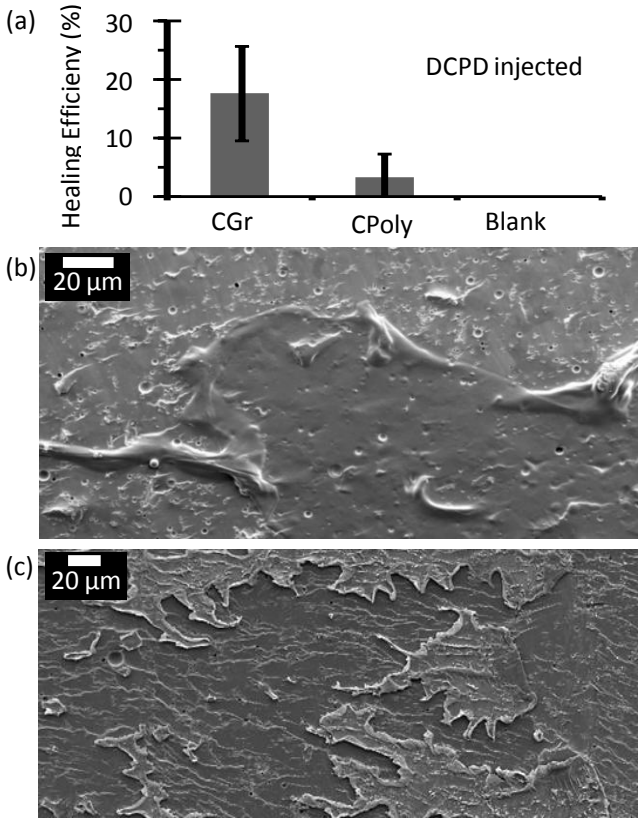

Figure 4.7. Samples containing catalyst particles (7 % w/w, CGr), polymer particles (7 % w/w) or no self-healing agents were injected with DCPD and clamped after virgin fracture. (a) Healing efficiency. SEM images of a portion of the crack surface where healing occurred is shown for samples containing (b) catalyst particles and (c) polymer particles.

4.5 Small Size-scale Self-healing in an Epoxy Matrix

TDCBs containing micron size capsules and catalyst particles retain approximately 20% of their original fracture toughness. The average healed peak load for this system is 15.0 N (**Figure 4.8a**). The load displacement curve shows brittle fracture of the healed material (Figure 4.8b). The fracture surface of the healed sample has a thin film across a fraction of the crack surface (Figure 4.8d). Samples containing catalyst alone or capsules alone show no healing. However, samples containing DCPD capsules and composite polymer particles without catalyst show healing similar to the samples with injected DCPD. As mentioned, this is attributed to capabilities of DCPD to dissolve the PS and redeposit it in the crack plane.

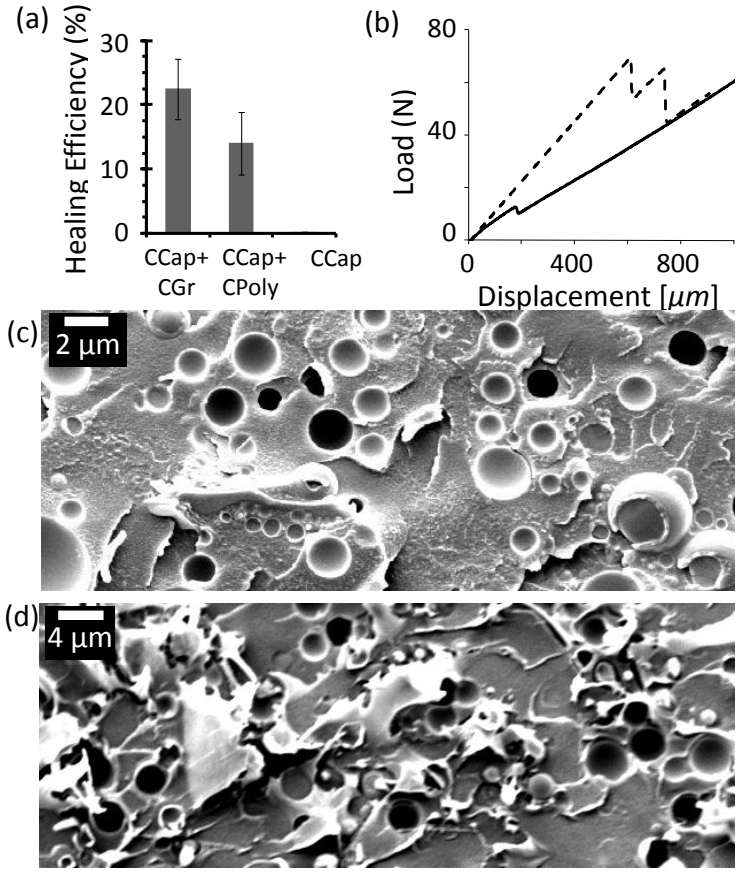

Figure 4.8. (a) Healing efficiency for short groove TDCB specimens containing capsules and catalyst particles (15 % w/w CCap; 7 % w/w, CGr), capsules and polymer (catalyst free) particles (15 % w/w CCap; 7 % w/w CPoly), or only capsules (15 % w/w, CCap), (b) Typical load displacement curve of a full sample (CCap + CGr) with both the virgin (dashed line) and healed (solid line) fracture. SEM of the crack surface of a sample containing capsules and catalyst particles (c) before and (d) after healing. A polymerized polyDCPD film can be seen on the crack surface.

4.6 Conclusions

Small size-scale self-healing in an epoxy matrix is demonstrated with DCPD-filled capsules and PS-protected catalyst particles on the order of 1 μm in diameter. Both components disperse well in epoxy at high concentrations and toughen epoxy through crack pinning and crack deflection. PS-protected catalyst particles, both 45 μm and sub-micron in diameter, successfully

catalyze the polymerization of DCPD injected into the crack plane. This confirms that the PS-protection scheme and manufacture process do not lead to significant catalyst deactivation. A portion of the healing observed when using sub-micron catalyst particles is a result of PS from the catalyst particles redepositing in the crack plane. TDCBs containing 15 wt.% DCPD-filled capsules and 7 wt.% catalyst particles recover a portion of the epoxy's initial properties. To accomplish this, force is applied across the crack plane to reduce the damage volume. An average healing efficiency of 20% is observed in the full system.

4.7 Experimental

4.7.1 Materials

Dicyclopentadiene (DCPD) was purchased from Alfa Aesar (90+%, stab. with 150-200ppm p-tert-butyl catechol). The DCPD was distilled to remove cyclopentadiene and any oligomeric units that might be present. Grubbs' catalyst and wax (mp=58-62 °C) were purchased from Aldrich. Grubbs' catalyst was kept in a nitrogen glovebox until use. Ammonium chloride (NH_4Cl) and urea were purchased from Sigma-Aldrich. Formaldehyde solution (37wt% formaldehyde in water) was purchased from Fisher Chemicals. Ethylene maleic anhydride copolymer was donated by Zeeland chemicals (EMA, MW=400000). This was used as a 2.5 % w/w solution in water. Polystyrene (PS, MW=280000), polymethylmethacrylate (PMMA, MW=120000), cetyltrimethylammonium bromide (CTAB), tetraethylorthosilicate (TEOS), and tetrabutylammonium fluoride (TBAF, 75wt% in water) were purchased from Sigma. TBAF was diluted to 0.75wt% for use. EPON 828 was purchased from Miller Stephenson and diethylaminetriamine (DETA) was received from Dow Chemical.

4.7.2 Self-healing Composites

DCPD capsules and Grubbs catalyst particles are synthesized according to the procedures described in Chapter 2 and Chapter 3. All micron size DCPD capsules were coated using the fluoride-catalyzed silica condensation chemistry. All sub-micron catalyst particles are made using the composite particle method. PS and polymethylmethacrylate (PMMA) protect the catalyst in the particle core while a silica shell is added using the fluoride-catalyzed silica condensation chemistry. 45 μm catalyst particles are only protected with PS using the emulsion solvent evaporation procedure with quench bath.

All self-healing samples were prepared by mixing EPON 828 and diethylenetriamine (DETA) at 12wt.% DETA in EPON 828. Vacuum was applied to the resin/hardener mixture for 10 minutes before adding the encapsulated healing agents. After the encapsulated healing agents were added, vacuum was reapplied for 5 minutes. The final mixture was poured into the appropriate mold and cured for 24 hours at room temperature followed by 24 hours at 35 °C.

Short-groove tapered double cantilever beam (TDCB) specimens were prepared as described previously [3] but with the changes described in Figure 2. After virgin fracture, Pressure was applied to the sample using spring-loaded clamps to minimize the crack width. The sample was then allowed to heal for 24 hours and retested. For injected healing tests, DCPD (5 μL) was injected into the crack plane before applying pressure to the sample. At least 3 samples were tested for each data point. Fracture toughness was calculated based on work by Brown *et al*.[6, 7]

The morphologioes of fracture planes were analyzed using SEM (Philips XL30 ESEM-FEG). To determine the width of the TDCB cracks while under pressure, superglue was added to the crack plane after virgin fracture. The samples were clamped and the superglue was dried for 24 hours. The crack width was estimated by analyzing at the edge of the crack plane using SEM.

4.8 References

[1] Blaiszik, B. J.; Baginska, M.; White, S. R.; Sottos, N. R. Autonomic Recovery of Fiber/Matrix Interfacial Bond Strength in a Model Composite. *Adv. Func. Mater.* **2010**, *20*, 3547-3554.

[2] Hayes, B. S.; Gammon, L. M. In *Optical Microscopy of Fiber Reinforced Composites* ASM International **2010**, pp 246.

[3] Rule, J. D.; Sottos, N. R.; White, S. R. Effect of microcapsule size on the performance of self-healing polymers. *Polymer* **2007**, *48*, 3520-3529.

[4] Patel, A. J.; Sottos, N. R.; Wetzel, E. D.; White, S. R. Autonomic healing of low-velocity impact damage in fiber-reinforced composites. *Comp. Part A - Appl. S.* **2010**, *41*, 360-368.

[5] Kirkby, E. L.; Michaud, V. J.; Månson, J. -. E.; Sottos, N. R.; White, S. R. Performance of self-healing epoxy with microencapsulated healing agent and shape memory alloy wires. *Polymer* **2009**, *50*, 5533-5538.

[6] Brown, E. N.; Sottos, N. R.; White, S. R. Fracture testing of a self-healing polymer composite. *Exp. Mech.* **2002**, *42*, 372-379.

[7] Brown, E. N.; White, S. R.; Sottos, N. R. Microcapsule induced toughening in a self-healing polymer composite. *J. Mater. Sci.* **2004**, *39*, 1703-1710.

[8] Blaiszik, B. J.; Sottos, N. R.; White, S. R. Nanocapsules for self-healing materials. *Compos. Sci. Technol.* **2008**, *68*, 978.

[9] Rule, J. D.; Brown, E. N.; Sottos, N. R.; White, S. R.; Moore, J. S. Wax-Protected Catalyst Microspheres for Efficient Self-Healing Materials. *Adv. Mater.* **2005**, *17*, 205-208.

CHAPTER 5

OPTICAL SELF-HEALING IN POLYMETHYLMETHACRYLATE

Parts of this chapter are submitted for publication to Advanced Functional Materials

5.1 Motivation

This chapter focuses on self-healing polymethylmethacrylate (PMMA) for optical applications but the concepts developed can be applied to other thermoplastic systems. PMMA is an important material used in optical materials [1, 2] and biomaterials.[3] Relevant optical applications include Fresnel lenses, lens coatings and protective coatings for artwork. Fresnel lenses made of PMMA are, for example, important in concentrating photovoltaic modules.[2] Microcracking often occurs as a result of the build-up of residual stresses during manufacture. The micro-cracks grow further when exposed to adverse environmental conditions, such as temperature cycling and humidity.[1, 2] The cracks can result in hazing and compromise the mechanical stability of the Fresnel lens. Similar damage in lens coatings and artwork coatings result in significant light scatter and environmental damage to the underlying substrate.

This research addresses these issues by autonomically healing the microcracking. This both reduces light scatter from microcracks and maintains the protective capabilities of the polymeric coating while retaining a portion of the mechanical properties in the coating. Along with utilization of a chemical system appropriate for healing a thermoplastic, the two primary challenges towards developing an optically transparent self-healing system are: (1) minimization of light scatter from capsules in the polymer matrix and (2) minimization of light scatter from the healed material in a polymer matrix. To develop a self-healing optical system containing capsules, index matching to minimize reflections or light scatter from interfaces between phases with differing refractive indices is necessary. Here we demonstrate a new self-healing chemistry that enables index matching of the matrix, the capsules, and the healed material, largely eliminating light scatter.

A thermoplastic solvent welding chemistry allows a relatively simple index matching scheme. In solvent welding, the polymer matrix swells in a solvent and deposits part of the matrix in the damaged area, fixing small defects in thermoplastic polymer.[4] For self-healing, the solvent simply needs to be encapsulated and appropriately dispersed in the thermoplastic matrix. As a crack propagates through the matrix, capsules are broken, and the solvent wicks into the crack plane initiating the solvent welding mechanism (**Figure 5.1**). Careful choice of the solvent and matrix can reduce light scatter from the capsules through index matching. If properly designed, the healed material can be designed to be inherently index matched to the polymer matrix, minimizing light scatter from the healed region.

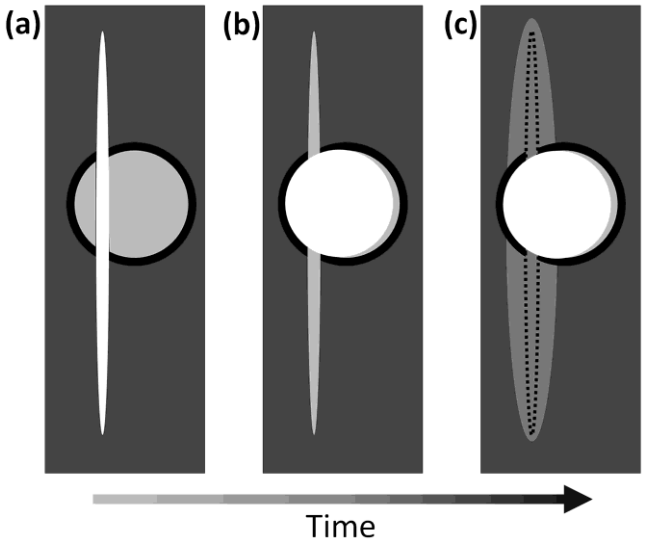

Figure 5.1. Schematic of the solvent welding mechanism in a polymer matrix. During a damage event, capsules rupture (a), releasing all or most of their contents (light gray) into the crack plane (b). Over time, the solvent in the crack plane diffuses into the polymer and the polymer swells and flows into the crack plane leaving a plasticized polymer (dark gray) in the healed region (c). Eventually the solvent disperses into the polymer, leaving behind essentially intrinsic material in the crack plane (not shown).

5.2 System Overview

The particular thermoplastic matrix studied in this work is PMMA. Prior work in solvent welding of PMMA used methanol (n=1.33) and ethanol (n=1.36),[4, 5] but these solvents are not readily encapsulated and are poorly index matched to PMMA (n=1.49). Useful solvents for solvent welding PMMA with refractive indices similar to PMMA include ethylphenyl acetate (EPA, n=1.50), and dibutyl phthalate (DBP, n=1.49). Although a research has been performed using DCPD filled capsules,[6-8] DCPD does not readily swell PMMA. Previous work has also demonstrated encapsulation of EPA for solvent welding.[9, 10] However, we chose DBP as a self-healing agent since it is more closely index matched to PMMA and has a larger molecular size, decreasing its permeability through the shell wall, resulting in capsules with better stability. Although DBP is left behind after healing due to its low volatility, its plasticization properties can plasticize the surrounding PMMA, increasing toughness in the healed region.

Control of the characteristic length scales of the healing agent is important as it can be used as a tool to minimize light scatter. Here, two sizes of capsules are considered: 1.4 μm and ~75 μm diameter capsules. For comparison to previous sonicated capsules, **Figure 5.2** shows the size distribution of 1.4 μm DBP capsules. In all cases, the capsule diameter must be less than the film thickness or a rough, highly scattering film will result. In optical lenses for example, coatings as thin as 10 μm are common, and thus only small capsules could be used. One advantage of using thinner films and smaller capsules is the reduced scatter and path length for light through the material. A difficulty in using smaller capsules, however, is the decreased quantity of healing agent supplied to the damaged region. Previous work demonstrated that, as the capsule size decreases, the amount of healing agent released into the crack plane decreases with a linear dependence on the capsule diameter,[11] limiting the size of cracks that can be healed by small capsules.

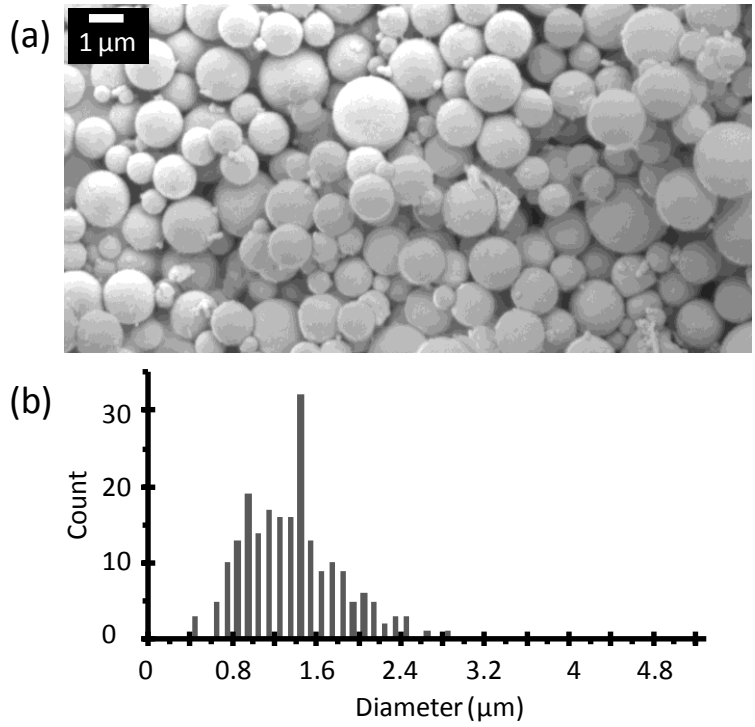

Figure 5.2 (a) SEM of DBP capsules and (b) size distribution of 1.4 µm DBP capsules as measured from SEM images.

Successful thermoplastic solvent-based self-healing requires a good understanding of capsule stability during their manufacture, the nature of the interface between the capsules and polymer matrix, and the upper bound to the extent of healing that can occur. As shown previously, solvent capsules have poor stability when extruded with a thermoplastic polymer as a result of the high temperatures and pressures required for processing.[10] Solvent casting minimizes shear, but the solvent used and the conditions required to remove the solvent must not damage the capsules. The capsules must survive both elevated temperatures and exposure to solvents at those temperatures with little or no loss of healing agent. This is demonstrated in Chapter 2 where both 75 µm capsules and 1.4 µm capsules lose none of their contents after 1 hour at 90 °C in anisole.

The interface between a capsule and its polymer matrix is important for capsule dispersion and capsule rupture during damage. For example, as discussed in chapter 4, silica

coated DCPD capsules disperse better than unmodified DCPD capsules in epoxy. For self-healing optically transparent materials, the capsules must be well dispersed in the polymer, and must be fractured by a damage event, both of which require a well engineered capsule-matrix interface. Both small and large capsules require interface engineering. As shown in **Figure 5.3a**, unfunctionalized, silica coated 1.4 μm diameter capsules aggregate during the spin coating procedure used to form PMMA coatings while methacryl functionalized silica-coated capsules disperse well (Figure 5.3b). Uncoated, 75 μm capsules also require interface engineering. When the composite coating is cracked, uncoated capsules pull out of the PMMA matrix instead of rupturing to release their contents (Figure 5.3c). Neither a silica coating nor methacryl functionalization provides obvious improvements for capsule rupture (unlike the case for the smaller capsules). Once the larger capsules are soaked in a solution of anisole and PMMA, or annealed in the dry state at 140 °C before dispersing them in PMMA, improved capsule rupture is observed. Figure 5.3d shows a representative image of successful capsule rupture in a PMMA matrix. It is important to note that 1.4 μm DBP capsules consistently rupture when damaged as observed by SEM (Figure 5.3e).

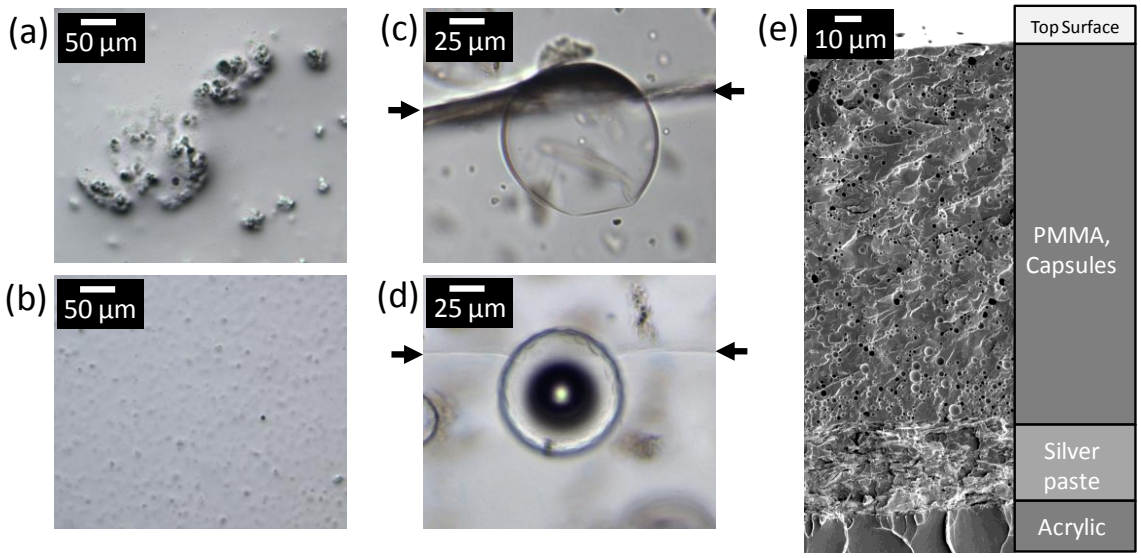

Figure 5.3. Transmission optical microscopy of capsules in PMMA: small coated capsules without functionalization (a); small coated capsules with methacryl functionalization (b); large uncoated, unmodified, capsules that do not ruptureas a result of crack damage (c) and large uncoated capsules, annealed prior to incorporation in PMMA, that do rupture as a result of crack damage (d). An SEM of a crack surface of PMMA containing 1.4 µm capsules (e). Arrows in (c) and (d) point to the crack damage in each sample.

5.3 Optical Properties of Capsule-containing Films

MIE scattering calculations for small, 1.4 µm, capsules enable determination of the effect of refractive index on light scatter from capsules and transmission through coatings containing the capsules. The calculations are based on Matlab code written by Bond et al. to calculate light scatter of particulate matter in an atmosphere.[12] Three refractive indices are important: that of the matrix (n_m), the capsule core (n_c) and the capsule shell (n_s). As the refractive index difference between the capsule core and matrix increases (Δn), the calculated transmission decreases. For a system containing 5 wt.% capsules, below $\Delta n \sim 0.02$, the calculated transmission is greater than 90% of the sample without capsules. EPA and DBP both have a refractive index within 0.01 of PMMA. As the refractive index of the capsule shell is varied, the calculated transmission is affected, but not by more than 5% for $\Delta n = 0.06$ (**Figure 5.4**). This is expected since the shell wall makes up only a small volume fraction of the final composite. The shell's thickness, only 70 nm, additionally reduces its scattering strength. Previous work [13] demonstrates that optical

composites with inclusions smaller than the wavelength of light can tolerate a larger mismatch in refractive index between the two phases than composites with inclusions larger than wavelength of light.

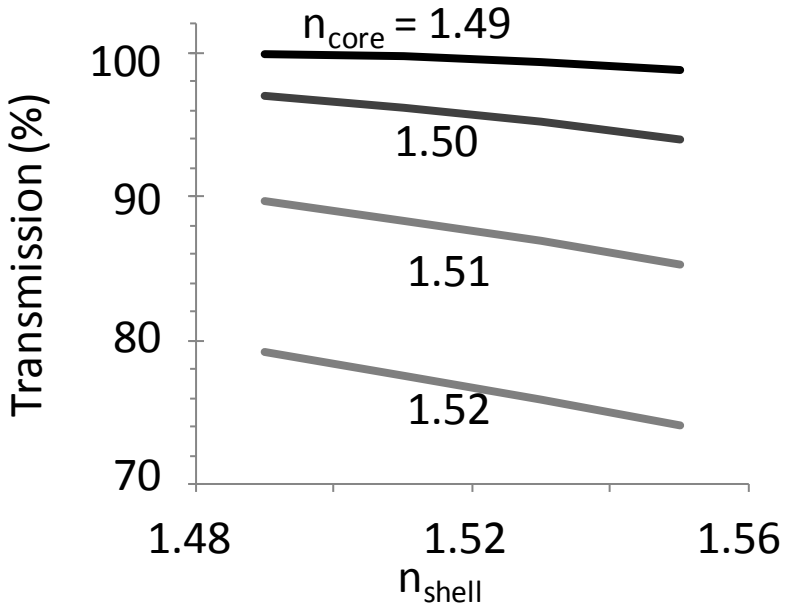

Figure 5.4: Theoretical calculation of transmission for various indices of refraction for the core material and shell material of micron size capsules. Here, the matrix index of refraction is taken as 1.489, the capsule diameter is 1.4 μm, the shell thickness is 50 nm, the wavelength is 550 nm and the capsules are dispersed at 5 wt.% in a 10 μm thick film.

Capsules deposited on a glass slide demonstrate how index matching the core material to the polymer matrix can reduce light scatter in the sample. For a submonolayer of capsules (surface coverage of ~35%), due to the index mismatch between air and the capsules, light scatters such that features beneath the sample are cloudy (**Figure 5.5**). For the same concentration of capsules in a PMMA coating, light scatter is nearly eliminated due to index matching and features beneath the sample can be seen (Figure 5.5b). Optical microscopy and UV-vis spectroscopy confirms that the light scatter from the capsules is minimal due to index matching (Figure 5.5c,d,e).

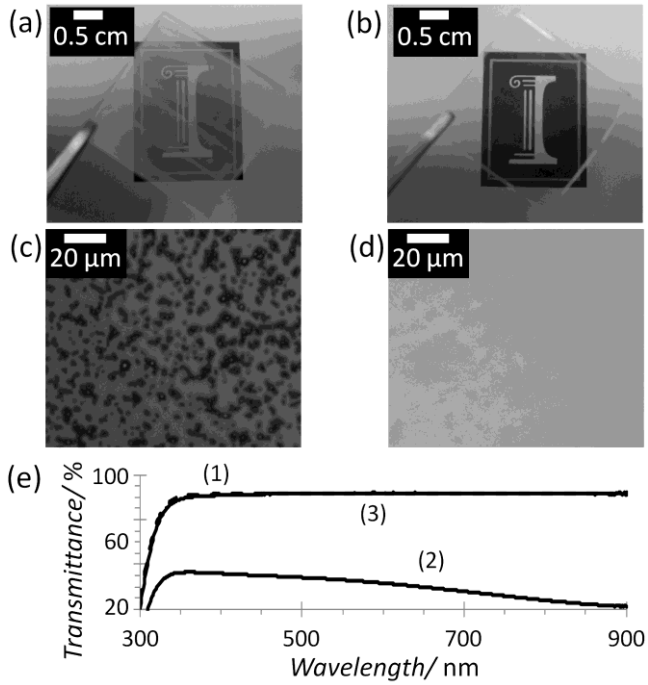

Figure 5.5. 1.4 µm uncoated capsules containing DBP (a) deposited on a glass slide and (b) after a 10 µm thick PMMA film is spun coat onto the same sample. Transmission optical microscopy images of the capsules (c) before and (d) after PMMA addition. (e) UV-vis of the glass slide (1, dashed), the glass slide with deposited capsules (2), and the glass slide with capsules in PMMA (3).

As expected, 75 µm capsules scatter more light than 1.4 µm capsules. When the large DBP capsules are dispersed in PMMA, light scatter is observed but the composite is relatively clear with a light transmission above 70% in the visible spectrum (**Figure 5.6**). In comparison, DBP capsules dispersed in polystyrene, which has poor index matching, scatter more light and light transmission is less than 50% throughout the visible spectrum. Much of the light scatter in the PMMA films is a result of PUF particles that could not be removed during the capsule work-up (Figure 5.6c). This scatter is still acceptable for applications that do not require high quality optics.

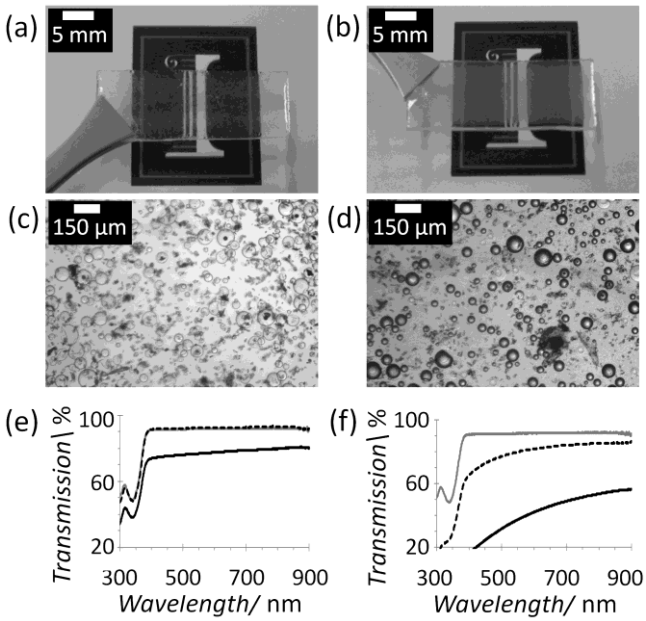

Figure 5.6. 6 wt.% 75 µm DBP capsules dispersed in (a) PMMA and (b) PS. Transmission optical microscopy of the capsules in (c) PMMA and (d) PS. UV-vis of the capsules in (e) PMMA and (f) PS. Acrylic substrates (gray lines) and acrylic substrates with respective polmyer films (dotted lines) are shown for comparison.

5.4 Optical and Barrier Properties of the Healed Polymer

The focus here is on sub-micron damage created by brittle cracking as a result of mechanical stresses. Healing occurs only when the crack is wet by healing agent. 15wt.% of the 1.4 µm diameter capsules are capable of delivering sufficient DBP to fill cracks up to 200 nm wide. 75 µm capsules contain enough healing agent at 5 wt.% in PMMA to fill cracks up to 7.5 µm wide. The final films are designed to be 100 µm thick for small capsules and 170 µm thick for large capsules. They are drop cast on acrylic and, based on SEM analysis, the actual thickness in the center of the samples (1.27 cm by 2.54 cm) varies by plus or minus 50 µm from the predicted values. The thickness tapers to 0 µm over a 200-500 µm wide area on the edge of the sample. Bending these films on acrylic substrates produces cracks narrower than 50 nm at the surface as observed by AFM and SEM and as large as 1 µm below the surface as observed by SEM (**Figure 5.7**). Some of the damage is a result of buckling as the edges of the crack come back together due to the restoring force from the acrylic substrate. Despite being smaller than the

wavelength of light, these cracks are optically visible (**Figure 5.8a**). Optical imaging also suggests that damage below the surface is more extensive but the extent of damage could not be determined quantitatively.

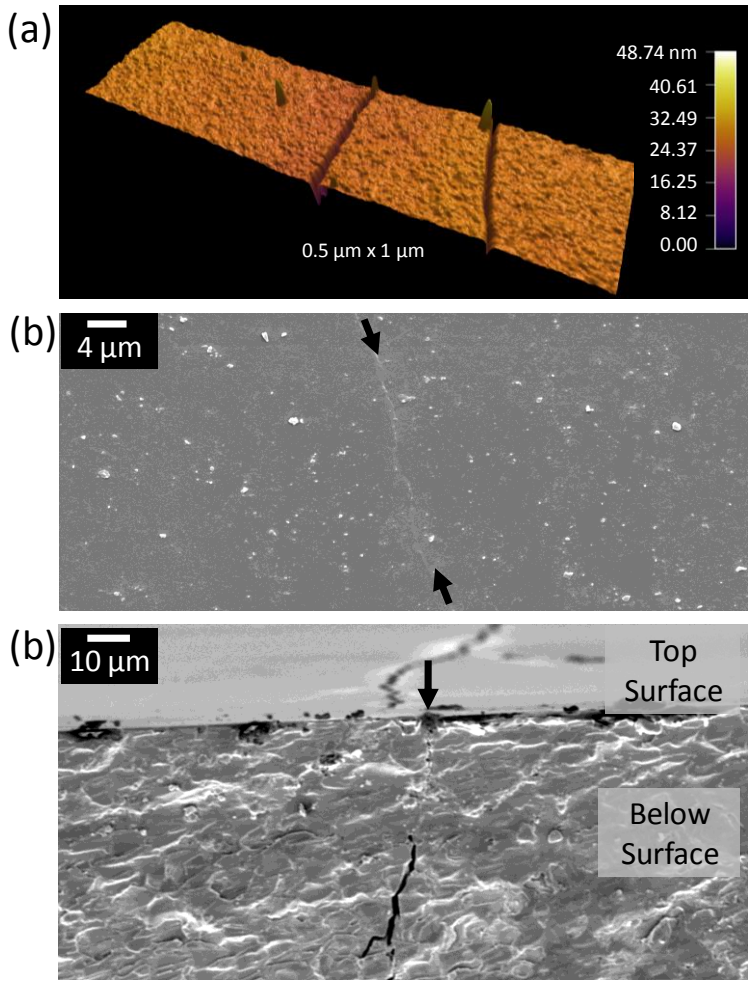

Figure 5.7. (a) AFM and (b) SEM of the top view of cracking in PMMA without capsules. (c) SEM of cracking extending below the surface. Arrows point to the crack observed in (b) and (c).

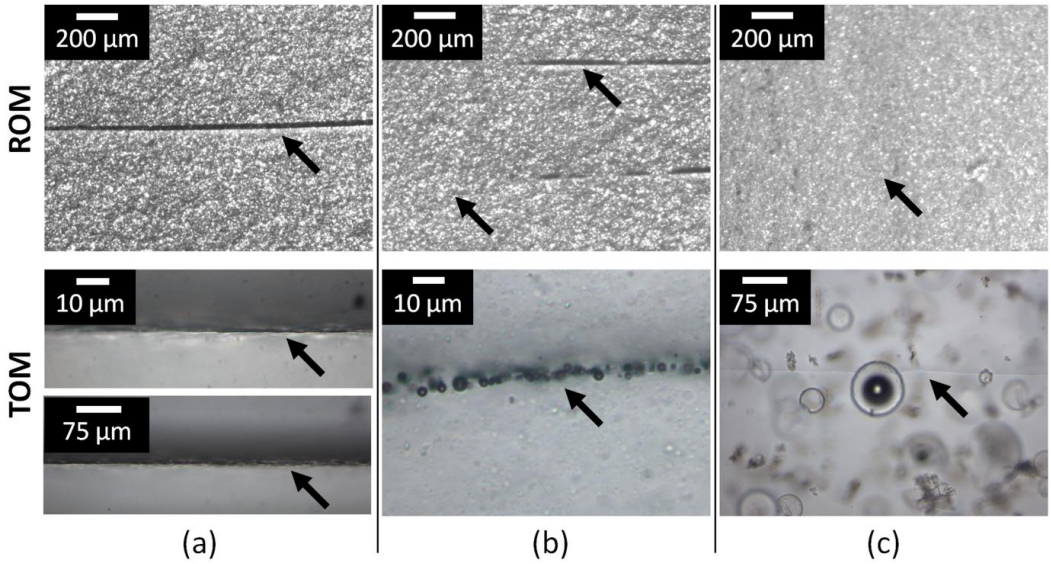

Figure 5.8. Transmission optical microscopy (TOM) and reflection optical microscopy (ROM) of cracks or healed cracks in (a) PMMA, (b) PMMA with 10 wt.% small capsules, and (c) PMMA with 6% large capsules. Arrows point to cracks or healed cracks in the samples.

An electrochemical setup, similar to the setup used by Cho *et al.* (**Figure 5.9**),[14] highlights regions where cracks are deep enough to provide a path between the surrounding environment and the substrate. Silver paste, coated onto the acrylic substrate, is the conductive substrate for these samples since the samples retain the mechanical properties of the acrylic substrate resulting in crack structure similar to samples without the silver paste. As a result, no substrate damage occurs during these tests due to the inertness of the silver. In cracked samples, a current is observed as a voltage is applied across the coating and solution since a conductive path exists between the electrode and the substrate (Figure 5.9b). For non-damaged or healed samples, no current is observed since the electrolyte solution does not come into contact with the substrate.

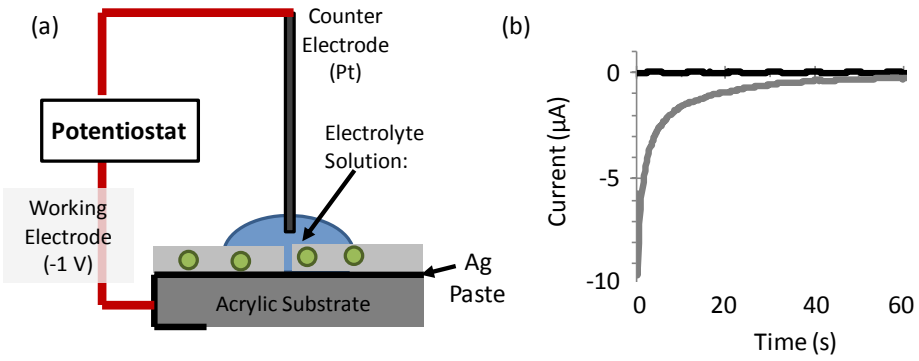

Figure 5.9. (a) the electrochemcial setup. (b) Current observed as voltage is applied across a virgin or healed substrate (black line) and a damaged substrate (gray line).

Small capsules, 1.4 μm in diameter, provide partial healing in PMMA. During initial damage, the sample is bent until the crack(s) initiated propagates across the width of the sample. Immediately after damage, portions of the crack fill in with DBP and are no longer visible by eye. After 24 hours, the healed regions remain invisible (Figure 5.8b) and electrochemical measurements in those areas demonstrate that the protective capabilities of the film are retained. Unhealed regions also exist and can be seen visually and probed electrochemically. Optical microscopy demonstrates that capsules rupture along the crack plane and leave behind empty voids as healing agent wicks into the crack plane (Figure 5.8b). The emptied capsules scatter less light than the initial crack, and do not affect optical healing at a macroscopic level. By measuring the total length of healed cracks and dividing by the total length of the crack, the healed fraction is found. For samples containing 3 wt.% small capsules in PMMA, approximately 30% of a crack is healed while for samples containing 15 wt.% capsules, approximately 40% is healed.

Large capsules, 75 μm in diameter, provide more healing agent to the crack plane and, as a result, can achieve full healing at low concentrations at the expense of increased light scatter. As discussed, annealing the capsules prior to dispersion in PMMA maximizes capsule rupture and healing efficiency. Below 6 wt.%, the annealed large capsules provide only partial healing similar to healing demonstrated for small capsules. At concentrations above 6 wt.%, large

capsules provide enough healing agent for full healing as observed both visually (Figure 5.8c) and electrochemically. The healing process starts quickly and can be seen as soon as healing agent is released into the crack plane. Especially at higher capsule concentrations, so much healing agent is released that pools of DBP form on the sample surface. Video of healing is available in the supplementary information. At all concentrations, the fraction of crack that is healed for the annealed capsules is higher than the fraction of crack that is healed for capsules not annealed (**Figure 5.10**).

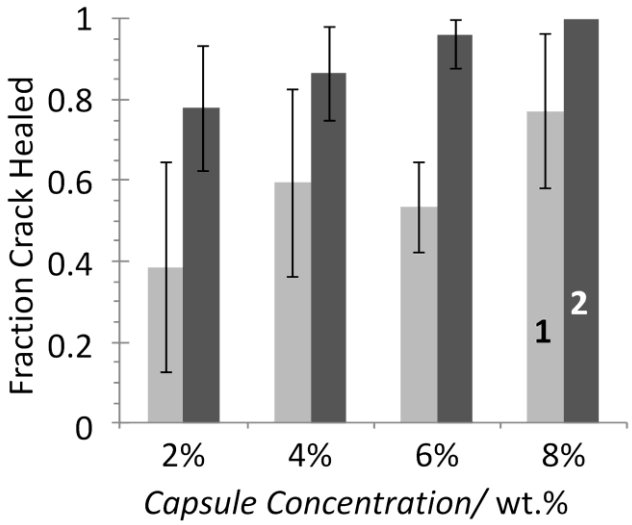

Figure 5.10. Fraction of crack healed for PMMA coatings containing 75 μm DBP filled uncoated capsules (1) and uncoated capsules annealed at 140 °C (2). Averages taken over at least 4 samples. Error bars are the standard deviation. For 8 wt.% annealed capsules, 100% healing was observed in all sample thus no error bar is shown.

5.5 Rate and Extent of Thermoplastic Self-healing

The time scale for healing and extent of healing are important for developing a better understanding of thermoplastic self-healing and optimizing the self-healing response. Although PMMA particles, as received from Sigma, remain unswollen after 72 hours in DBP, imaging of cracked regions in self-healing samples after 72 hours suggest that diffusion of DBP into the PMMA matrix does occur. In samples healed for 1 minute, the original cracks open across the

length of the crack beginning at low bending strains, indicating healing has not occurred. These cracks grow in width as more strain is applied. Liquid healing agent that remains in the crack plane reduces light scatter from the crack when open and remains in the crack plane after the bending strain is removed, resulting in recovery of the initial optical properties of the healed polymer (**Figure 5.11a**). After 72 hours, the original cracks are not observed until a sufficient bending strain is applied to recrack the cracks. Cracks typically re-initiate from defects in the healed region, especially emptied capsules (Figure 5.11b). The cracks remain visible after the bending strain is released suggesting that DBP had first promoted chain entanglement in the crack plane and subsequently diffused far into the PMMA after 72 hours.

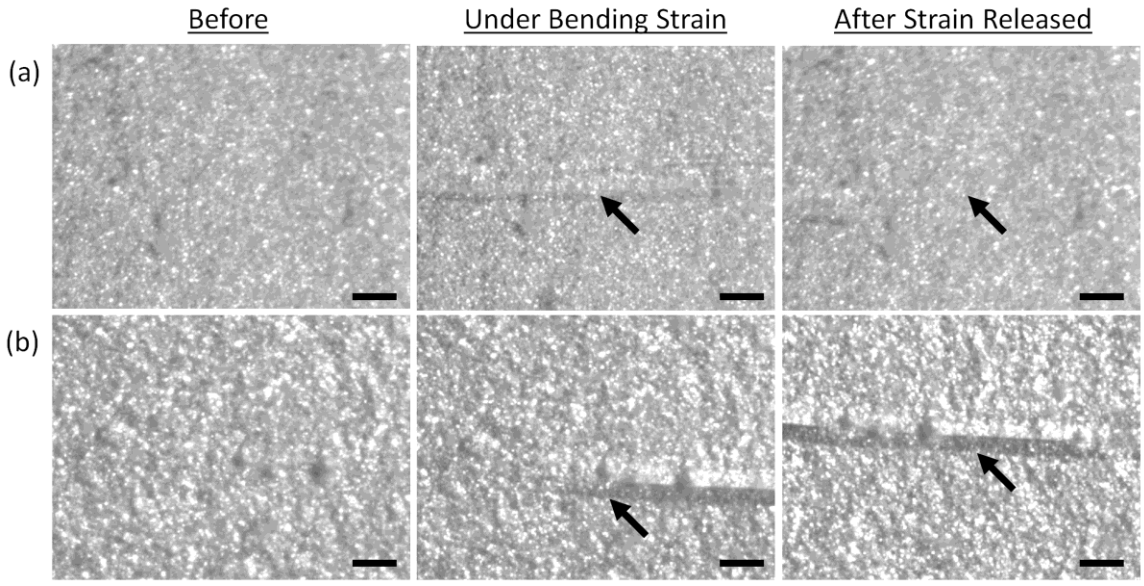

Figure 5.11. (a) Reflection optical microscopy images of PMMA films containing 6 wt.% DBP capsules after healing for 1 min followed by bending. (b) Samples are then allowed to heal for 72 hours before re-testing. Scale bars are 200 μm; arrows point to locations of healed cracks.

The healing capabilities of a single capsule demonstrate the extent of healing that can occur in this system. In damaged samples, a single large capsule can heal a crack as long as 1 cm. This is approximately half of the healing expected from volume calculations: assuming a 50nm wide crack in a 200 μm thick coating, and 75 μm capsules, a single capsule should heal as

much as 2 cm. A number of factors reduce the actual healing. First, healing agent exits the top of the crack plane and forms pools on the sample surface. In addition, capsules often release only a portion of their contents (Figure 5.8c) perhaps due to the thinness of the cracks being tested. Finally, the crack may be wider than 50nm in some regions.

5.6 Conclusions

A solvent welding self-healing system is developed for the optical thermoplastic polymer PMMA. By employing index matching between the healing agent and polymer matrix, thin films of PMMA containing DBP capsules transmit sufficient light to be useful for optical applications. Two capsule sizes are studied: small, 1.4 μm, capsules are important for thin film applications in which larger capsules will not fit; and large, 75 μm, capsules are important for applications where more healing agent is required. In both cases, the capsules retain most of their contents during work-up, are well dispersed and rupture well during a crack event. Partial healing occurs for 50 nm cracks in PMMA containing either size capsule. Because the healed material is inherently index matched to the polymer matrix, light scatter from the damaged area is minimized allowing recovery of the optical properties of the polymer film after cracking. The protective capability in the healed areas is also regained as demonstrated by potentiostat measurements. Full healing of the crack occurs in PMMA samples with more than 6 wt.% large capsules. After 72 hours, polymer diffusion occurs in the crack plane and mechanical healing is observed. Finally, healing in thin films is only limited by the thickness of the film. The healing capabilities of a single capsules is approximately half of what is expected based on geometry calculations. The remaining healing agent pools on the surface of the film.

5.7 Experimental

5.7.1 Materials

Ammonium chloride was purchased from Sigma. Monobasic sodium phosphate and sodium chloride were purchased from Fisher Scientific. Brij 97, Resorcinol, urea, dibutylphthalate (DBP), ethyl phenyl acetate (EPA), formaldehyde solution, tetrabutyl ammonium fluoride (TBAF), and tetraethylorthosilicate (TEOS) were purchased from Sigma-Aldrich. Formaldehyde was purchased as a 37.5 wt.% solution and TBAF was purchased as a 75 wt.% solution in water. For all experiments, 1 mL TBAF was diluted with 100 mL Millipore water. Ethylene maleic anhydride (EMA) surfactant was donated by Vertellus (chemical name ZeMac). For all experiments, a 2.5 wt.% solution of EMA in water was made and used. Polymethylmethacrylate (PMMA, 35000 g/mol), methyltriethoxy silane (MTMS), cetyltrimethylammonium bromide (CTAB), and anisole were purchased from Acros. Methacryloxypropyltrimethoxy silane (MPTMS) was purchased from Gelest. Cast acrylic (0.06" thick) was purchased from McMaster Carr. Silver paste was purchased from Ted Pella.

5.7.2 Fabrication of Self-healing Coatings

1.4 μm capsules and 75 μm capsules were both synthesized based on the procedures outlined in chapter 2. 1.4 μm capsules contained DBP and were coated using the fluoride-catalyzed silica condensation chemistry.

Self-healing coatings were fabricated via one of two solvent casting methods. Self-healing coatings less than 10μm thick were prepared via spin coating. A solution of 30 wt.% PMMA in anisole was first prepared. Next, 1.4 μm, uncoated capsules were deposited on a 1 mm thick glass slide using a method similar to convective assembly of colloid crystals described elsewhere.[15] The solution was then spun coat at 3000 rpm for 30 seconds and dried in an oven at 90 °C for 12 hours. Two layers of PMMA without capsules were spun coat as a capping layer to assure that no capsules penetrated the surface of the samples.

Self-healing coatings 100-500 μm thick were prepared via drop casting. A solution of 20 wt.% PMMA in anisole was prepared and the desired fraction of capsules added. Vacuum was pulled on the mixture to remove any trapped gas. The solution was dropped onto a 1" x 0.5" x 0.06" acrylic substrate in a quantity corresponding to the anticipated thickness based on volume calculations. For small capsules, 0.15 mL of the solution containing capsules and polymer was dropped onto the substrate while 0.25 mL of solution was used for large capsules. The sample was dried in an oven at 140 °C for 15 hours forming a polymer film.

0.06" thick acrylic substrates were used for all samples analyzed using transmission optical microscopy. For reflection optical microscopy and electrochemical experiments, a reflective substrate was required. To achieve this while maintaining similar cracking properties to the acrylic substrate, silver paint was applied to one side of an acrylic substrate and dried for 1 hour at 140 °C before the solvent casting step.

Large capsules required one of two methods to ensure efficient rupture in PMMA. In the first method, capsules were heated in the dry state to 140 °C for 15 minutes before being incorporated into the PMMA solution described above. In the second method, capsules were soaked in the PMMA solution for 1 hour before drop casting.

5.7.3 Analysis of Self-healing Coatings

Simulations of transmission were done using Matlab code developed by Bond *et al*.[12] Small capsules are modeled with a 1.4 μm diameter core and 70 nm shell. To calculate transmission, the PMMA sample is modeled as a 10 μm thick film containing 5 wt.% capsules. All UV-vis measurements were done with air as background in a UV-vis spectrometer (Shimadzu UV-2450 Spectrophotometer).

To induce damage in the PMMA films, samples were bent in a 3-point bend configuration. Sufficient force was applied to cause cracking across the full sample. Unhealed damage was analyzed in AC mode on an Asylum Cypher AFM in air using oxide-sharpened

silicon probes having a resonance frequency in the range of 280–320 kHz (MikroMasch–NSC15). The cross-section of the crack was prepared by first cracking through the PMMA film in one direction followed by cracking through the PMMA and substrate in the perpendicular. Unhealed and Healed damage was analyzed by optical microscopy and electrochemical measurements.

An electrochemical setup similar to previous research [14] was used to demonstrate the protective capabilities of the self-healing coating. An image of the setup is included in the supplementary information. Briefly, substrates of acrylic coated with silver paste were used in the drop casting step. The silver layer was connected to a reference electrode while a working electrode was brought into contact with a drop of electrolyte solution on the sample surface. To assure that the electrolyte solution had wicked into the crack plane, the sample was flexed to temporarily widen visible cracks without re-damaging any healed regions. The electrolyte solution consisted of 1M NaCl and 1 wt.% Brij 97. 1 V was applied across the electrodes and the current recorded over 60 seconds.

5.8 References

[1] Ishiyama, C.; Sakuma, T.; Shimojo, M.; Higo, Y. Effects of humidity on environmental stress cracking behavior in poly(methyl methacrylate). *J Polym Sci Pol Phys* **2002**, *40*, 1-9.

[2] Miller, D. C.; Gedvilas, L. M.; To, B.; Kennedy, C. E.; Kurtz, S. R. Durability of poly(methyl methacrylate) lenses used in concentrating photovoltaic modules. *Proc SPIE* **2010**, 777303.

[3] Biggs, P.; Jones, L.; Wellborn, B.; Lewis, G. A Self-healing PMMA Bone Cement: Influence of Crystal Size of Grubbs' Catalyst. *IFMBE Proceedings* **2009**, *24*, 147-150.

[4] Lin, C. B.; Lee, S.; Liu, K. S. Methanol-Induced crack healing in poly(methyl methacrylate). *Polym. Eng. Sci.* **1990**, *30*, 1399--1406.

[5] Hsieh, H.; Yang, T. J.; Lee, S. Crack healing in poly(me-thyl methacrylate) induced by co-solvent of methanol and ethanol. *Polymer* **2001**, *42*, 1227--1241.

[6] Brown, E. N.; Kessler, M. R.; Sottos, N. R.; White, S. R. In situpoly(urea-formaldehyde) microencapsulation of dicyclopentadiene. *J. Microencapsul.* **2003**, *20*, 719-730.

[7] Blaiszik, B. J.; Sottos, N. R.; White, S. R. Nanocapsules for self-healing materials. *Compos. Sci. Technol.* **2008**, *68*, 978.

[8] Jackson, A. C.; Bartelt, J. A.; Marczewski, K.; Sottos, N. R.; Braun, P. V. Silica-Protected Micron and Sub-Micron Capsules and Particles for Self-Healing at the Microscale. *Macro. Rap. Comm.* **2010**, *31*, 82-87.

[9] Caruso, M. M.; Delafuente, D. A.; Ho, V.; Sottos, N. R.; Moore, J. S.; White, S. R. Solvent-Promoted Self-Healing Epoxy Materials. *Macromolecules* **2007**, *40*, 8830-8832.

[10] Caruso, M. M.; Blaiszik, B. J.; Jin, H.; Schelkopf, S. R.; Stradley, D. S.; Sottos, N. R.; White, S. R.; Moore, J. S. Robust, Double-Walled Microcapsules for Self-Healing Polymeric Materials. *ACS Appl. Mater. Interfaces* **2010**, *2*, 1195-1199.

[11] Rule, J. D.; Sottos, N. R.; White, S. R. Effect of microcapsule size on the performance of self-healing polymers. *Polymer* **2007**, *48*, 3520-3529.

[12] Bond, T. C.; Habib, G.; Bergstrom, R. W. Limitations in the enhancement of visible light absorption due to mixing state. *J. Geophys. Res.* **2006**, *111*, D20211.

[13] Beecroft, L. L.; Johnen, N. A.; Ober, C. K. Covalently Linked, Transparent Silica-Poly(imide) Hybrids. *Polym. Adv. Technol.* **1997**, *8*, 289-296.

[14] Cho, S. H.; White, S. R.; Braun, P. V. Self-Healing Polymer Coatings. *Adv. Mater.* **2009**, *21*, 645-649.

[15] Prevo, B. G.; Velev, O. D. Controlled, Rapid Deposition of Structured Coatings from Micro- and Nanoparticle Suspensions. *Langmuir* **2004**, *20*, 2099-2107.

CHAPTER 6:

CONCLUSIONS AND FUTURE DIRECTIONS

6.1 Conclusions

Small size-scale self-healing systems for composites and optical materials are successfully developed and analyzed. In particular, liquid-filled capsules and active particles on the order of 1 μm in diameter are synthesized and modified such that that minimal aggregation and loss of healing agent occurs during processing. Silica condensation onto 1.4 μm capsules is particularly effective at improving capsule dispersion in both epoxy and polymethylmethacrylate (PMMA). The coatings do not significantly improve capsule stability, however during this work it was found that capsule stability can be significantly enhanced through appropriate work-up conditions. Catalyst is successfully protected by polymer and silica in sub-micron particles. The silica coating is important for making reducing catalyst deactivation when the particles are cured in epoxy. These capsules and particles are implemented in an epoxy system where the size of damage must be less than 1 μm wide for effective healing to occur. Similarly, partial healing can occur in thermoplastic materials containing micron size dibutyl-phthalate (DBP) capsules.

Silica-coated capsules are coated using three different methods: Stöber condensation, fluoride-catalyzed silica condensation, and fluidized bed reactor chemical vapor deposition (FBR-CVD). Stöber chemistries are well understood and have been shown to build dense silica shells on a variety of surfaces but the alcohol solvents required for the chemistry limit its use. Capsules larger than 20 μm cannot be coated using this method because the alcohols weaken the shell wall resulting in capsule bursting under mild stirring conditions. 1.5 μm diameter DCPD filled capsules formed via sonication assisted synthesis can be coated in an alcohol solution as long as

the alcohol solution is first saturated with DCPD. This requirement limits the Stöber chemistry to capsules containing solvents that can form saturated solutions in alcohols. FBR-CVD does not require solution conditions and is capable of coating a variety of surfaces with functionalities not amenable to solution processing techniques. This method, however, requires that the interactions between capsules be less than the shear forces available in the FBR. Fluoride-catalyzed chemistries are the most promising route to a generalized silica condensation method for capsules. Although the surface chemistry of the capsules is important, polyureaformaldehyde capsules at all size scales are successfully coated using this method by controlling the solution ionic environment. For 1.5 μm capsules, the silica coating is necessary as the coated capsules can be dried to a dry powder for incorporation into a polymer matrix. This is not possible with uncoated capsules.

Although the silica coating process adds an extra diffusion barrier to the capsules, no significant changes in capsule stability are observed. Instead, in depth studies of capsule stability demonstrate other important parameters for minimizing content loss in a variety of conditions. The capsule work-up conditions have the greatest impact on thermal stability. In particular, ethanol-rinsed PUF capsules perform significantly better than water-rinsed capsules. It is expected that this is a result of the ethanol washing out trapped solvent molecules in the capsule wall and this results in pore closure as the ethanol evaporates. The molecule size also plays an important role as capsules containing DBP have a consistently smaller diffusion coefficient in PUF than capsules containing DCPD or EPA. Of particular interest is that DCPD capsules have a consistently lower diffusion coefficient in PUF than EPA despite having a smaller molecular weight and higher volatility at 20 °C. This demonstrates the importance of the interactions between solvent molecules and the PUF shell on stability. Solvent stability is also a key component for understanding capsule stability and is important for applications requiring solvent casting processing. Although quantitative data could not be collected, qualitatively, the size of

the solvent molecule also plays an important role on healing agent loss in a good solvent. In fact, while EPA capsules tend to lose a portion of their contents in anisole at 80 °C, no loss is observed from DBP capsules under the same conditions.

Grubbs' catalyst particles are also subject to healing agent loss under adverse conditions and polymer encapsulation plays an important role in minimizing loss. While wax has been used previously to protect the catalyst particles, the size of the particles cannot be reduced to match the size scale of the 1.5 μm DCPD capsules coated in Chapter 2 due to aggregation. In addition, the wax particles break down above 35 °C and dissolve in epoxy during a cure cycle at 50 °C. Polystyrene (PS), on the other hand, can be made into sub-micron particles using an emulsion solvent evaporation procedure and these particles remain well dispersed after drying. On the micron size-scale, PS is insufficient to protect the catalyst in epoxy so polymethylmethacrylate (PMMA) and silica are used with the PS to build stable particles. At larger sizes, above 15 μm, PS is sufficient to protect the catalyst and the particles can survive intact in air up to 65 °C. Unlike the wax particles, they also remain intact while curing epoxy, containing the particles, at 50 °C.

The 1.5 μm coated DCPD capsules and sub-micron catalyst particles are effective at healing damage events on the order of 100 nm in epoxy using a short-grove tapered double cantilever beam (TDCB) specimen. Both components disperse well and remain active during the epoxy curing procedure. A pressure applied across the crack plan reduces the crack width in regions of the TDCB to as small as 100 nm simulating the smaller damage events that can be healed with the limited healing agent available in the 1.5 μm capsules. Healing in the full system approaches 22%. Part of this healing is a result of PS redistribution in the crack plane and mechanical interlocking with the crack plane.

Coated liquid capsules also open new possibilities for self-healing in transparent thermoplastic polymers. In particular, DBP filled coated capsules, both 1.5 μm and 80 μm, are used to heal PMMA while maintaining a good transparency in the polymer. 1.5 μm capsules require a silica shell to remain dispersed during the solvent casting steps for building a PMMA film. 1.5 μm capsules are incorporated at up to 15 wt.% in PMMA and partial healing is observed both optically and by testing the protective capabilities of the healed films. Full healing is obtained with larger capsules that supply more healing agent. 80 μm heal both the optical and protective properties of PMMA above 6 wt.%. A portion of the mechanical properties are also healed as observed visually. When recracked after 3 days, the cracks propagate through the PMMA and can be seen after recracking suggesting that the DBP had diffused into the PMMA leaving a plasticized polymer in the healed region.

6.2 Future Directions

This works opens several important directions that will contribute to the success of future self-healing system. First, capsule stability is an important component for determining the lifetime of these self-healing materials but quantification of the stability is not trivial. Thus, the various capsule parameters that may affect capsule stability and possible methods for quantifying capsule stability are discussed. Second, self-healing polymer particles offer a wide range of possibilities for new self-healing chemistries where chemical reactions are eliminated, reducing the need to protect reactive components from deactivating species and high temperature. Finally, several comments are included discussing how this research can help to advance research on other thermoplastic self-healing systems.

6.2.1 Capsule Stability

Several parameters are important for changing the properties of liquid-filled capsules and their thermal stability in air. Shell material is the most important parameter and is typically chosen based on the solvent that will be encapsulated.[1-4] Isocyanates, for example, cannot be encapsulated using a polyureaformaldehyde (PUF) shell due to reactions with the urea but can be encapsulated in a polyurethane shell.[2] Previous work[3, 5] shows that the shell thickness has an important effect on the strength of the capsules and the time for diffusion of the inner contents across the shell wall. Appropriate choice of the core material is also important. The core liquid properties and its interactions with the shell wall are also important for stability as described in **Table 6.1** and discussed in Chapter 2. Finally, the capsule work-up is an extremely important component to recording consistent data. While washing the capsules with ethanol affects capsule properties the most, many of the factors shown in Table 1 also cause slight changes in the capsule properties.

Parameter	***What it affects***
Shell material	Shell wall quality
Shell thickness	Time for core diffusion across shell wall
Core interactivity with shell	Shell wall quality
Core volatility at RT	Evaporation from shell wall
Core molecule size	Diffusion coefficient across shell wall
Core boiling point	Upper bound for use
Core solubility in matrix resin	Diffusion from shell wall during manufacture
Core solubility in polymer matrix	Diffusion from shell wall during normal operation
Work-up Parameters: *Solvent wash, wash time, dry time, sieve time*	Shell Quality

Table 6.1. Capsule properties and their effects on the capsule stability.

While thermal stability in air has been the primary measure of capsule stability,[3, 6] it should only be used as an approximation of capsule stability since capsules will rarely see high temperatures during storage. Instead, **Table 6.2** highlights recommended tests to mimic more realistic conditions. For many applications, storage stability is the most important capsule property since capsules only need to retain their contents until they are incorporated into a polymer. As a result, capsules can be classified as: stable for short-term storage and stable for long-term storage. The acceptable contents loss can be determined by the application and can be measured by TGA. Once in a polymer, the shell wall becomes a thin diffusion barrier compared to the matrix itself requiring matrix stability tests. Similar to the procedures outlined in Chapter 2, the loss of contents from the matrix can be determined from XRay Computed Tomography (Xray CT) although light microscopy can be used to find the volume loss from capsules in a transparent polymer matrix. The initial matrix stability is important for determining what capsules can be incorporated into a given polymer with minimal healing agent loss. Accelerated matrix stability can be used to determine an approximate lifetime for a given self-healing polymer. The final capsule environment that should be tested is solvent stability and is important for quantifying content loss during typical processing conditions and the solvent tested should include any resins, monomers, or organic solvents to which the capsules may be exposed. Of these tests, short-term air stability, initial matrix stability and solvent stability are the most important parameters for academic research while specific applications will determine the exact requirements for the other tests.

Type of stability	*Environment*	*Application*
Short-term air stability	Capsules stored in air for 1 week. T = 25 C	Self-healing polymer manufactured within 1 week of capsule synthesis
Long-term air stability	Capsules stored in air for 6 months T=25 C	Long-term capsule storage required prior to manufacture
Initial matrix stability	Capsules stored in final polymer matrix for 1 week. T= variable	Benchmarking test
Accelerated matrix stability	Capsules stored in final polymer matrix for 2 months. T>application temperature	Benchmarking test
Long-term matrix stability	Capsules stored in final polymer matrix for expected life of polymer at application temperature	Comparing capsule stability across various applications
Solvent stability	Solvent, temperature, and time are variable and should reflect the expected environment during self-healing polymer manufacture	Quantifying capsule contents loss during typical polymer processing conditions.

Table 6.2. Potential Stability tests and their applications.

6.2.2 Active Particle Stability

Many of the parameters that apply to capsules also apply to particles. As a result of the solid nature of active particles, the key differences between these and capsules are:

(1) Diffusion of species into the particle can lead to deactivation.

(2) Quantification of active material cannot easily be done in real time.

To date, active particle stability has focused primarily on Grubbs' catalyst particles for use in epoxy matrices. Loss of the catalyst results from diffusion of deactivating molecules into the particle. Therefore, the environment has a key impact on how much healing agent is lost during storage and use. Beyond the environment, the type of encapsulating material used plays the primary role in particle stability as discussed in Chapter 3.

Many of the tests used to find the stability of liquid-filled capsules can be used to test active particles. Because the quantity of healing agent in the particles cannot easily be measured

in real time, active particles are deemed to be those that have a minimum concentration of active material remaining after exposure to the different environments. In Chapter 3, the catalyst activity is demonstrated by gel time in DCPD. Particles that gelled DCPD in a certain time are deemed active. This works well with catalyst where the concentration of catalyst in monomer can change without having a deleterious effect on the final healed polymer. Other systems, however, may require more quantitative measurement techniques such as NMR or UV-vis. One of the challenges to determining the quantity of Grubbs' catalyst using these methods was the deactivation of the catalyst during the measurement process. As a result, care must be taken to develop a procedure to separate the active particles from their environment without accidental loss of healing agent.

6.2.3 New Applications with Thermoplastic Self-healing

One of the exciting aspects of the polymer particles developed in Chapter 3 is that they can be re-dissolved and deposited into the crack plane forming their own healed material without any chemical reactions taking place. Therefore, temperature and matrix reactive groups do not play a role in deactivating the self-healing components. Possible interactions between the healed polymer and polymer matrix include hydrogen bonding, Van der Waals bonding or mechanical interlocking. For the system described in Chapter 4, polystyrene (PS) does provide some healing in epoxy but much of this is expected to be mechanical interlocking since PS particles larger than 40 μm do not show similar results and the primary difference between the two samples is the surface roughness of the crack plane. Other polymers form better interactions with the crack plane through hydrogen bonding. Proteins, for example, are known to adsorb strongly to a wide variety of surfaces.[7]

A particularly intriguing thermoplastic system is one where a microfluidic network delivers a good solvent to the thermoplastic components. The primary challenge with developing

this type of system is protecting the polymer matrix from dissolving into the solvent healing agent during normal operation. CVD and ALD may be one possible solution for protecting the microfluidic channels. In addition to the promise of multiple healing events, advantages to this system are similar to those discussed in Chapter 5: the healed material is the same as the initial polymer, allowing full healing, and index matching can result in optically clear self-healing polymers containing microfluidic networks.

6.3 References

[1] McIlroy, D. A.; Blaiszik, B. J.; Caruso, M. M.; White, S. R.; Moore, J. S.; Sottos, N. R. Microencapsulation of a Reactive Liquid-Phase Amine for Self-Healing Epoxy Composites. *Macromolecules* **2010**, *43*, 1855-1859.

[2] Yang, J.; Keller, M. W.; Moore, J. S.; White, S. R.; Sottos, N. R. Microencapsulation of Isocyanates for Self-Healing Polymers. *Macromolecules* **2008**, *41*, 9650-9655.

[3] Caruso, M. M.; Blaiszik, B. J.; Jin, H.; Schelkopf, S. R.; Stradley, D. S.; Sottos, N. R.; White, S. R.; Moore, J. S. Robust, Double-Walled Microcapsules for Self-Healing Polymeric Materials. *ACS Appl. Mater. Interfaces* **2010**, *2*, 1195-1199.

[4] Yuan, Y. C.; Rong, M. Z.; Zhang, M. Q.; Chen, J.; Yang, G. C.; Li, X. M. Self-Healing Polymeric Materials Using Epoxy/Mercaptan as the Healant. *Macromolecules* **2008**, *41*, 5197-5202.

[5] Yuan, L.; Liang, G.; Xie, J.; Li, L.; Guo, J. The permeability and stability of microencapsulated epoxy resins. *J. Mater. Sci.* **2007**, *42*, 4390-4397.

[6] Kessler, M. R.; Sottos, N. R.; White, S. R. Self-healing structural composite materials. *Comp. Part A - Appl. S.* **2003**, *34*, 743-753.

[7] Tzannis, S.; Hrushesky, W. J. M.; Wood, P. A.; Przybycien, T. M. Adsorption of a Formulated Protein on a Drug Delivery Device Surface. *J. Colloid Interf. Sci.* **1997**, *189*, 216-228.

AUTHOR'S BIOGRAPHY

Aaron Jackson was born on April 27, 1984 in Wilmington, DE to Elaine and Scott, both Chemical Engineers graduated from Cornell. Following their footsteps in science, he attended Charter School of Wilmington High School, a math and science magnet school. There he firmly planted himself in the engineering field, participating in a variety of Science Olympiad building events and making it to the national Science Olympiad tournament his sophomore and junior years. Outside of the classroom, he played soccer, piano, clarinet, and golf. He earned the Eagle Scout award in 2001.

From 2002 to 2006, Aaron attended his parents' alma mater, Cornell University, in Ithaca, NY where he majored in Materials Science and Engineering. He became interested in alternative energies especially fuel cells and began his research career with Uli Weisner under the mentorship of Scott Warren. He studied fuel cell catalysts and helped to develop the poly-thiol process for producing nanoparticles using a relatively safe and green thiol reduction chemistry. He had the opportunity to work in the fuel cell industry through summer internships at United Technologies Corporation's Fuel Cell Department and at W. L. Gore. For those visiting Cornell, Aaron strongly recommends the Finger Lakes region just north of Ithaca for those interested in scenic wine tours.

Aaron's enjoyment of research led him to the University of Illinois for graduate school. Taking a hiatus from energy research, Aaron joined the Braun group where he focused on self-healing materials. He enjoyed his teaching assistant responsibilities in the Introduction to Materials Science class and hopes he can continue to use his expertise to teach younger students the exciting potential of materials science in every day applications. Outside of research, he enjoyed the social aspects of Graduate student life where he captained the materials science flag football team and organized prospective graduate student visits. He hopes that his Friday games

competitions continue to bring together the MSE department and other departments for years to come. Aaron is excited to continue polymer research at the Army Research Labs in Maryland.